IMPACT OF URBAN MORPHOLOGY ON THE ENERGY EFFICIENCY OF TIRANA NEW BOULEVARD PROJECT

A THESIS SUBMITTED TO
THE FACULTY OF ARCHITECTURE AND ENGINEERING
OF
EPOKA UNIVERSITY

BY

LEZO KROJ

IN PARTIAL FULFILLMENT OF THE REQUIREMENTS
FOR
THE DEGREE OF MASTER OF SCIENCE
IN
ARCHITECTURE

July, 2021

Approval sheet of the Thesis

This is to certify that we have read this thesis entitled **"Impact of urban morphology on the energy efficiency of Tirana New Boulevard project"** and that in our opinion it is fully adequate, in scope and quality, as a thesis for the degree of Master of Science.

_____

Dr. Edmond Manahasa
Head of Department
Date: July, 22, 2021

Examining Committee Members:

Prof. Dr. Sokol Dervishi (Architecture) _____

MSc. Ina Dervishi (Architecture)_____

Dr. Fabio Naselli (Architecture) _____

I hereby declare that all information in this document has been obtained and presented in accordance with academic rules and ethical conduct. I also declare that, as required by these rules and conduct, I have fully cited and referenced all material and results that are not original to this work.

Name Surname: Lezo Kroj

Signature: _____

ABSTRACT

IMPACT OF URBAN MORPHOLOGY ON THE ENERGY EFFICIENCY OF TIRANA NEW BOULEVARD PROJECT

Kroj, Lezo
M.Sc., Department of Architecture
Supervisor: Prof. Dr. Sokol Dervishi

The reason why Smart Cities is a very popular topic amongst researchers is because they provide effective and efficient ways of collecting, managing and distributing resources to their residents. Energy-efficiency is a major contributor of sustainable cities, that affects the end-consumer directly. It plays a vital role on a persons' economical expenses. This study focuses on the importance that urban morphology plays towards the energy efficiency by analyzing four different urban fabrics within the New Boulevard project in Tirana. The selection of these four zones was made considering that they cover a significant percentage area of the overall site, properly represent the predominant building and district morphologies and any results reflected about these areas will have a notable significance for the site on the whole. It achieves this by measuring 8 different urban morphology indicators (UMIs): Gross space index, Floor space index, Façade-to-site ratio, Average building height, Volume area ratio, Building aspect ratio, Sky factor of building facades, Open space ratio. These UMIs are gathered as important statistical data and serve as a comparison ground for the four districts between them. For this study AutoCAD 3D is used to model the site and prepare the file for CitySim Pro, Revit Architecture for modeling the site envelope and later run a solar analysis with Insight Plugin for Revit, and CitySim Pro software to investigate and optimize the energy efficiency parameters. The results of this study serve as a role model for the contemporary buildings of the future in Tirana especially after considering that no previous observations of this nature that take the Mediterranean climate into account are made here.

Keywords: *Urban morphology, Smart Cities, Sustainable Urban Design, Energy Efficiency in Urban Scale, Urban Scale Simulation*

ABSTRAKT

IMPAKTI I MORFOLOGJISË URBANE NË EFIÇENCËN ENERGJITIKE TË PROJEKTIT NË BULEVARDIN E RI

Kroj, Lezo

Master Shkencor, Departamenti i Arkitekturës

Udhëheqësi: Prof. Dr. Sokol Dervishi

Arsyeja pse tema e Qyteteve Inteligjente është shumë e përhapur mes kërkuesve vjen sepse ato mundësojne rrugë efektive për grumbullimin, menaxhimin dhe shpërndarjen e burimeve tek banorët e tyre. Efiçenca energjitike është një kontributor madhor i qyteteve të qëndrueshme, që ndikon përdoruesin përfundimtar në mënyrë direkte. Ajo luan një rol jetik tek shpenzimet e një personi. Ky studim përqëndrohet në rëndësinë që morfologjia urbane luan te efiçenca energjitike duke analizuar katër struktura urbane në projektin e Bulavardit te Ri ne Tiranë. Përzgjedhja e këtyre katër zonave është bërë duke patur parasysh që ato mbulojnë një përqindje të konsiderueshme të territorit të përgjithshëm, përfaqësojnë në mënyrë korrekte ndërtesat dhe morfologjitë urbane predominante dhe cdo rezultat i reflektuar për këto zona do të ketë nje domethënie të veçantë për territorin në përgjithësi. Kjo gjë arrihet duke matur tetë indikatorë të ndryshëm urban: Koeficienti i shfrytëzimit të territorit (KSHT), Indeksi i hapësirave të dyshemeve, Raporti fasadë-parcelë, Lartësia mesatare e ndërteses, Raporti volumetri-sipërfaqe, Raporti sipërfaqe-volumetri, Shikueshmëria e qiellit nga cdo pikë e fasadave, Raporti i hapësirave të hapura. Këta indikatorë janë matur dhe më pas grumbulluar si të dhëna statistikore të rëndësishme dhe shërbejnë si një mjet krahasimor për të katër zonat mes tyre. Për këtë studim janë përdorur programet AutoCAD 3D për modelimin e sipërfaqes mbështjellëse të territorit të përgjithshëm dhe pregatitjen e dosjes per në CitySim Pro, Revit Architecture për modelimin e territorit ku më pas bëhet analiza diellore me anë te shtojcës Insight për

Revit, dhe programi CitySim Pro për të investiguar dhe optimizuar parametrat e efiçencës energjitike. Përfundimet e këtij studimi shërbejnë si një shembull për ndërtesat kontemporane të së ardhmes në Tiranë, veçanërisht pasi merr në konsideratë që asnjë vrojtim i mëparshem i kësaj natyre në kontekstin e klimës Mesdhetare të jetë bërë këtu.

Fjalët kyçe: *Morfologji urbane, Qytete inteligjente, Dizenjime urbane të qëndrueshme, Efiçencë energjitike në shkallë urbane, Simulime në shkallë urbane.*

Dedicated to my family

ACKNOWLEDGEMENTS

I would like to express my gratitude to Prof. Dr. Sokol Dervishi, who supported me throughout the process and his guidance was crucial in making a great final product. I thank him for his dedication of time, patience, honesty and dynamic energy, which motivated me to work harder.

Also, I am appreciative of all the professors who have been part of my architectural education since the first year.

Most importantely I thank my parents whose advices I have always listened very carefully and my sister who has played a huge part on making me a better person. I am grateful to them.

TABLE OF CONTENTS

LIST OF TABLES

LIST OF FIGURES

CHAPTER 1

INTRODUCTION

1.1 Motivation

Recently, the topic of smart cities has become quite popular to the public and has gained global attention as a reaction to the challenge of urban sustainability (Bibri 2017). Ecologically and advanced nations in particular are facing such tough challenge. Developing countries as well need to start tackling their energy problems early on by foucusing on sustainable solutions and observe the intelligent solutions that smart cities unfold. A closer look into individual consumption reveals that there is more than the occupant's behaviour affecting it. (Holden 2004) assumed that household consumption is impacted to a large extent by the physical living conditions such as: design and location of buildings. This also relates to the energy used for heating and technical appliances. (Mauree 2019) focuses on environmental sustainability and shows how it has an economical impact. He depicts a link between urban climate, building energy demand, outdoor thermal comfort, energy systems and suggests that an interface where all the abovementioned factors are taken into account, is constructed, in order to tackle the high amount of energy that is currently used in our societies. (Calvillo et al. 2016) reviews similar work on energy and proposes an improved energy model in the smart city context. He concludes that detailed modelling and simulation is required to verify and develop existing and new systems. (Okeil 2010) demonstrates a general energy efficient building morphology that is obtained by cutting solar profiles. The results indicate that the proposed form can maximize the potential of passive solar energy. (Sharifi 2016) reviews literature concerning energy resilience to establish a scheme for estimating urban energy resilience. The study attempted to consolidate the existing information on urban energy resilience and develop a methodological framework for urban energy assessment and present

different design solutions and planning principles to be used for urban energy evaluation.

This investigation develops upon the field of urban sustainability and focuses in particular on the impact that building morphology plays towards energy efficiency and how building systems are affected in this process. The Mediterranean climate lacks such investigations, particulary our country that is in the development process, and those few studes conducted are limited in their depth of analysis. A strong emphasis is put on the methodological framework as it combines an analysis of 4 different urban typologies individually and together, concerning: energy use, surface temperatures and UMIs, shown in ***Figure 1.***

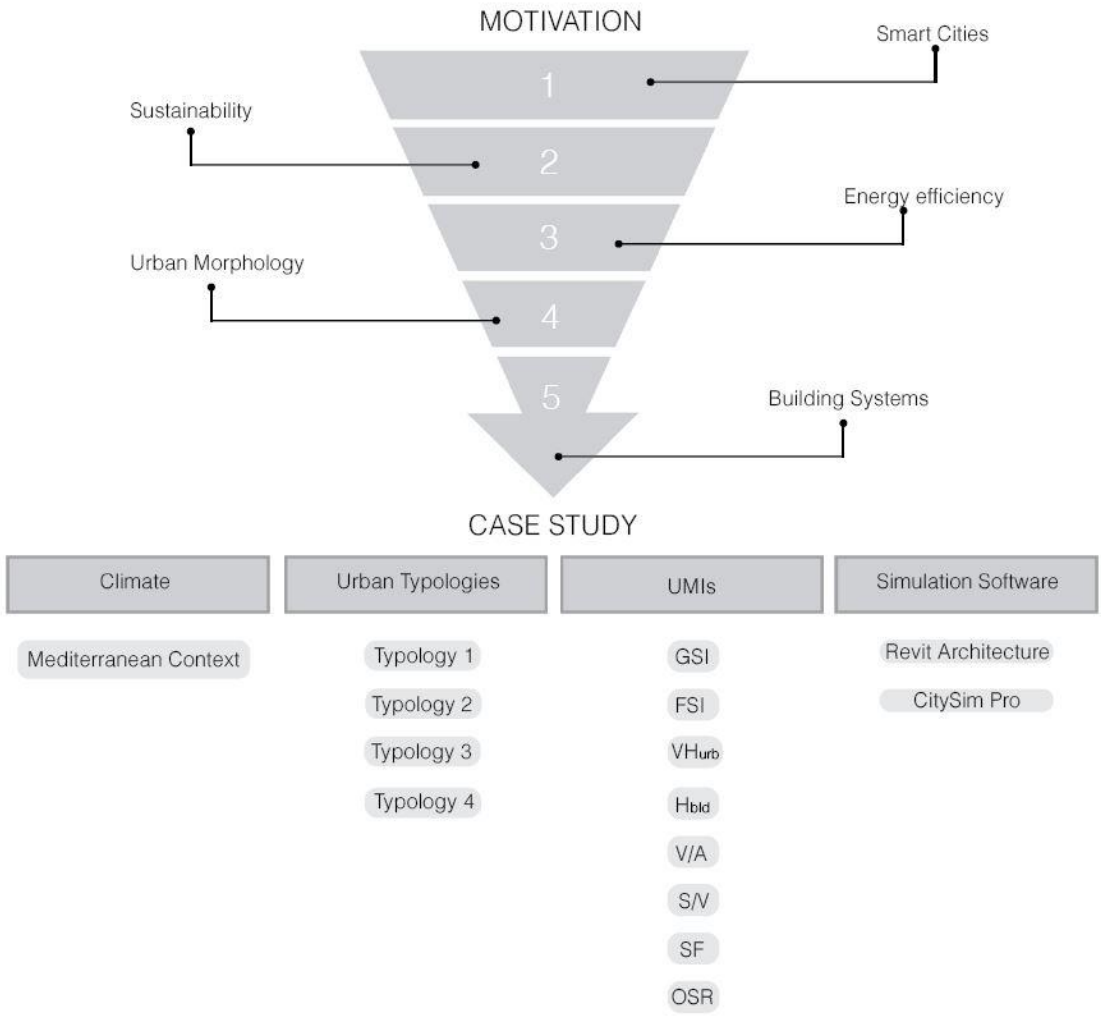

Figure 1. Motivation scheme

1.2 Problem statement

The capital of Albania, Tirana is undergoing a rapid development and urbanization process. New neighborhoods and buildings are shaping the city as we know it. With these contemporary constructions, innovative solutions are required, not merely for the building's physical components, but also the energy-costs related ones. Any metropolitan area that aspires to have a more sustainable approach and solve the problems of the future with competence, needs to answer the cost related questions with a certain responsibility to the citizens physical and economical comfort and adaptability to the recent technological advancements for its urban planning and infrastructure. To hit this target, an interference since the early stages of the design process is required. The preliminary, form-giving sketches of an architect often considered as an idyllic portrayal of his visions, are about more than meets the eye. In the case of an apartment building for example, they, often unintentionally, establish the long run expenses that an apartment will produce and that a family will pay. On a larger scale, the urban form significantly affects the total energy consumed by the inhabitants of the neighbourhood. Consequently, the morphology and its impact on energy efficiency is an issue that needs to be addressed as early as the design process. Such observations for the Mediterranean climate are few, and the need arises naturally to have a better perception of such problematics in order to make better decisions in the future.

1.3 Thesis objective

The objective of this investigation is to assess the importance of building morphology towards energy efficiency, at an urban and building level, and the evaluation of the effectiveness of preliminary design decisions that will unfold along the way for this project. More precisely this researches intent is to unfold:

1. What are some positive urban morphology examples for having an efficient energy performance for the Mediterranean context?

2. How does the courtyard affect the abovementioned performance in building scale and urban scale?
3. How is the energy performance affected if alterations of different metrics are made?

Our hypothesis is that blocks with courtyards will perform more efficiently than compact ones, and the courtyards dimension plays an important role regarding the energy efficiency.

CHAPTER 2

LITERATURE REVIEW

2.1 Introduction

The literature collected for this study leans mainly in the energy-efficiency domain. However, this topic is related to the concept of Smart Cities so inevitably a collection of such literary works is made as well. The topics included for enriching this research include the following: Sustainability, Urban and Building Morphology, Building Scale Energy, Urban Scale Energy, shown in ***Table 1*** below.

Table 1. Reviewed scientific literature

Contribution area	Authors	Description
Sustainability	Holden (2004)	Provided empirical and theoretical knowledge for discussing principles about sustainable urban development.
	Calvillo et al. (2016)	Reviewed energy-related work within the smart-city scope.
	Mauree et al. (2019)	Focused on environmental sustainability and shows how it has an economic impact.
	Okeil (2010)	Holistic approach for energy efficient building forms.
	Sharifi (2016)	Reviewed literature related to energy resilience.
	Bibri (2017)	Provides an extensive overview of the field of smart and sustainable cities.
Urban and building morphology	Rode et al. (2014)	Analyzed the effect of urban morphology on the heat-demand of buildings.
	Wong et al. (2011)	Estimated the building energy consumption with varying urban morphology conditions.
	Urquizo et al. (2017)	Explored the combination of four urban morphological characteristics in order to draw conclusions about their effect on energy-efficiency.
	Salvati et al. (2020)	Showed that the density of the urban texture affects significantly the urban climate and subsequently the annual energy demand.
	Ka¨mpf et al. (2010)	Minimized the urban shape volume and identified the cases which minimize the energy consumption for a given volume.
	Chatzipoulka et al.(2016)	Urban layout affects solar availability on ground and facades.
	Chatzipoulka (2018)	Geometric analysis of different urban forms, their solar access and statistical exploration of thee results.
	Javanroodi et al. (2018)	Investigated the impact of urban morphology on cooling load reduction and the potential of ventilation enhancement.
	Cheng et al. (2006)	Insights for planning solar cities by analyzing different generic models. Studied the urban form and its implication on urban climate to regenerate and change the use for meeting housing need.
	Futcher et al. (2013)	Reviewed studies on pedestrian level urban greening and geometry to improve thermal comfort in cities.
	Jamei et al. (2016)	Identified a set of urban morphology indicators that correlate with solar availability on facades.
	Morganti et al. (2017)	Explored the effect of geometrical forms of buildings on their use of energy. The effect of urban morphology on buildings energy performance in the Mediterranean climate.
	Steadman et al. (2013)	
	Salvati et al. (2015)	

Building scale energy	Lombard et al. (2007)	Analyzed the available information on energy consumption in buildings especially related to HVAC systems.
	Allegrini et al. (2012)	Used detailed building energy simulation to estimate the effect of adjacent buildings on space cooling and heat demand.
	Evins et al. (2015)	Identified following impacts on building energy use.
	Futcher et al. (2018)	Studied office buildings uses to identify the best urban design.
	Hui (2001)	Investigated low energy buildings
	Lauzet et al. (2019)	Reviewed different methods to take into account in building design simulations.
	Salvati et al. (2017)	Urban effect on building energy performance.
	Wu et al. (2017)	Presents a method for optimization of building energy systems.
	Allegrini et al. (2016)	Showed the impact of neighboring buildings on the space cooling demands.
Urban scale energy	Wang et al. (2017)	Constructed an urban energy performance evaluation system.
	Allen et al. (2020)	Used energy modeling to compare district thermal energy systems at the urban level.
	Allegrini et al. (2015)	Reviewed previous studies on district energy systems.
	Orehounig et al. (2014)	Revised the current energy systems and aims to rely on local renewable energy sources.
	Reinhart (2016)	Reviewed simulation methods for urban energy models.
	Keirstead et al. (2012)	Proposed a theoretical definition of urban energy system models by reviewing different papers.
	Chen et al. (2019)	Analyzed the spatial relation between energy demand and urban morphology indicators.
	Fichera et al. (2018)	Provided a combination of spatial and energy issues with optimization methods for urban energy strategies.
	Frayssinet et al. (2017)	Gave an overview of city energy simulation models.
	Perera et al. (2021)	Proposed a methodology for urban energy systems optimization.
	Sola et al. (2018)	Reviews existing tools for urban scale energy models.
	Tardioli et al. (2020)	Presented a calibration method for groups of buildings.

2.2 Related theoretical background

2.2.1 Urban and building morphology

The impact of shape in the energy performance is of a great influence. It has been previously examined by many authors and the results provided have shown that it is one of the key factors to a buildings or urban areas energy performance. A relation of form and the preliminary stage of design is intended, as on of the aims of this study is to find the most efficient ways of shape-giving in the first phases, and in relation with the final phase; its impact on energy efficiency of the building itself.

[2] analyzed the effect of urban morphology on the heat-demand of buildings. The theoretical conclusions suggested that the urban-morphology generated, heat-energy performances are important. Having kept all variables fixed except for the urban form showed fluctuactions in energy demand up to a factor of 6.

[4] estimated the buildings energy consumption with varying urban morphology conditions. It was concluded that urban morphology plays an important role in deciding the alterations of the temperature at the micro level. Also, it can have a cooling load reduction, when altering the urban morphology, from 5 to 10%.

The combination of four urban morphological characteristics was explored in order to draw conclusions about their effect on energy-efficiency. It was shown that building layout, compactness and orientation design are great influencers of the energy consumption [5].

The density of the urban texture affects significantly the urban climate and subsequently the annual energy demand, showed (Salvati, 2020). The study also showed that the site coverage ratio and the average building height are credible factors for a building's energy consumption in various urban textures. Also, on a previous study [40] the effect of urban morphology on buildings energy performance in the Mediterranean climate was presented.

An interesting method was used to minimize the energy consumption for a given volume by [8]. He minimized the urban shape volume and identified the factors that lower the energy demand.

[15] explained how urban layout affects solar availability on ground and facades by analyzing 24 urban forms in London. On a later study by the same author, it was shown a geometric analysis of different urban forms, their solar access and statistical exploration of the results (Chatzipoulka, 2018).

An investigation by [19] showing the impact of urban morphology on cooling load reduction and the potential of ventilation enhancement in the city of Tehran was made. There were shown 16 best scenarios out of 1600 cases where urban density, urban building form, urban pattern was considered. It was concluded that urban morphology has a significant role on the energy consumption of a building by lowering the cooling load by 10% and rise the ventilation potential by 15%.

[21] provided insights for planning solar cities by analyzing different generic models. It concluded that built form plays an important role in deciding the façade daylight availability.

A ‘’form first’’ approach was suggested by [25] so that each building should be designed according to its particular function. After having studied the urban form and its implication on urban climate to regenerate and change the use for meeting housing need it was concluded that offices that operate during the day need to get rid of internal heat and narrow streets provide best way of shading in such case.

Another study whose focus lies more at the preliminary stages of planning, reviewed previous work on pedestrian level urban greening and geometry to improve thermal comfort in cities. The later was classified by aspect ratio, street orientation, sky view factor and local neighborhood scale [28].

[31] identified a set of urban morphology indicators that correlate with solar availability on facades in the Mediterranean climate. GSI, $VH_{urb,}$ SF are the most advisable indicators for solar analysis in a Mediterranean urban context.

The effects of geometrical forms and buildings on their use of energy were studied by [38]. It was shown that plan depth above 14m has an effect on electricity.

2.2.2 Building scale energy

An overview of previous work done in building scale energy performance is necessary as they provide valuable information to be taken as example in this study. Closely related with the ‘’Morphology’’ section reviewed above, this part gives a great deal of attention in neighbouring buildings influence towards the buildings operating systems, how the affect the overall energy consumption and how to optimize them.

Such is the case of [7]. This study analyzed the available information on energy consumption in buildings especially related to HVAC systems. It showed that energy consumption in building scale accounts for 20-40% of the overall use.

[10] used detailed building energy simulation to estimate the effect of adjacent buildings on space cooling and heat demand while on another study (Allegrini, 2016) showed the impact of neighboring buildings on the space cooling demand.

[22] identified suceeding impacts on building energy use. Building area accounted for the factor with the most impact in overall heating loads. When building area was normalized the most effecting factor was fabric properties.

[26] studied office buildings uses to identify the best urban design. The results show that the yearly energy demand is dictated by the cooling load that can be lowered through street design that provides shading.

[21] investigated low energy buildings. The study found that highly populated cities can have their positive and negative effect on the overall energy consumption.

A review of different methods that need to be taken into account in building design simulation wsa made [29]. It concluded that building energy modelling is very responsive to the climate.

By analyzing the urban effect on building energy performance [35] confirmed that compact urban textures with a site coverage ratio higher than 0.5 are a huge contributor in reducing energy demand in the Mediterranean climate.

[41] presents a method for optimization of building energy systems and provides instructions for building owners presenting several transformation options.

2.2.3 Urban scale energy

After having reviewed a number of studies on building scale, the focus comes more towards the urban scale energy systems where this researches aim is to find the factors that contribute on its energy consumption. Different methods are used for the evaluation of this scale and larger districts are reviewed here.

[1] constructed an urban energy performance evaluation system for the city of Beijing and selected different indicators according to proper theoretical contributions of the past such as: capital, labor, population, climate etc.

Another author [3] used energy modeling to compare district thermal energy systems at the urban level. The study concluded that hydronic HVAC systems score 49% lower than air-based ones but the high infrastructure costs block the adoption of such systems.

[11] reviewed previous studies on district energy systems and thus helping other researchers in finding reliable information for selecting suitable models and related tools to tackle different problems at an urban scale.

[13] revised the current energy systems and aims to rely on local renewable energy sources. For the case study selected which is a village in Switzerland, an energy efficiency of 83% is achieved by installing PV panels and other contributors.

[43] reviewed simulation methods for urban energy models and suggested that building inhabitants should be considered individually rather than identical group operating the same way each day.

[18] proposed a theoretical definition of urban energy system models by reviewing different papers and came up with the conclusion that urban energy system modelling is the best tool to estimate better designs energywise.

An analysis of the spatial relation between energy demand and urban morphology indicators was made by [20]. The results showed that the most necessary urban morphology indicators in explaining building energy consumption are: height, plot area, normalized difference vegetation index.

A combination of spatial and energy issues with optimization methods for urban energy strategies is provided by [23]. This study allows to indentify the buildings that are capable to activate the greater number of connections.

2.3 Previous related studies on (UMIs)

Table 2. Data available in scientific literature for UMIs

Authors	Year	UMI	Software	Case study model
Rode	2014	Building density Building height Surface coverage of buildings Surface to volume ratio Open space ratio	GIS ESRI-ArcInfo	Dominant residential building typologies Idealised Samples
Wong	2011	Green plot ratio (GnPR) Sky view factor (SVF) Building density Wall surface area Pavement area Albedo	TAS STEVE	PIXEL building
Urquizo	2017	Shape and size Building massing Plot ratio Layout and orientation	NOT SPECIFIED	Lower 3-4 storey and smaller flats, detached and linked Low terraces, 2 storeys with large T-rear extensions Low terraces, small Standard size semis Low terraces, small Smaller detached houses Non-residential building Lower 3-4 storey and smaller flats, detached and linked
Salvati	2020	Site coverage ratio Average building height Façade to site ratio Ratio of building length to street width	NOT SPECIFIED	Simplified urban model
Futcher	2018	Building height Street width	Virtual Environment (VE)	Office buildings
Morganti	2017	Gross space index Floor space index Façade to site ratio Average building height Volume area ratio Building aspect ratio Sky factor of building facades	HELIODON 2	Normalize models

To better understand the various morphology indicators and the way they are incorporated into a research framework, the following papers are reviewed in depth, as shown in ***Table 2***.

[2] analyzes different types of urban form in Paris, London, Berlin, Istanbul. The analysis footprint is made within a 500x500m square and focuses on heat-energy efficiencies created by the spatial configuration of cities. Furthermore, this paper tries

to fill a void in literature concerning the effect of urban morphology on the heat-demand of buildings. The features analysed for the urban morphology are: building density, building height, surface coverage of buildings, surface to volume ratio, open space ratio. The results show that with regards to building typology compact urban blocks consistently perform best, detached housing worst. Considering density, minimum building density appears to guarantee the maximum heat-energy demand. Average building height, was found to be a strong contributor to heat-energy demand with the later decreasing with increasing height.

[4] compared how the air temperature variation of urban condition can affect the building energy consumption in tropical climate of Singapore. In order to achieve this goal, a series of numerical calculation and building simulation are utilized. A total of 32 cases, considering different urban morphologies, are identified and evaluated to give better a understanding on the implication of urban forms, with the reference to the effect of varying density, height and greenery density. The results show that GnPR, which related to the present of greenery, have the most significant impact on the energy consumption by reducing the temperature by up to 2 C. The results also strongly indicate an energy saving of 4.5% if the urban elements are addressed effectively. The methods used are by alternating GnPR, Height, Density, Height and Density, GnPR and Height, GnPR and Density, GnPR Height and Density.

[5] identifies differences and similarities between three districts in the United Kingdom (UK) and draws conclusions which prove to be useful to interpret other districts in the city and provide general rules for energy efficiency measures and distributed supply interventions in Newcastle upon Tyne, UK, and potentially beyond. This methodology explores the potential application of the close relation between four urban morphological characteristics and the spatial aggregated building energy end-use in the roll-out strategy of interventions.

The morphology is characterized by the shape and size, the building massing and the plot ratio (the ratio of the building floor area to the land area in a given territory), the layout and design of the neighbourhood.

[6] contributes to fill the gap by describing a chain strategy to model urban boundary conditions suitable for annual simulations using dynamic thermal simulation tools. The methodology brings together existing physical and empirical climate models and it is applied to 10 case studies in Rome (Italy) and Antofagasta (Chile). The results show that urban climate varies significantly across a city depending on the density of urban texture and its impact on the annual energy demand depends on the region's climate. The urban shadows are crucial in cooling-dominated climates (Antofagasta) while the urban heat island intensity is more important in temperate climates (Rome). The results of the case studies also showed that two morphology parameters – the site coverage ratio and the average building height – can be good predictors of the building energy performance in different urban textures. This could be applied to map the energy performance variability across a city and to foster targeted refurbishment strategies depending on the characteristics of the urban texture.

[26] examines the energy demand of a city street in London, UK, which is comprised of typical office buildings with internal energy gains associated with daytime occupancy. Simulations are performed for office buildings placed in urban canyons that are defined by the ratio of building height (H) to street width (W). The results show the annual energy demand is dominated by the cooling load, which can be significantly reduced through street design that provides shading by increasing H/W. However, the 'best' street design for modern office buildings may be incompatible with that for residences or, for that matter, outdoor climates.

[31] identifies a set of urban morphology indicators that show the most accurate relations with the solar availability on façades in the Mediterranean context. The analysis that relates to 14 urban textures of Rome and Barcelona comprises seven UMIs: gross space index, floor space index, façade-to-site ratio, average building height, volume-area ratio, building aspect ratio and sky factor of building façades.

Results suggest that gross space index, façade-to-site ratio and sky factor show very good correlation with SIy ($R2 = 0,91$) and could be used to develop a comparative assessment tool of solar performance at fabric scale. This could ease the work of urban planners and architects in the early stage of design, reducing both data and time normally needed to perform solar analyses at urban scale.

2.4 Aim and originality of the study

The reviewed literature shows the effect of urban morphology on the energy demand of individual residential buildings and urban districts as a whole, and states the need for more precise results of energy performance, by taking into account a number of other factors. Having depicted a few potential areas for development, this study builds upon providing authentic contributions by addressing the following knowledge gaps:

- No other studies make use of modelling softwares such as Revit and detailed urban simulation softwares like CitySim Pro used here. Also, to gain more perspective on the site's solar availability, Insight Plugin for Revit is used to conduct a solar study. Other authors mentioned here like (Rode 2014) use GIS and ESRI-ArcInfo tools, or, [4] uses TAS STEVE. [26] and [31] use Virtual Environment and HELIODON 2 respectively.
- 8 different UMIs are analyzed here: GSI, FSI, $VH_{urb,}$ $H_{bld,}$ V/A, V/A, SF, OSR. No previous studies have analyzed all these parameters except [31] who covers 7 of them and correlates them with the solar availability on facades. The difference with this study is that all indicators are used to show their correspondence concerning energy demand within the builings and the typologies chosen. Other authors mentioned in the literature review that have calculated UMIs are: [2], [4], [5], [6], [26].
- Only two authors [31] with Rome and Barcelona, and [6] with Rome and Antofagasta, have fully conducted the research within the Mediterranean climate, while [2] includes Istanbul as one of the four cities mentioned in that study, raising the need for more investigations in this region. This study takes into consideration the Mediterranean context, by being carried on in the city of Tirana. Furthermore, it shows results for a whole year-round observation of the chosen typologies. Others range to places like: Singapore [4], UK [7], London [26].

- No previous simulation-assisted inquiries have been examined on the impact of different urban typologies on the energy performance, at this depth.

Therefore, an original methodological framework consisting of advanced urban simulation software like CitySim Pro and statistical analysis approach to interpret the results is proposed. The software uses detailed input variables (district properties, building properties, composites and insulation, opening properties, visible surface properties, grounds properties and occupancy) described more in detail in section 3.5.3, Figure 22, and extracts many outputs from which heating demand, cooling demand and surface temperatures are analyzed.

CHAPTER 3

METHODOLOGY

3.1 Case Study Selection Criteria

The selection of this case study was based upon it being a significant intervention in the city, by covering a large area territorially and making for an important district of the capital's canvas, its impact will be felt all over. Socially, it will be a focal point, where each age will have dedicated areas of recreation and interaction, and economically, will affect the entire region with many attractions to be used not only by locals but from tourists as well.

Therefore, it is imperative to stress the importance of doing thorough research of this project, as it will affect the end user directly. How cost-efficient will it be to live there and how well-designed is the whole district concerning the energy-efficiency, are two very important questions that need a precise answer for the capitals new residential, commercial and cultural centre of the future.

3.2 Case Study Description

3.2.1 Overview

The ''New Boulevard'' project designed by Grimshaw architecture studio, will cover almost one-fifth of the capitals surface area and will change its urban layout largely. Covering 15 sq km and expanding upon the end of the citys main boulevard by adding another 3 km in length, it makes for an influential segment in the city that will join the two waterways that cross the city in its entire length. The general layout is predominated by a central axis which is the continuity of an existing artery. It starts with a wide public square in the south that connects the existing boulevard with the new one and elongates towards the north. It expands along the way, to three more

public squares that act as urban rooms. On the northern point of the site, it culminates with Tirana River, that flows down to the outskirts of the city. The site is characterized by blocks with courtyards that vary in shape and size. There are 4 selected zones with different urban fabrics that are chosen for this study: *Typology 1* with Organic Inner Streets, as shown in ***Figure 2***, *Typology 2* with Big Regular Shaped Courtyards and the main road included, as shown in ***Figure 3***, *Typology 3* with a big urban courtyard enclosed by building blocks, as shown in ***Figure 4***, *Typology 4* with Smaller Courtyards as shown in ***Figure 5.*** For each of them these 8 urban morphological indicators are measured: Groos Space Index, Floor Space Index, Façade-to-Site-Ratio, Average Building Height, Volume-Area Ratio, Building Aspect Ratio, Sky Factor of Building Facades, Open Space Ratio, as shown in ***Figure 6***.They are weighed against each-other in order to have a clear view of the differences and similarities between them in a statistical manner.

A solar study is conducted using Insight Plugin for Revit and the results, shown in ***Figure 7***, indicate how the overall envelope of the site is impacted from natural sunlight and shadows.

Once the analysis points out the the final results of the observation, a final stage is conducted where correlations between UMIs and total energy consumption is made in order to find which indicator has the most impact.

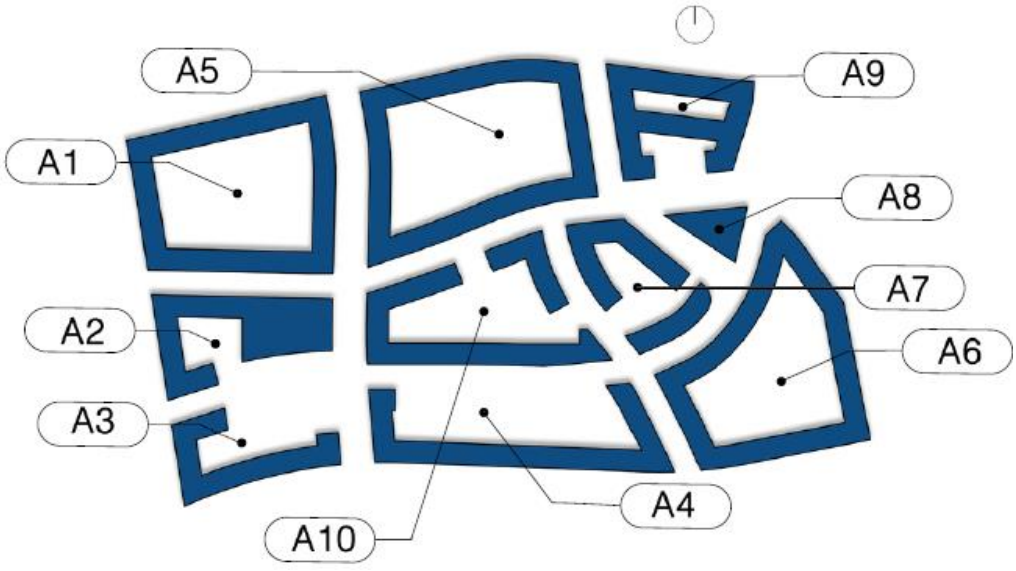

Figure 2. Typology 1 building keys.

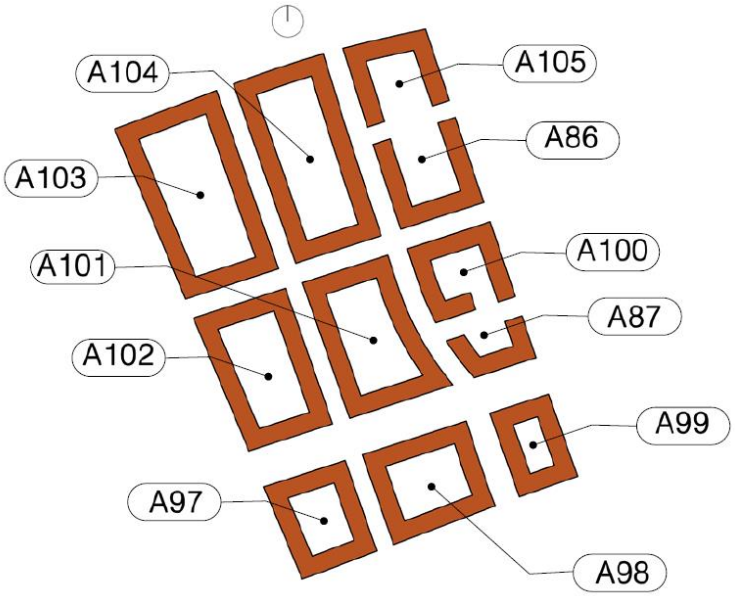

Figure 3. Typology 2 building keys.

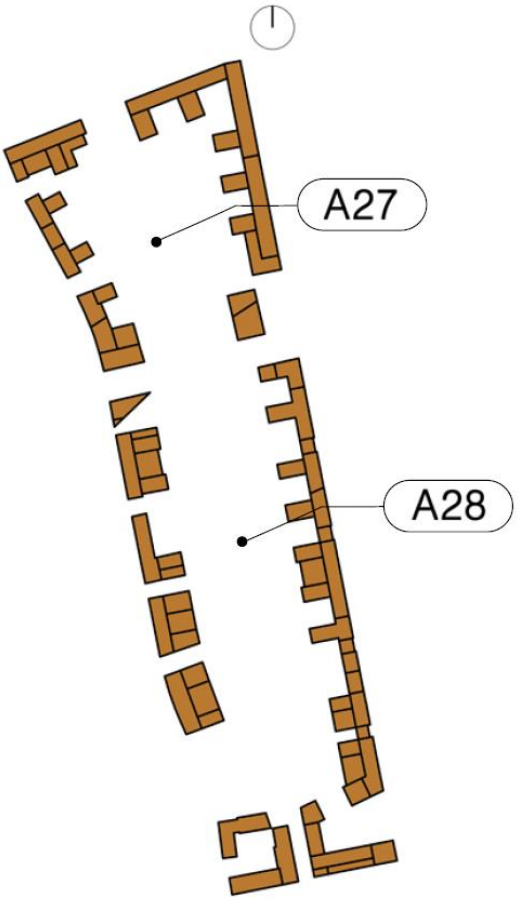

Figure 4. Typology 3 building keys.

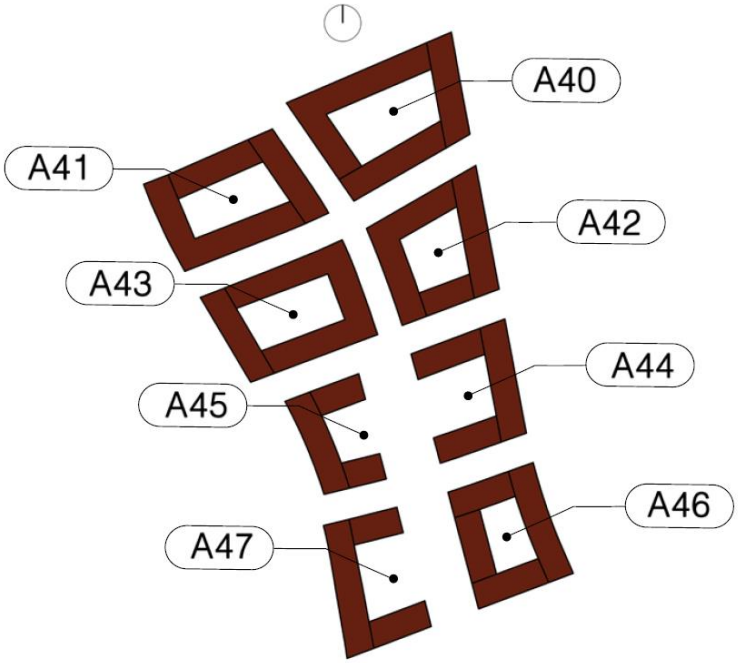

Figure 5. Typology 4 building keys.

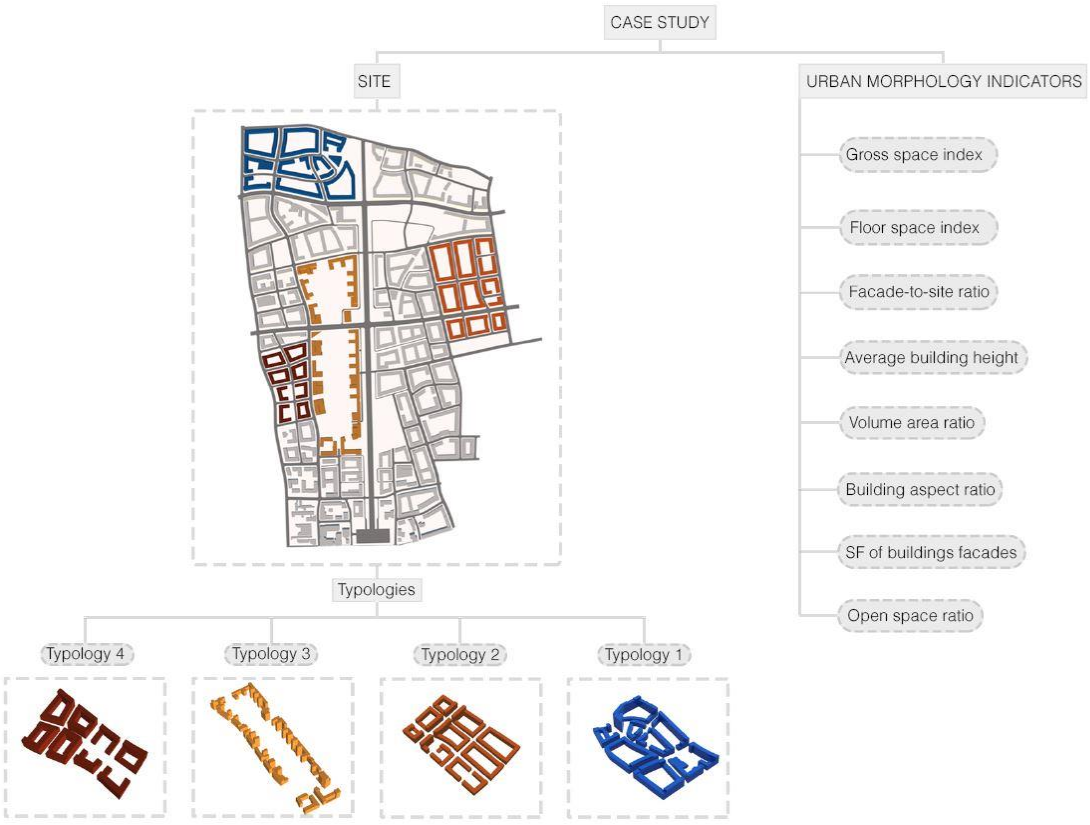

Figure 6. Site layout, zones selected and UMIs calculated for each typology.

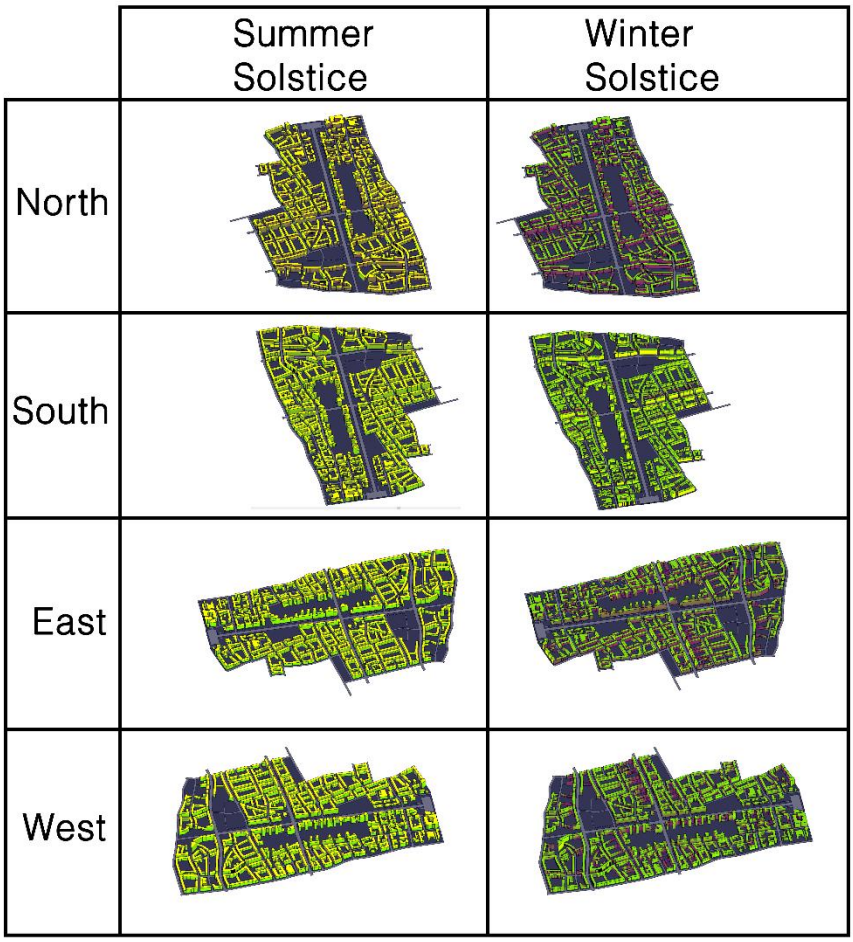

Figure 7. Summer Solstice and Winter Solstice Solar Study

3.2.2 Typology 1

The first urban morphology is located in the northern part of the site plan and contains 10 building blocks organized in an organic manner with 4 of them being closed-courtyard blocks and the rest semi-open and open ones. Its northern and western building blocks stand on the edges of the site as shown in ***Figure 8***. The average floor number is 8.36, with an average building area of 3966.7 msq and average building plot area of 12240.5 msq.

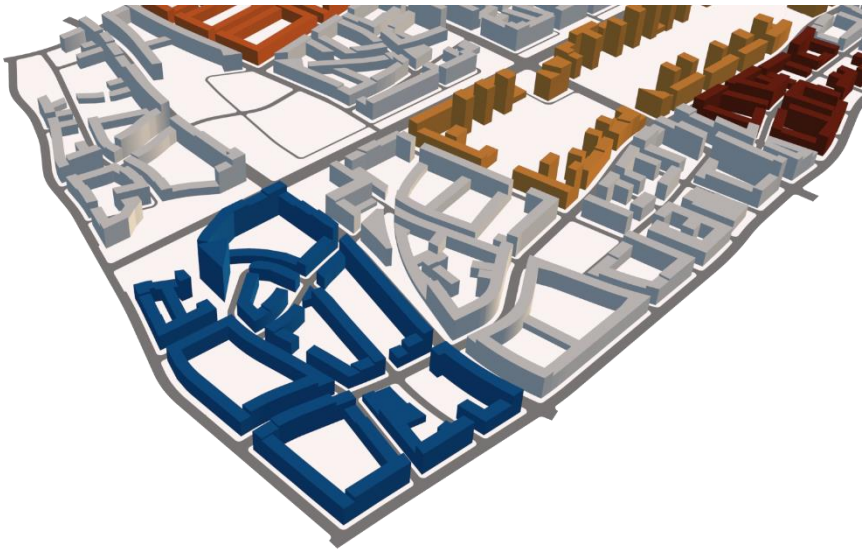

Figure 8. Typology 1 layout.

3.2.3 Typology 2

The second urban morphology, shown in ***Figure 9*** is located in the eastern part of the site and has 11 blocks defining it. Its eastern building blocks are positioned on the edge of the site. It consists of big regularly shaped courtyards with 2 of them not being closed-courtyard blocks. It has the most regularly shaped courtyards and building forms of all four chosen typologies. The average floor number is 8.32, average building area 3414.36 msq and average plot area of 9421.45 msq.

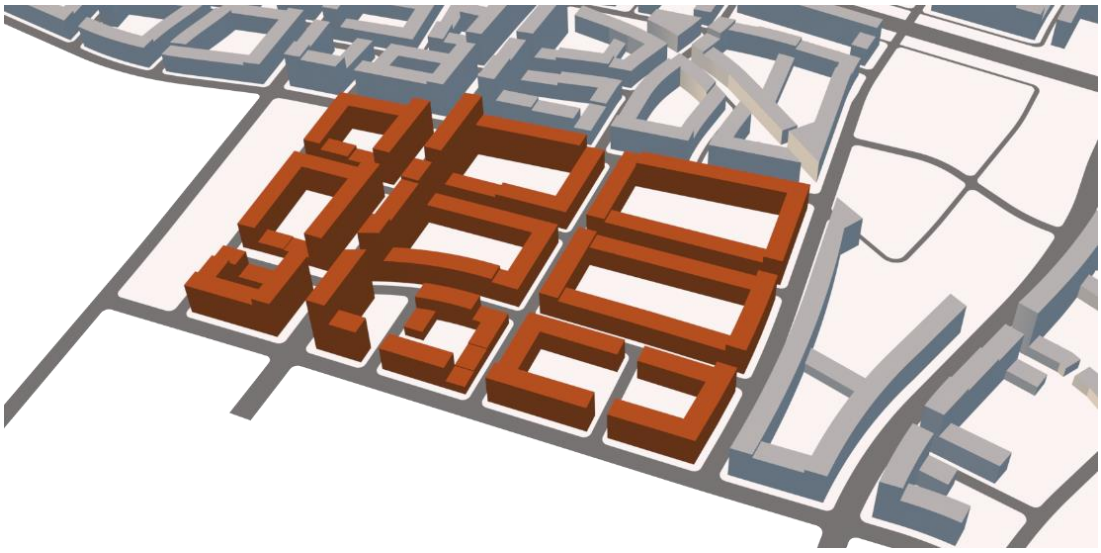

Figure 9. Typology 2 layout.

3.2.4 Typology 3

The third urban morphology is located near the center of the site, with its eastern buildings being the front row building blocks that face the New Boulevard, as shown in ***Figure 10.*** It has a large open space surrounded by only 2 long building blocks attached to each-other, defining a larger area of the site. The average floor number here is 10.26, with an average building area of 20077.5 msq and average plot area of 77617.5 msq.

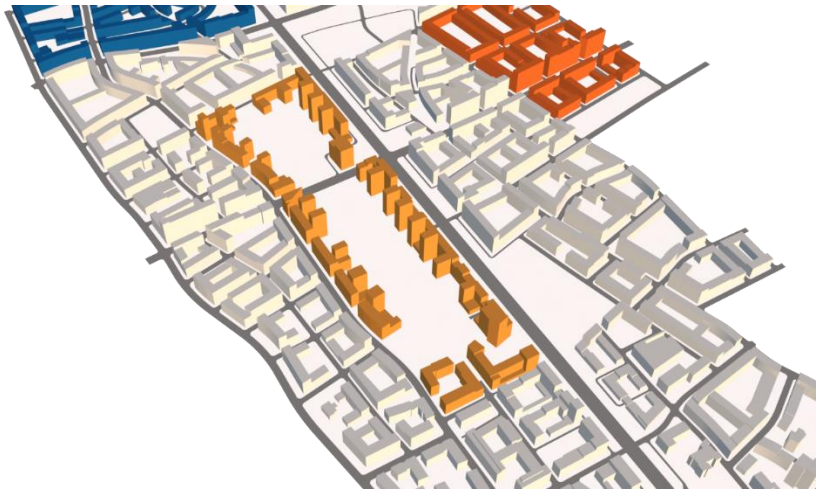

Figure 10. Typology 3 layout.

3.2.5 Typology 4

The last morphology selected for this site is located on the western section of the master plan. Its western building blocks face the edge of the site and its eastern blocks stand next to the western part of the third morphology. This zone is characterized by small courtyard blocks, as shown in ***Figure 11***. It has an average floor number of 7.44, average building area of 19112 msq and average plot area of 51254 msq.

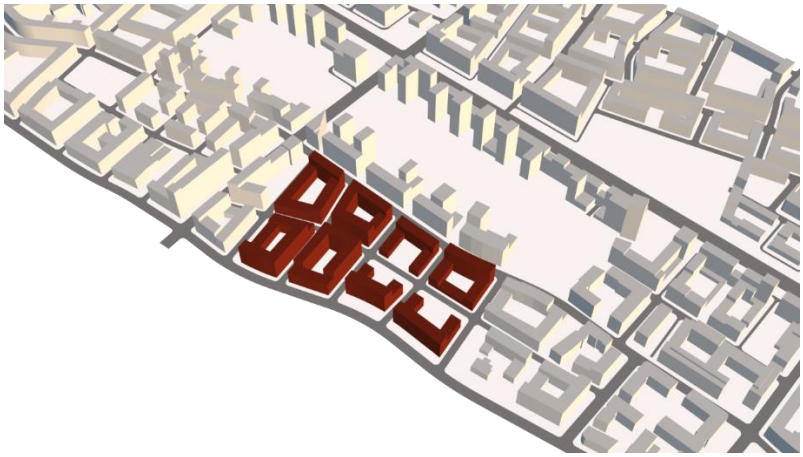

Figure 11. Typology 4 layout.

3.3 Urban Morphology Indicators

3.3.1 Description

Gross Space Index (GSI) represents the ratio of the built-up area to the urban site area ***Figure 12***. *Floor Space Index* (FSI) is the ratio of the total floor area to the urban site area ***Figure 13***. GSI expresses the compactness of buildings in urban textures and FSI their intensity. These two are of the most typical density indicators (Morganti 2017).

Façade-to-Site Ratio (VH_{urb}) is the ratio of the building's façade area to the urban site area ***Figure 14***. It is an indication of vertical density of a building thus it is proportional to the number of vertical planes of the block in a given urban context.

Average Building Height (H_{bld}) expresses the ratio of the buildings volume to the built-up area ***Figure 15***.

Volume-Area Ratio (V/A) shows the ratio of the buildings volume to the urban site area ***Figure 16***. It expresses building density in a given urban area but in volume units.

Building Aspect Ratio (S/V) is an index needed at building scale energy analysis rather than urban scale and is determined as the ratio of the building's envelope to the buildings volume ***Figure 17***. It is related to the compactness of shape.

Sky Factor of Buildings Facades (SF) is the mean value of the ratio of the solid angle of visible sky from each point of the façade to the sky vault ***Figure 18.*** This index is relatable for energy analysis in an ''urban canyon'' context, such as solar access, daylight availability and urban heat island. It is not a morphological indicator but has been included for this study because it gives information on the position and morphology of surrounding buildings which determine obstructions to direct and indirect solar irradiation.

Open Space Ratio (OSR) is the amount of open space in a residential zoning lot ***Figure 19.***

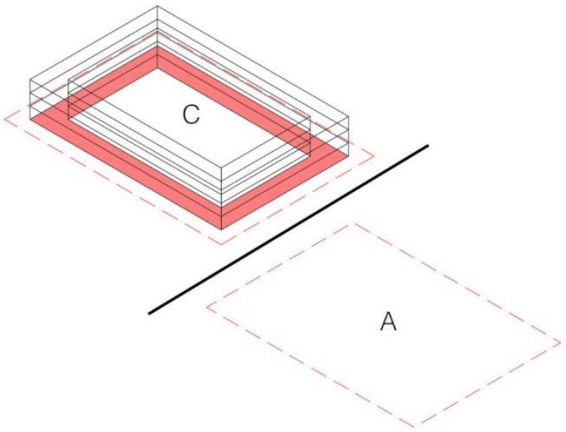

$$GSI = \frac{\sum_{i}^{n} = 1C_i}{A}$$

Figure 12. Gross Space Index (GSI).

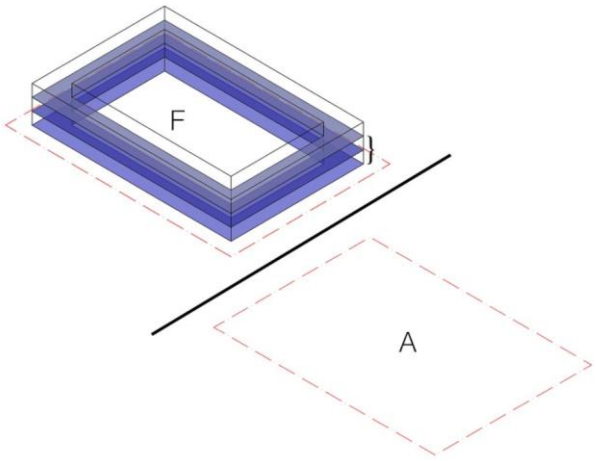

$$FSI = \frac{\sum_i^n = 1F_i}{A}$$

Figure 13. Floor Space Index (FSI).

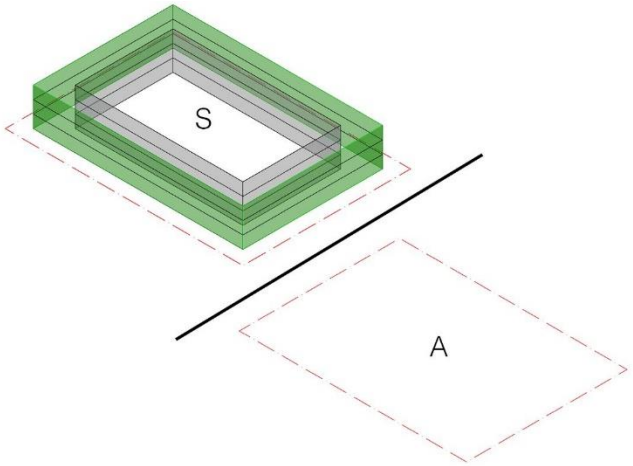

$$VH_{urb} = \frac{\sum_i^n = 1S_i}{A}$$

Figure 14. Façade-to-Site Ratio (VH_{urb}).

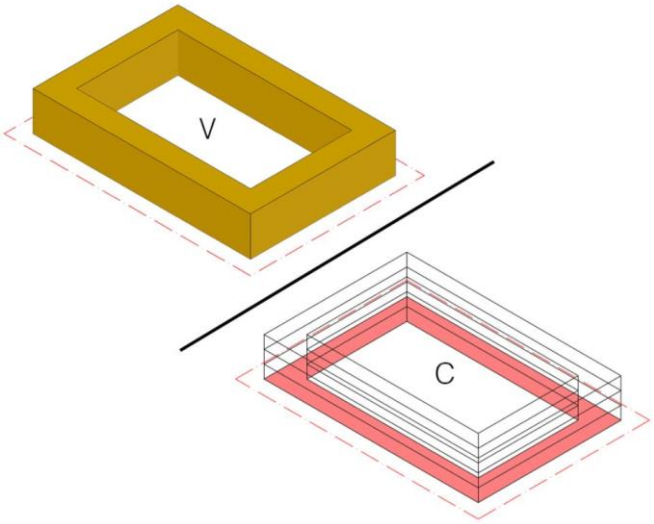

$$H_{bld} = \sum_{i=1}^{n} \frac{V_i}{C_i}$$

Figure 15. Average Building Height (H_{bld}).

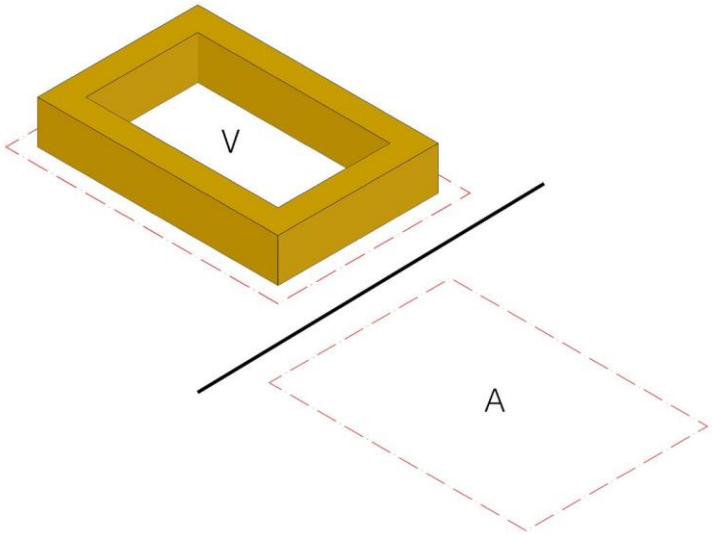

$$V/_A = \frac{\sum_i^n = 1V_i}{A}$$

Figure 16. Volume-Area Ratio (V/A).

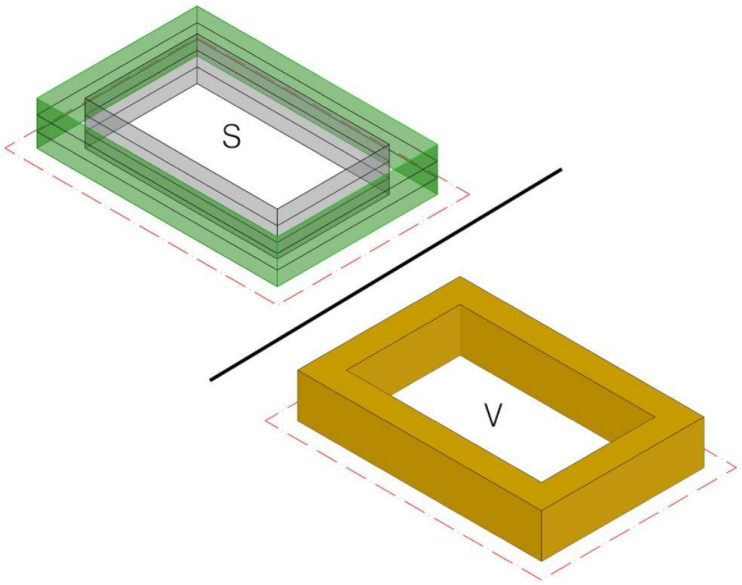

$$S/V = \sum_{i=1}^{n} \frac{S_i}{V_i}$$

Figure 17. Building Aspect Ratio (S/V).

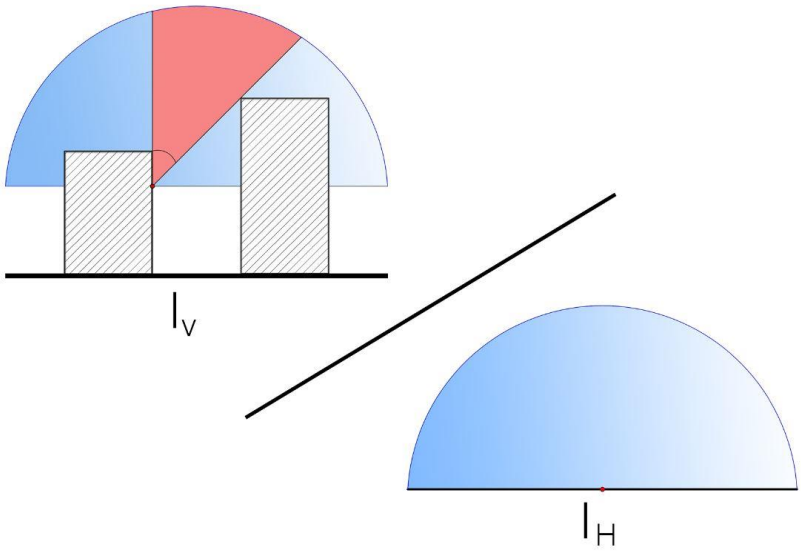

$$SF = \frac{l_V}{l_H}$$

Figure 18. Sky Factor of Buildings Facades (SF).

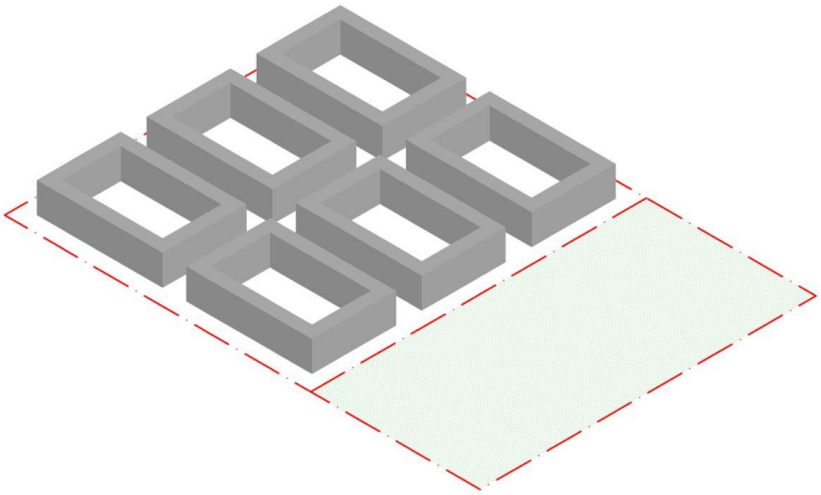

$$OSR = \frac{P - A}{P}$$

Figure 19. Open Space Ratio (OSR).

3.3.2 Typology 1 UMIs

For the first typology, all 8 UMIs have been measured and for each of the 10 building blocks, in this area, their average values have been calculated for each indicator as shown from ***Figure 20*** to ***Figure 27***. The results show that the main density indicators *GSI* and *FSI* have an average value of 0.33 and 2.71 as shown in ***Figure 20*** and ***Figure 21*** respectively. Building *A2* reaches the highest value while building *A3* the lowest one. VH_{urb} average value is 1.75 as shown in ***Figure 22,*** with building *A8* reaching the highest value and building *A5* the lowest one. H_{bld} averages to 25.8 with building *A8* having the greatest number of floors and building *A2* the least, as shown in ***Figure 23***. *V/A* ratio mean value is 8.33, as shown in ***Figure 24***, with building *A8* having the highest value and building *A2* the lowest one. *Building Aspect Ratio* value averages to 0.21 with building *A2* having the highest value and building *A8* the lowest one, as shown in ***Figure 25***. *SF*, shown in ***Figure 26***, averages to 0.34 with building *A8* having the highest value and building *A7* the lowest. *Open Space Ratio* mean value is 0.67, as shown in ***Figure 27***, with both buildings *A3* and *A4* having the same value and building *A2* having the lowest one.

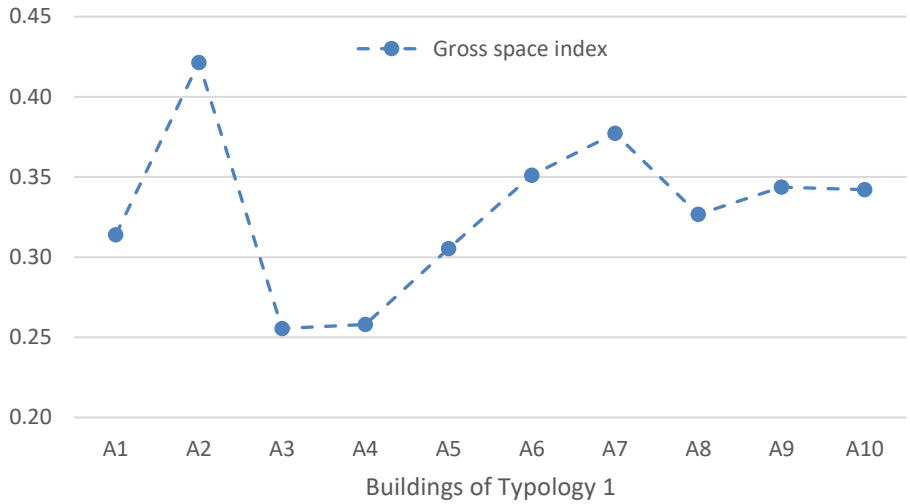

Figure 20. Gross Space Index (GSI).

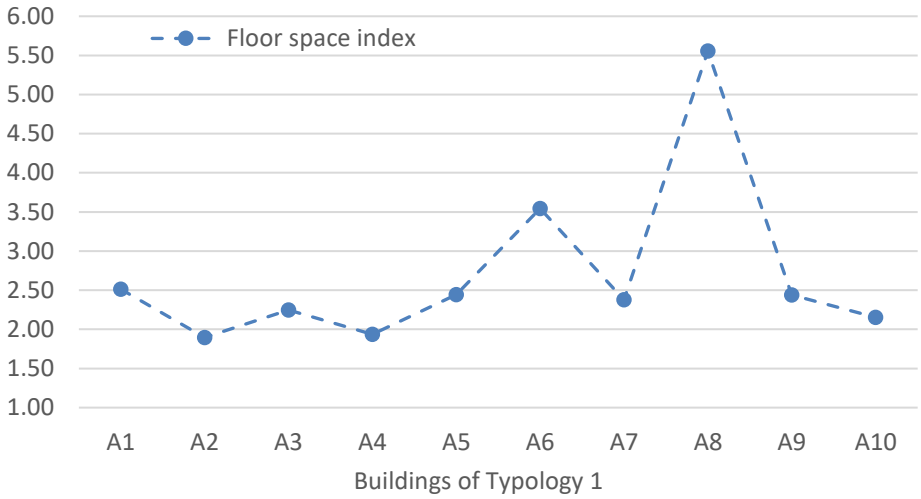

Figure 21. Floor Space Index (FSI).

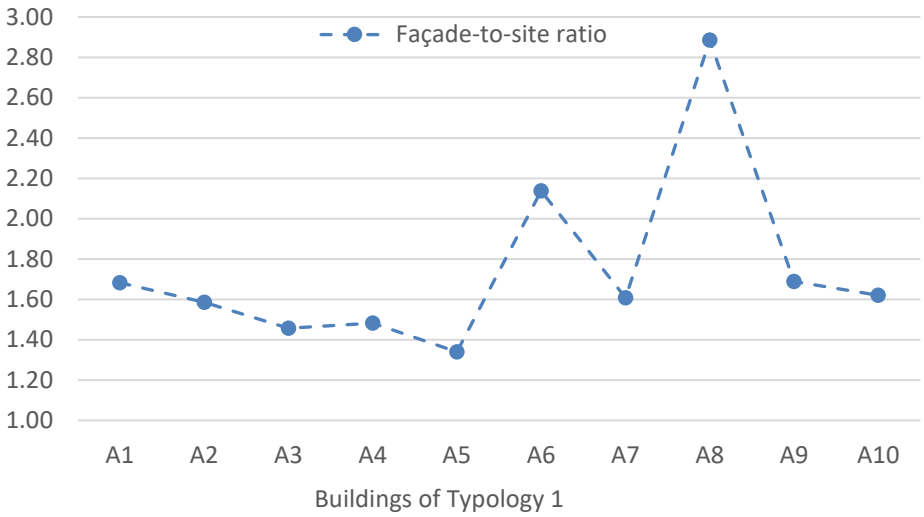

Figure 22. Façade-to-site ratio (VH_{urb}).

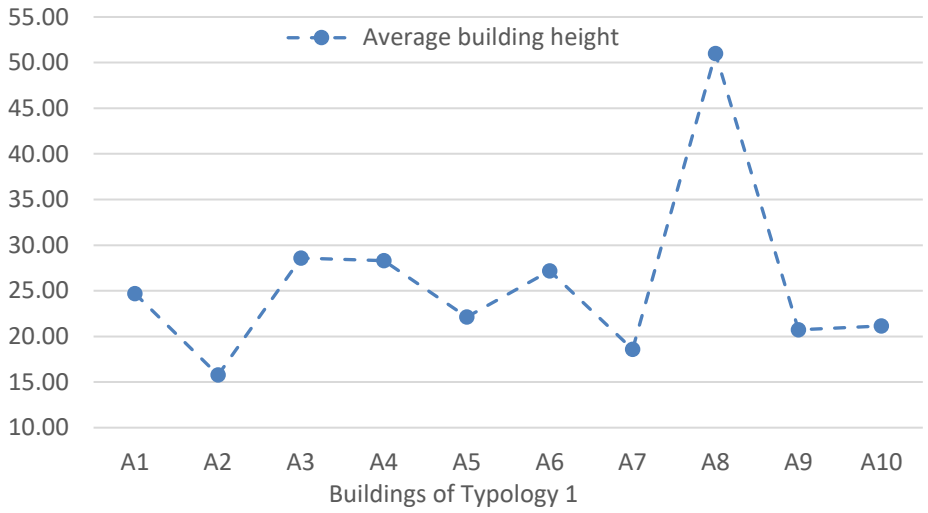

Figure 23. Average building height (H_{bld}).

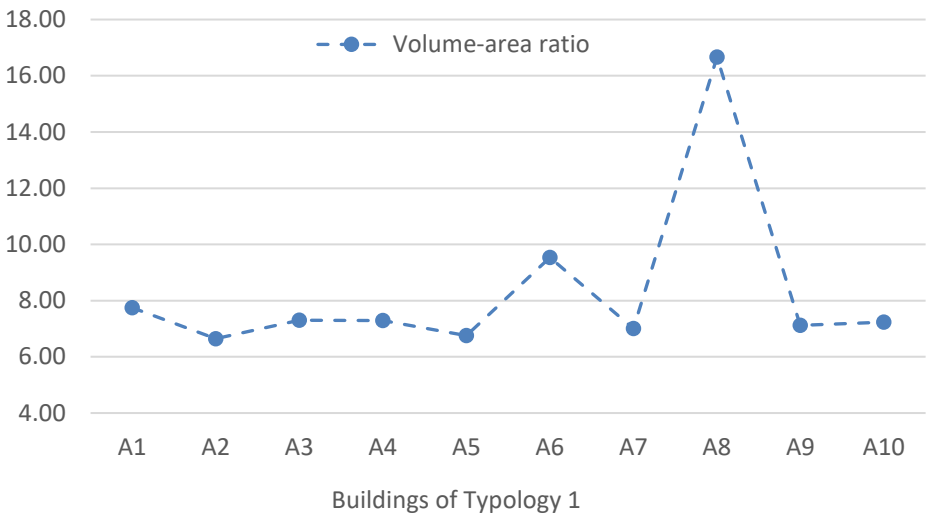

Figure 24. Volume-area ratio (V/A).

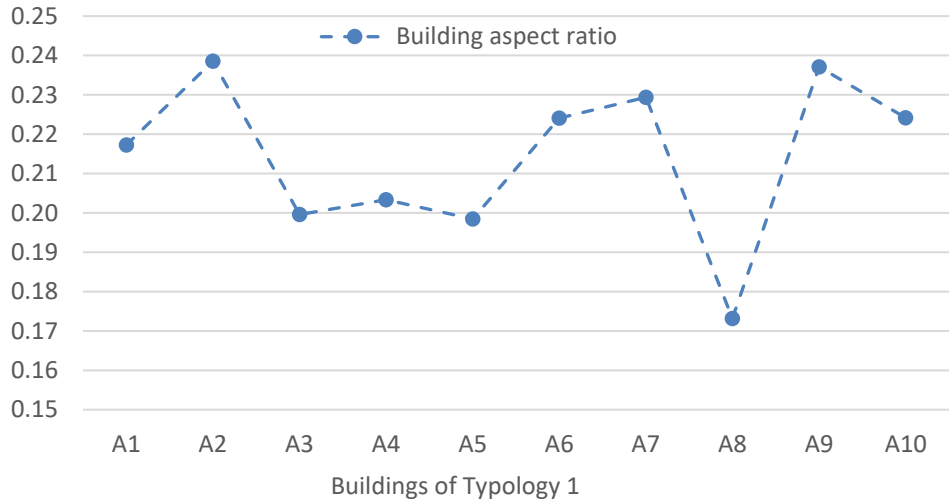

Figure 25. Building aspect ratio

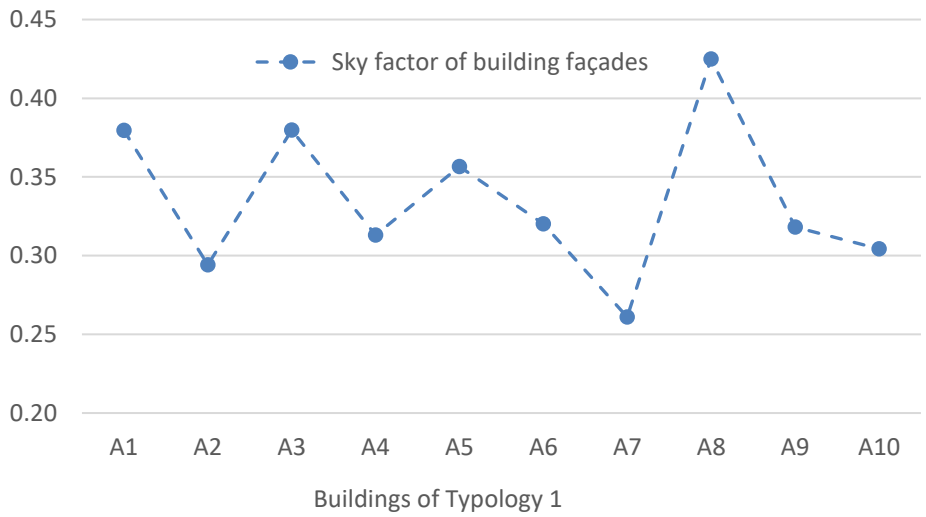

Figure 26. Sky factor of building façades (SF).

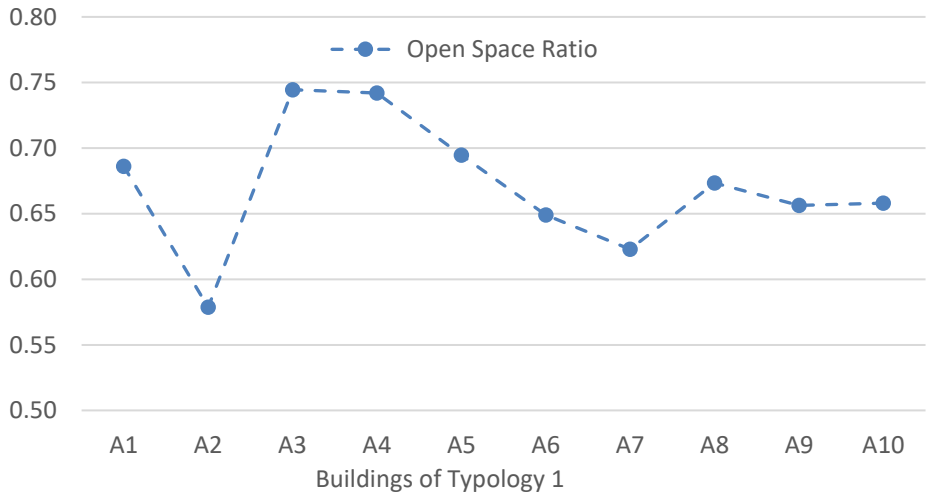

Figure 27. Open Space Ratio (OSR).

3.3.3 Typology 2 UMIs

The second typology contains 11 regularly shaped blocks and ***Figure 28*** to ***Figure 35*** displays the mean values of each UMI in the following order: *GSI* has a mean value of 0.36, as shown in ***Figure 28***, with building *A99* having the highest value and building *A87* the lowest. *FSI* averages to a value of 3.00, as shown in ***Figure 29***,

with building *A99* having the highest value and building *A100* the lowest. VH_{urb} has an average value of 2.09, with building *A99* having the highest value and building *A100* the lowest one followed closely by buildings *A103*, *A104*, *A105*, as shown in ***Figure 30***. H_{bld}, as shown in ***Figure 31***, reaches an average value of 24.97, with building *A99* being the tallest and building *A100* the shortest. *V/A* ratio has an average value of 9.00, as shown in ***Figure 32***, with building *A99* having the highest value and building *A100* the lowest. *Building Aspect Ratio* averages to 0.23, as shown in ***Figure 33.*** Building *A98* has the highest value closely followed by *A97* and *A100*, and the remaining ones have similarly lower values. SF has a mean value of 0.31, as shown in ***Figure 34***, where building *A86* has the highest value and *A100* and *A102* both have the lowest ones. *Open Space Ratio* averages to 0.64, where building *A87* has the highest value and building *A99* has the lowest, as shown in ***Figure 35***.

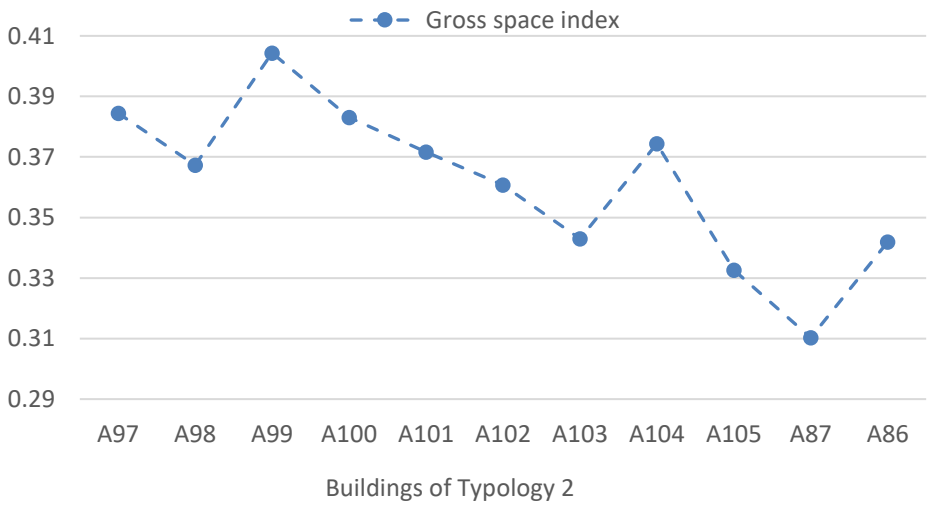

Figure 28. Gross space index (GSI).

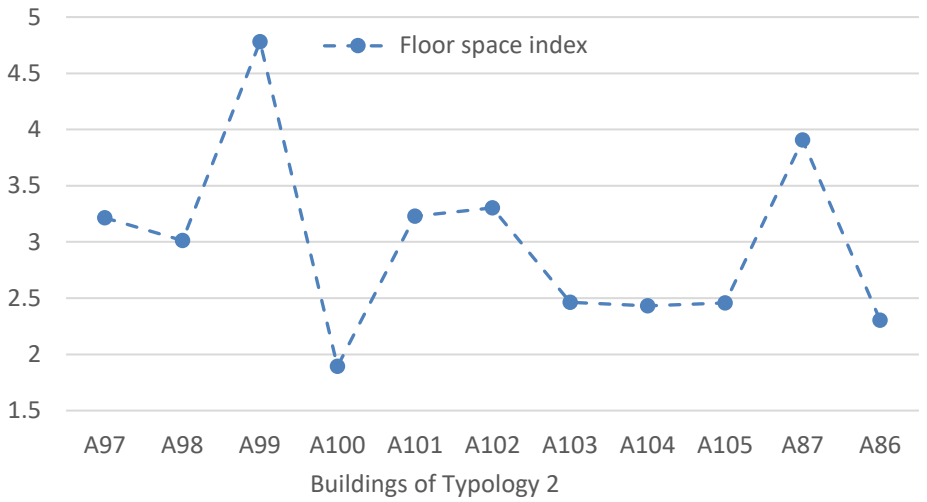

Figure 29. Floor space index (FSI).

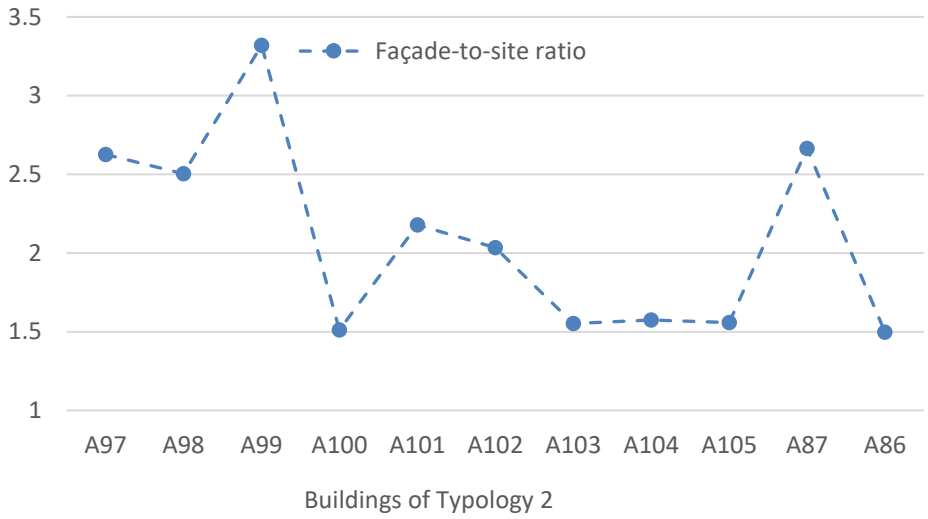

Figure 30. Façade-to-site ratio (VHurb).

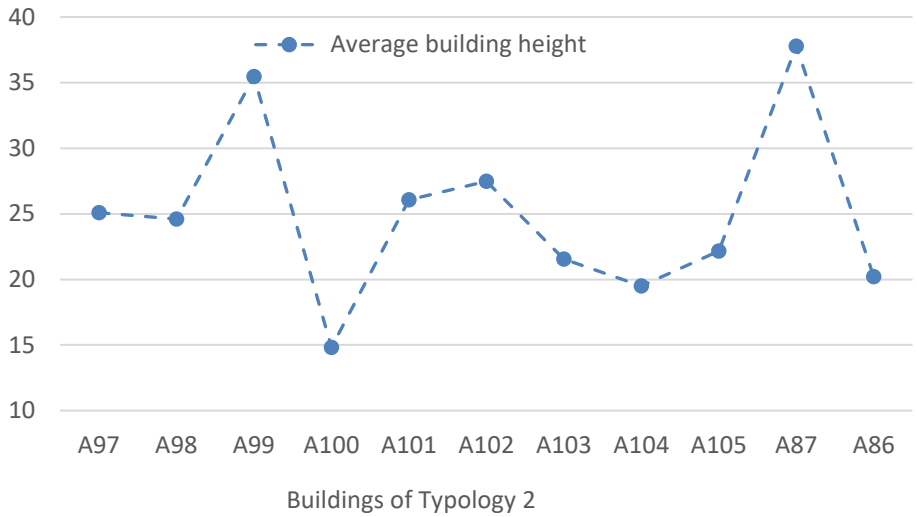

Figure 31. Average building height (Hbld).

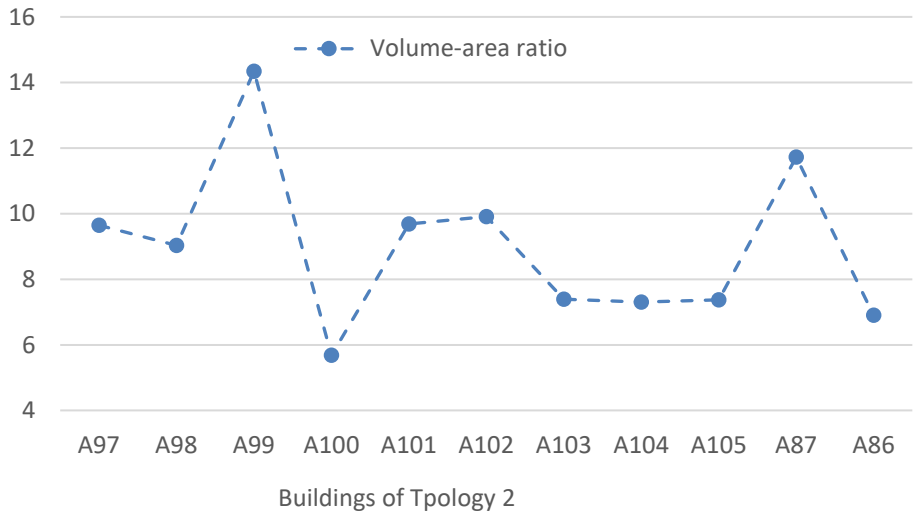

Figure 32. Volume-area ratio (V/A).

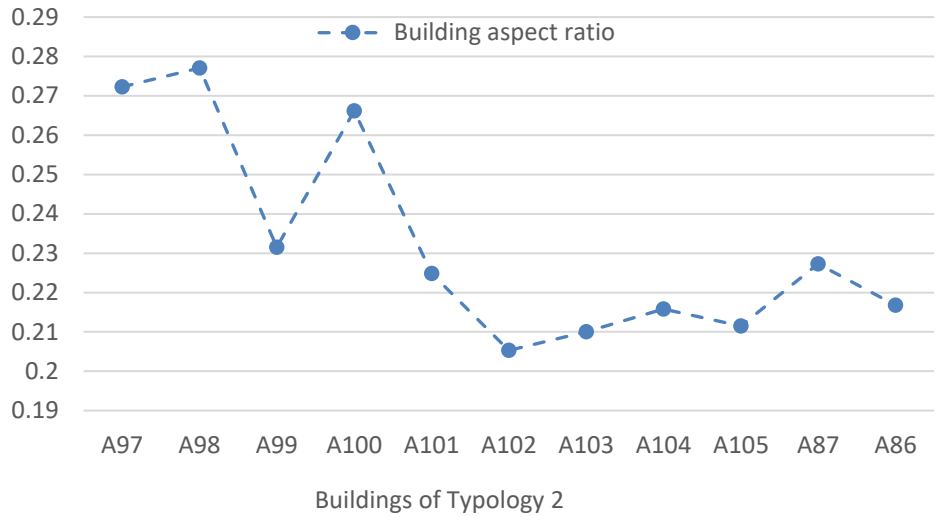

Figure 33. Building aspect ratio.

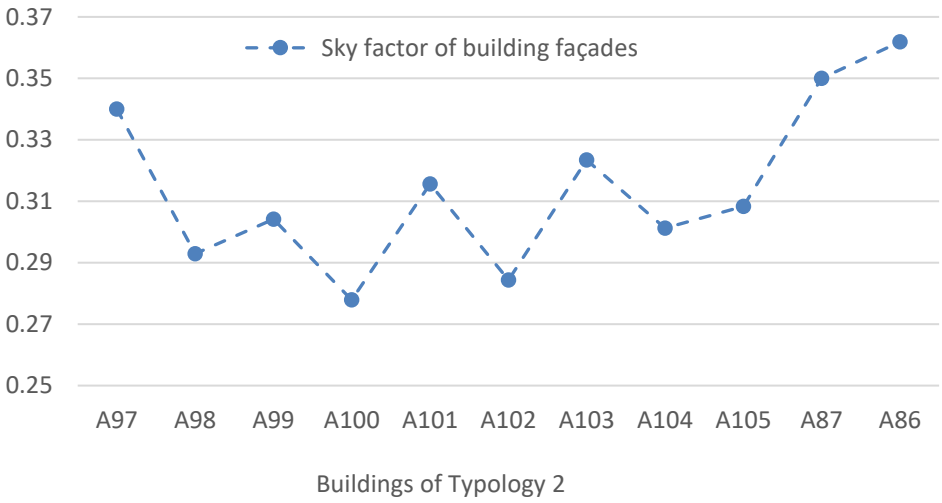

Figure 34. Sky factor of building façades (SF).

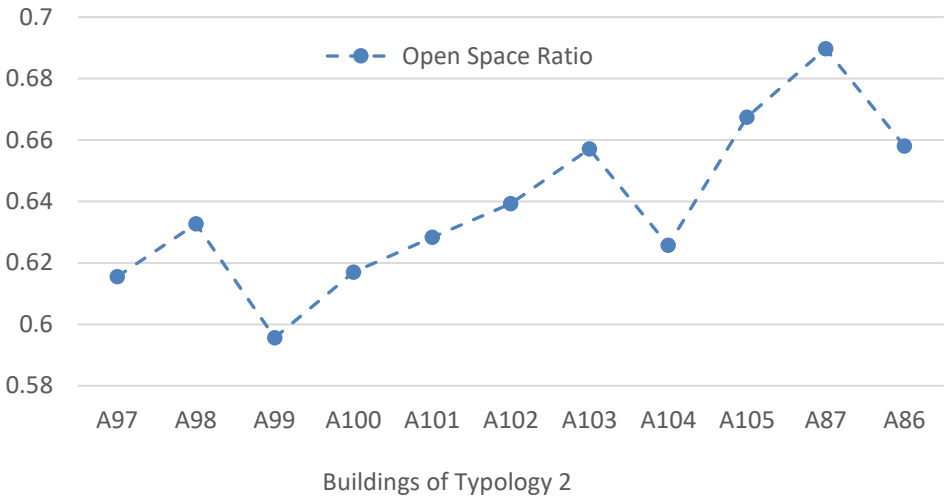

Figure 35. Open Space Ratio (OSR).

3.3.4 Typology 3 UMIs

Being the most unusual urban typology of the overall site and of all the 4 typologies chosen, it is divided in two large building blocks, *A28* and *A29*. ***Figure 36*** to ***Figure 43*** shows the average values for each UMI. *GSI* averages to a value of 0.26, where the highest value is in block A28 and the lowest in block *A27*, as shown in ***Figure 36***. *FSI*, as shown in ***Figure 37,*** has a mean value of 2.65, where block *A28* has the highest value. VH_{urb} has an average value of 1.81, with block *A28* having the highest value, as shown in ***Figure 38***. H_{bld} averages to 30.78, as shown in ***Figure 39*** and block *A27* has the greatest height. *V/A ratio* has a mean value 7.94, with block *A28* having the highest one, shown in ***Figure 40***. *Building Aspect Ratio*, shown in ***Figure 41,*** has a mean value of 0.23, where block *A28* has the highest one. *SF* averages to 0.31 with block *A27* having the highest value, as shown in ***Figure 42***. *Open Space Ratio* has an average value of 0.74, reaching its highest value in block *A27*, as shown in ***Figure 43.***

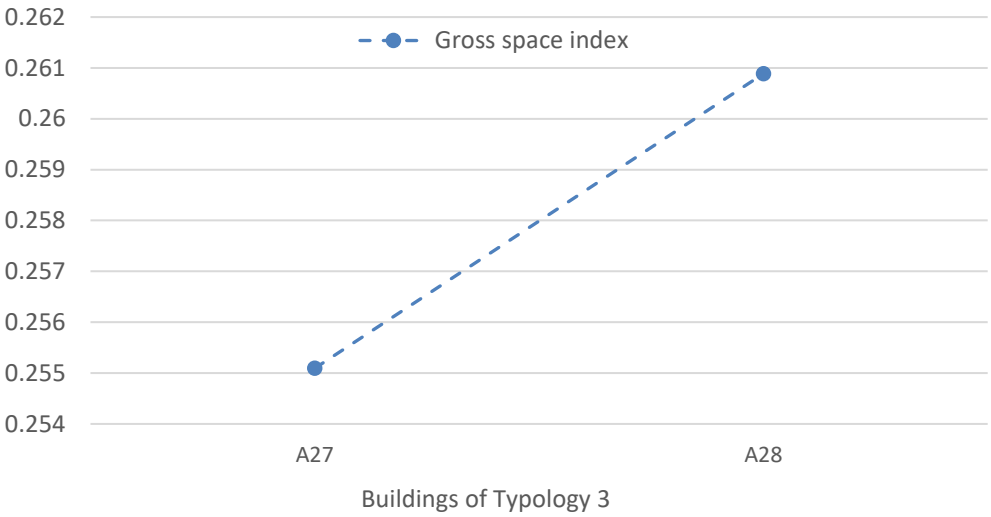

Figure 36. Gross space index (GSI).

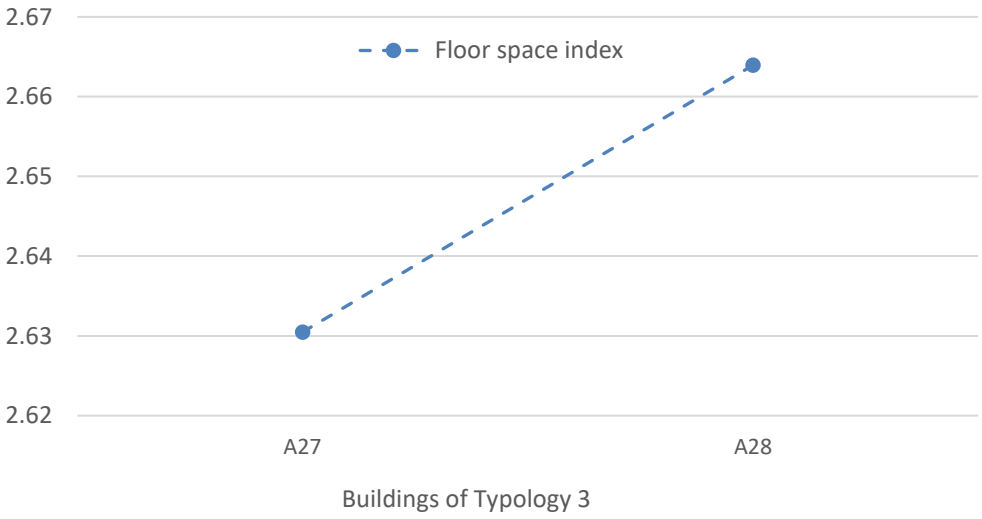

Figure 37. Floor space index (FSI).

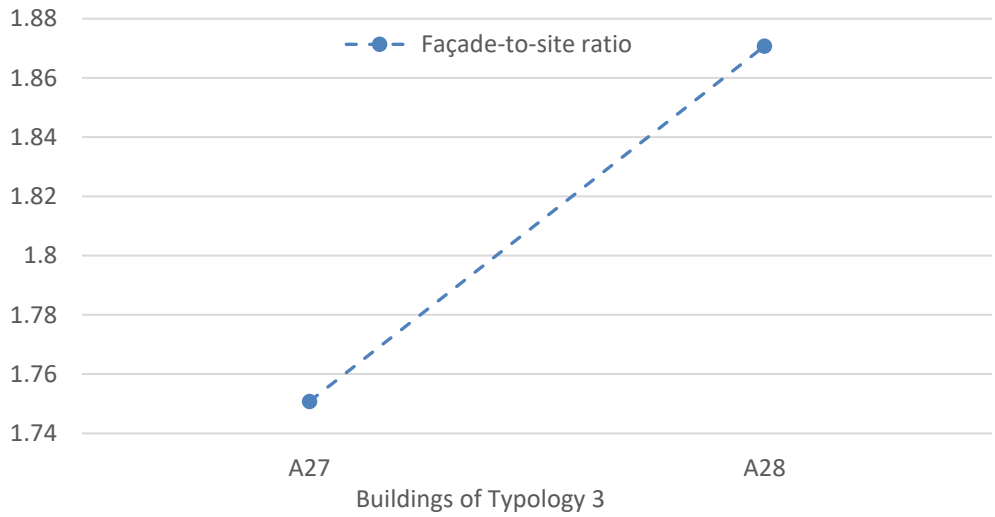

Figure 38. Façade-to-site ratio (VHurb).

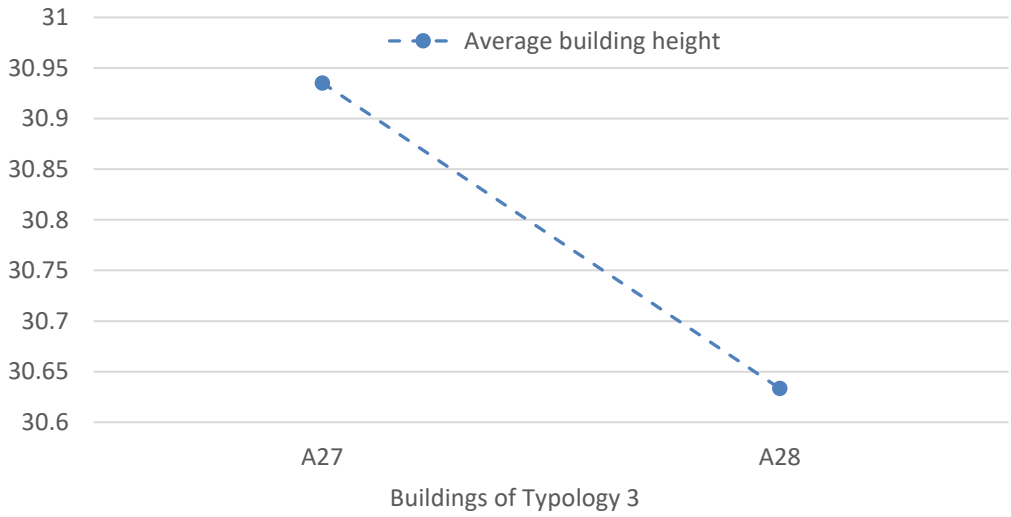

Figure 39. Average building height (Hbld).

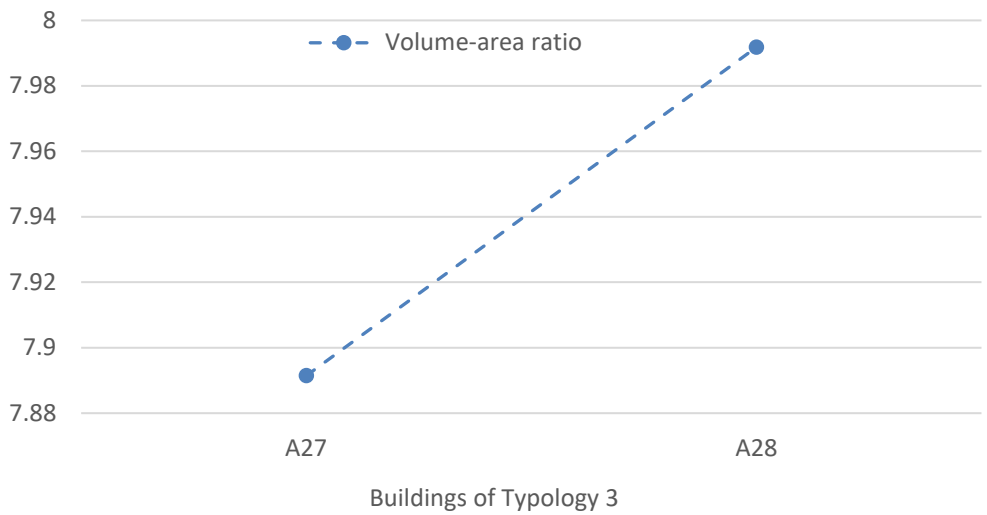

Figure 40. Volume-area ratio (V/A).

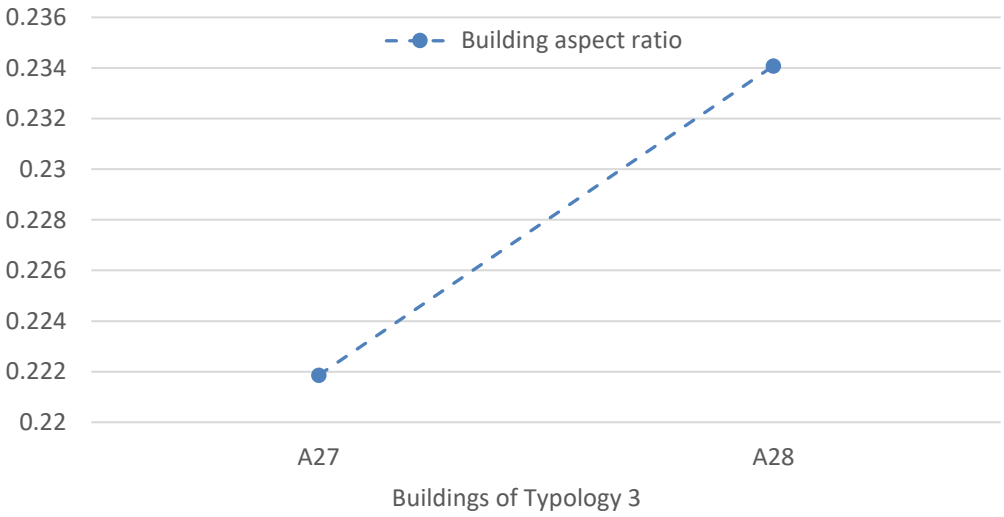

Figure 41. *Building aspect ratio.*

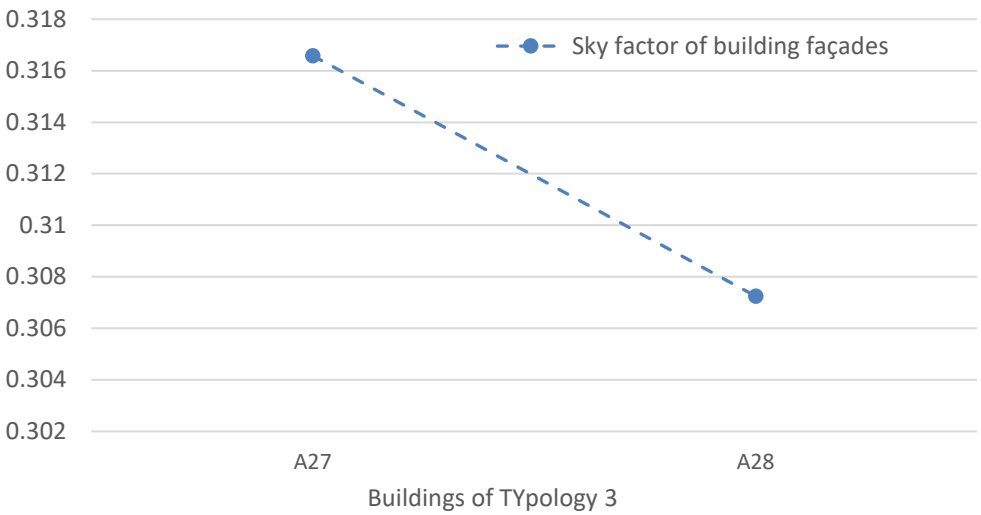

Figure 42. Sky factor of building façades (SF).

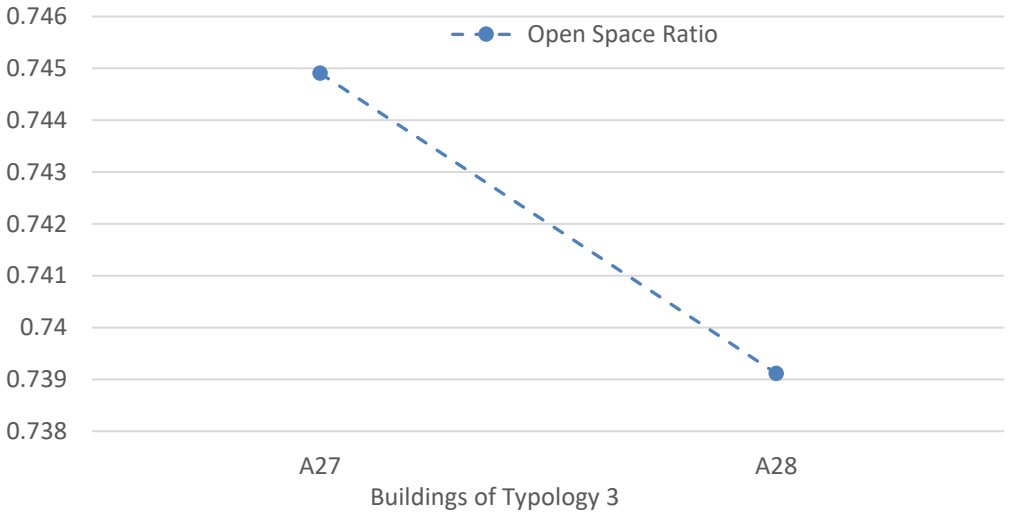

Figure 43. Open Space Ratio (OSR).

3.3.5 Typology 4 UMIs

The last urban typology chosen consists of 8 building blocks and their UMIs mean values are shown from ***Figure 44*** to ***Figure 51***. *GSI* has an average value of 0.37, as shown in ***Figure 44***, where building *A46* has the highest value and building *A45* has the lowest one. *FSI*, as shown in ***Figure 45***, has a mean value of 2.79, where

building *A43* has the highest value, closely followed by building *A42*, and building *A44* has the lowest value. VH_{urb} averages to a value of 1.84, where building *A42* has the highest one and *A44* the lowest, shown in ***Figure 46***. H_{bld}, shown in ***Figure 47***, has a mean value of 22.33, with both buildings *A42* and *A43* having the same height, and building *A44* being the lowest. *V/A ratio* averaging to 8.36, reaches the highest value in building *A42* and *A43*, and the lowest value in building *A44*, shown in ***Figure 48***. *Building Aspect Ratio*, shown in ***Figure 49***, averages to 0.22, with building *A44* having the highest value and *A43* the lowest. *SF* mean value is 0.31, as shown in ***Figure 50***, where building *A47* has the highest value, while building *A44* has the lowest. *Open Space Ratio* averages to 0.63, with building *A45* having the highest value and *A46* the lowest, as shown in ***Figure 51***.

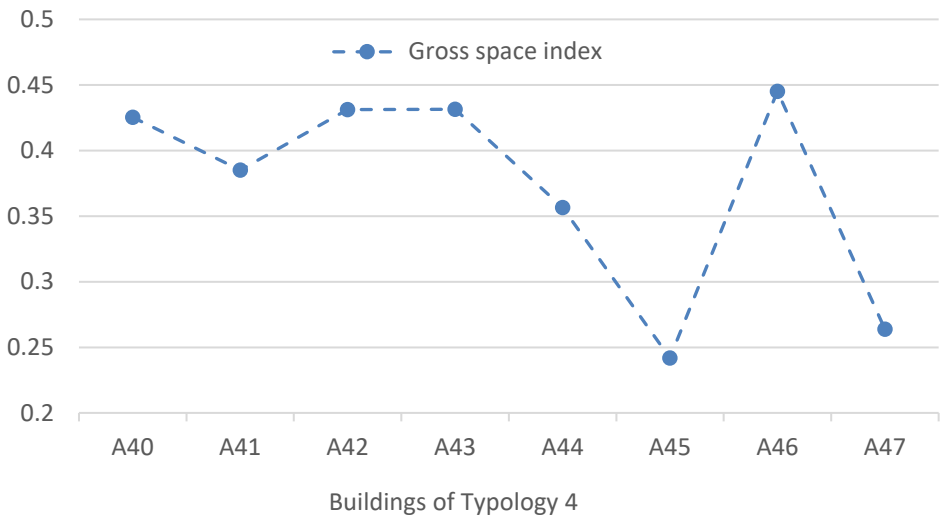

Figure 44. Gross space index (GSI).

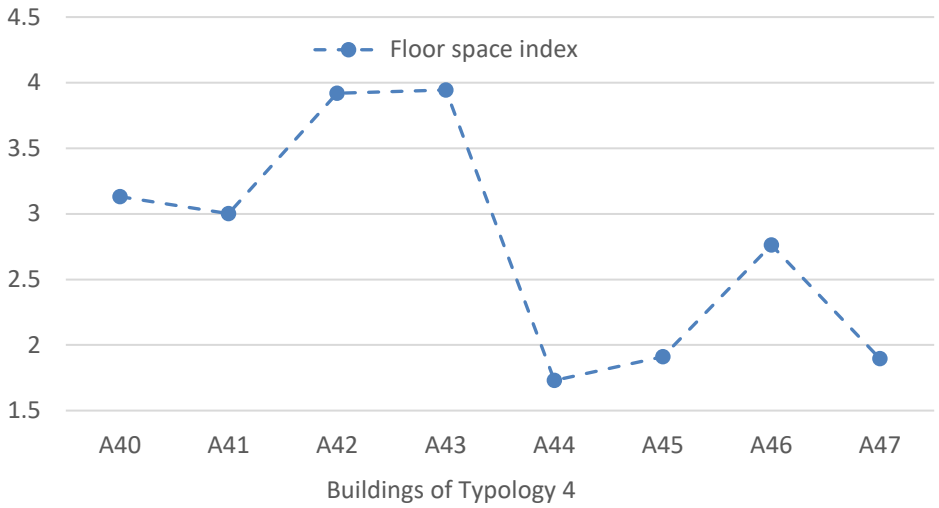

Figure 45. Floor space index (FSI).

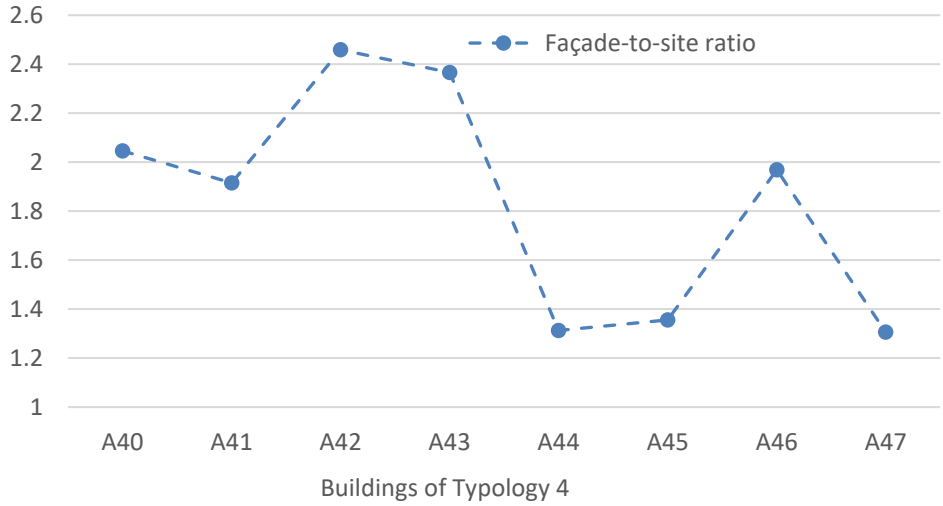

Figure 46. Façade-to-site ratio (VHurb).

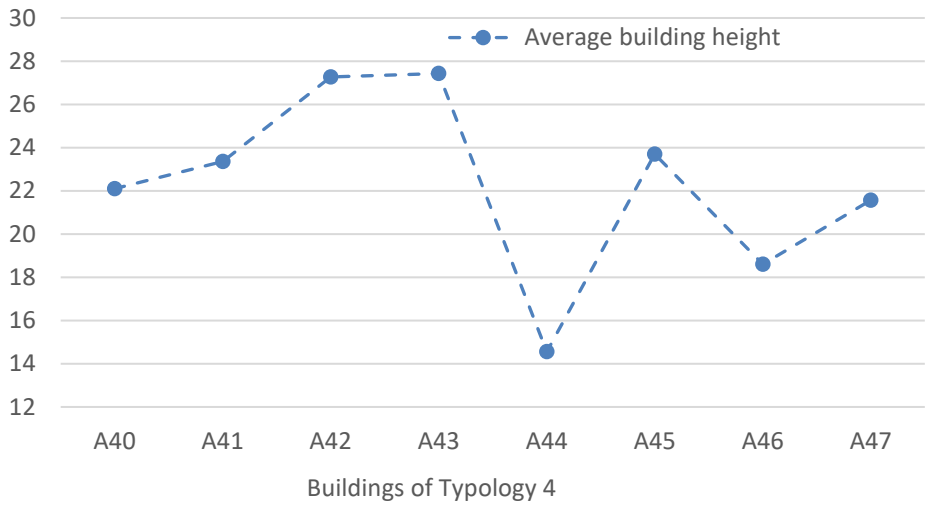

Figure 47. Average building height (Hbld).

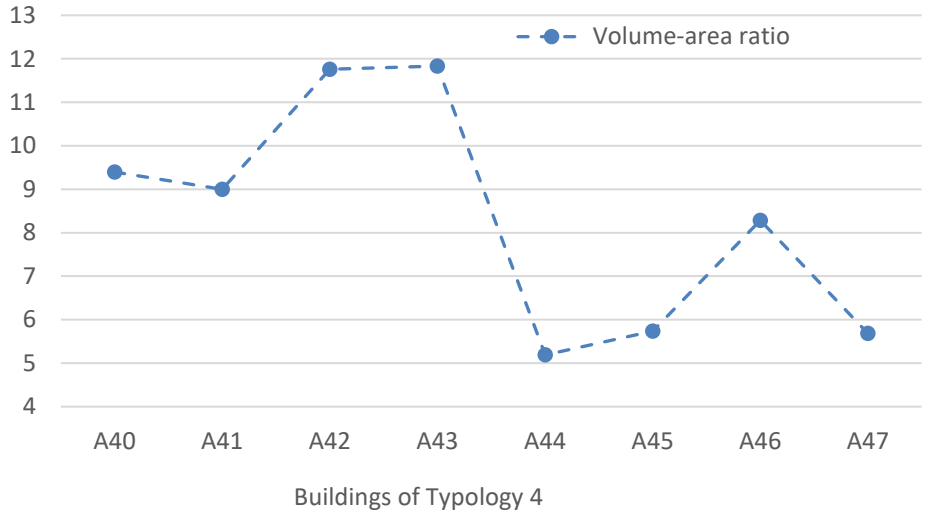

Figure 48. Volume-area ratio (V/A).

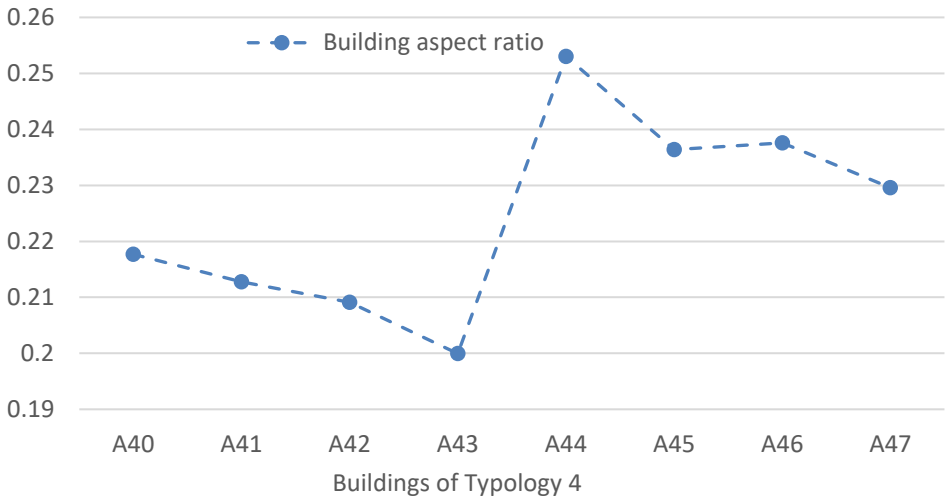

Figure 49. Building aspect ratio.

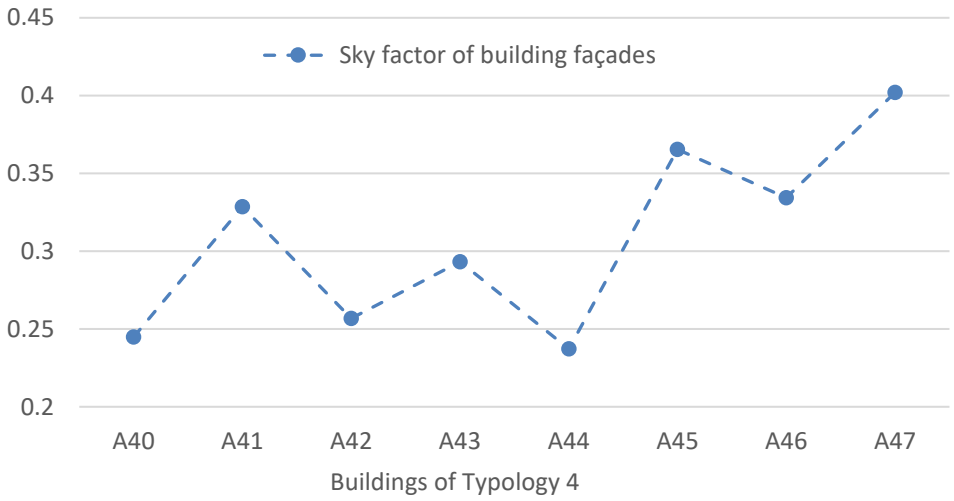

Figure 50. Sky factor of building façades (SF).

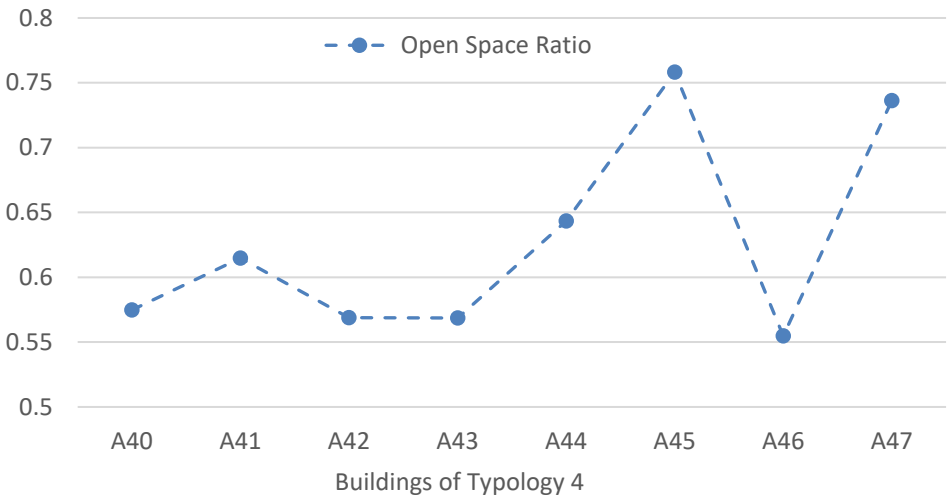

Figure 51. Open Space Ratio (OSR).

3.3.6 Comparison

The differentiations between the indicators are shown from ***Figure 52*** to ***Figure 59*** as follows: *GSI* has the highest value in *Typology 4* closely followed by *Typology 1* and *2*. The lowest value is in *Typology 3* as shown in ***Figure 52***. The reason for this outcome is that *Typology 3* has a much larger plot area contrary to the other ones. *FSI* values score the lowest in *Typology 3*, with *Typology 1* and *4* being close, shown in ***Figure 53***. On the other hand, *Typology 2* has the highest value. The main reason for this is the large plot surface area of *Typology 3*. VH_{urb}, shown in ***Figure 54***, has the highest value in *Typology 2* and the lowest one in *Typology 1*. The rest are closer to the lowest value, reason for that being *Typology 1* has the highest plot area of the two. H_{bld} has the highest value in *Typology 3* and the lowest one in *Typology 4*, shown in ***Figure 55***. *V/A ratio,* shown in ***Figure 56***, is the lowest in *Typology 3* because it has the largest plot area, and highest in *Typology 2*. *S/V ratio* is highest in *Typology 2* and lowest in *Typology 1*, as shown in ***Figure 57***. *SF*, as shown in ***Figure 58***, has the highest value in *Typology 1* and the lowest in *Typology 4*. As expected *OSR* has the highest value in *Typology 3* and the lowest value in *Typology 4*, shown in ***Figure 59***. The latter is a far denser zone than the first one.

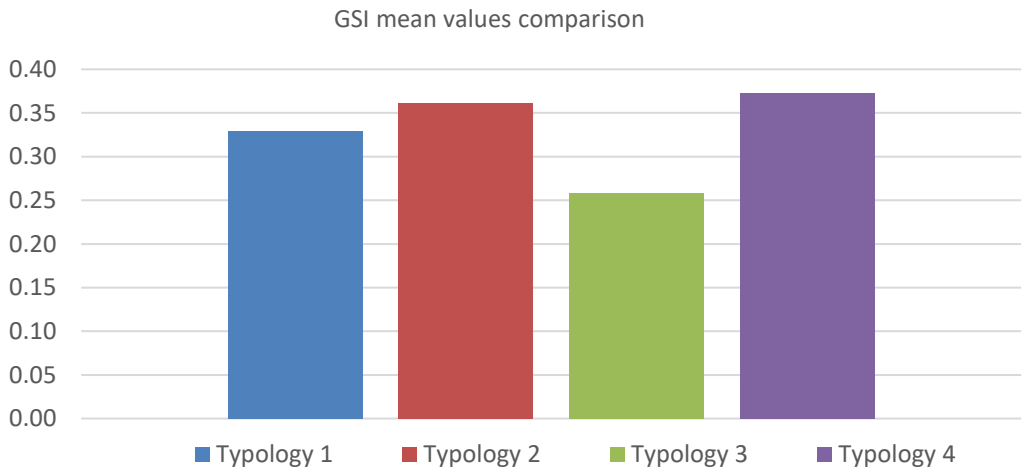

Figure 52. GSI mean values comparison.

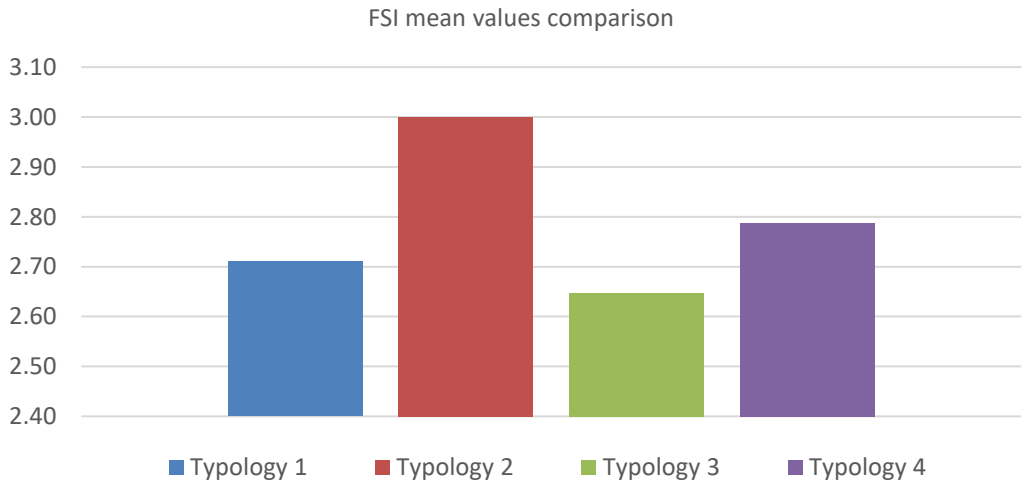

Figure 53. FSI mean values comparison.

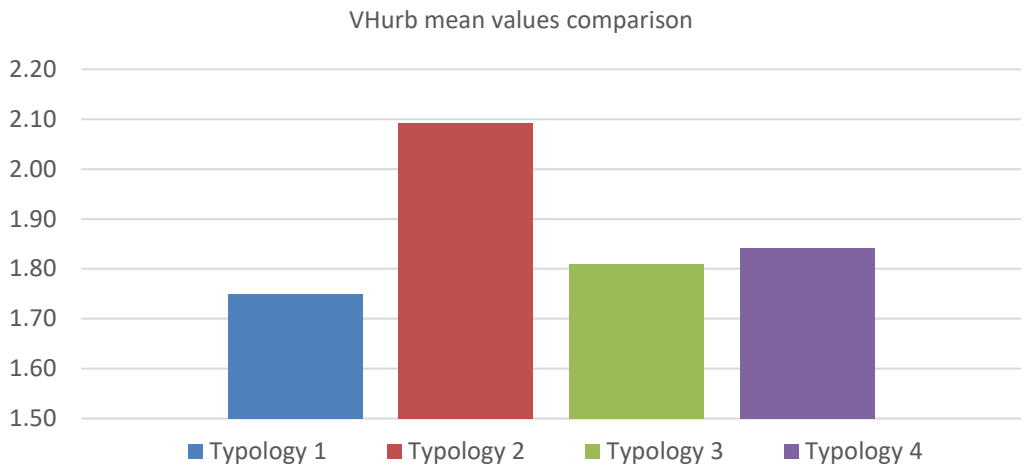

Figure 54. VH_{urb} mean values comparison.

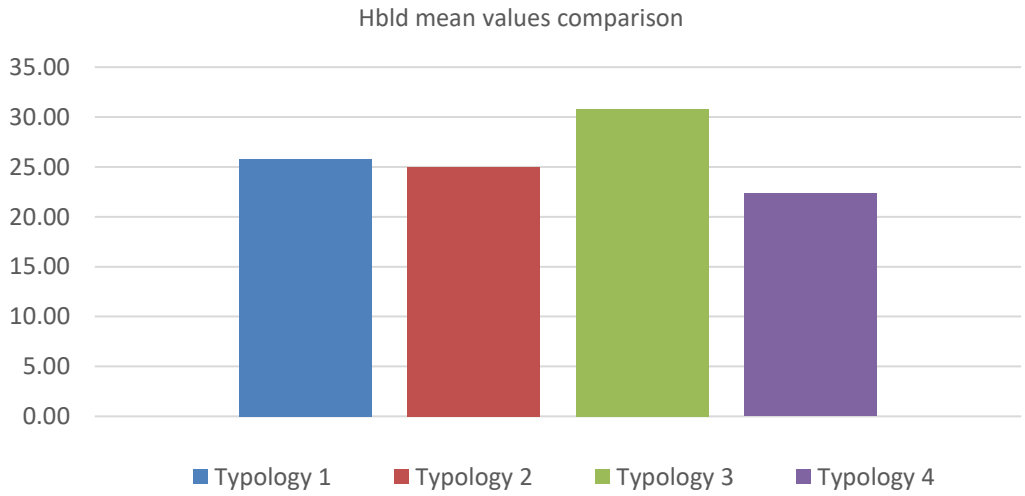

Figure 55. H_{bld} mean values comparison.

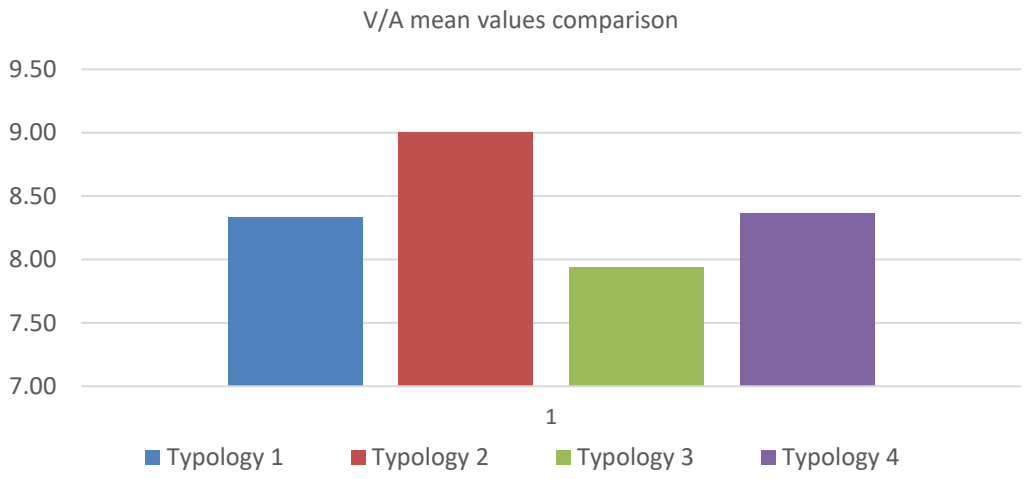

Figure 56. V/A mean values comparison.

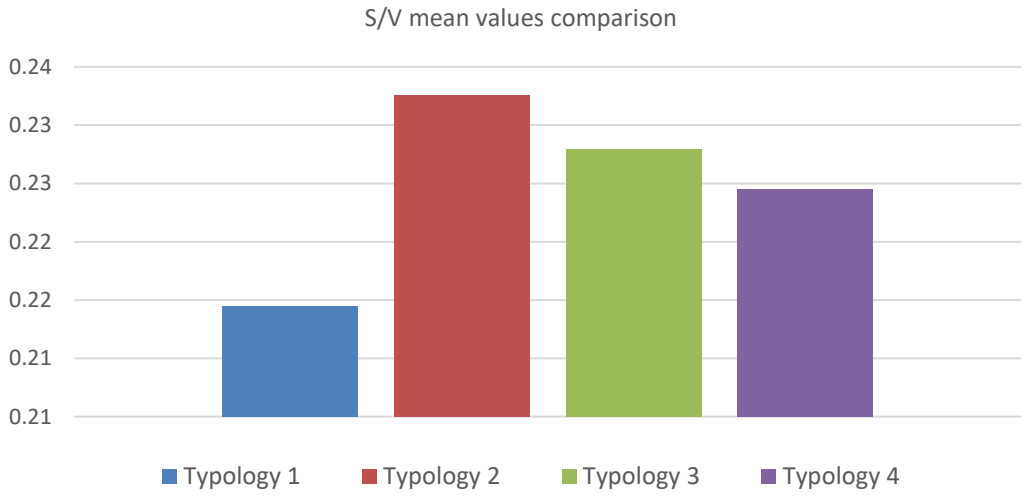

Figure 57. Building aspect ratio mean values comparison.

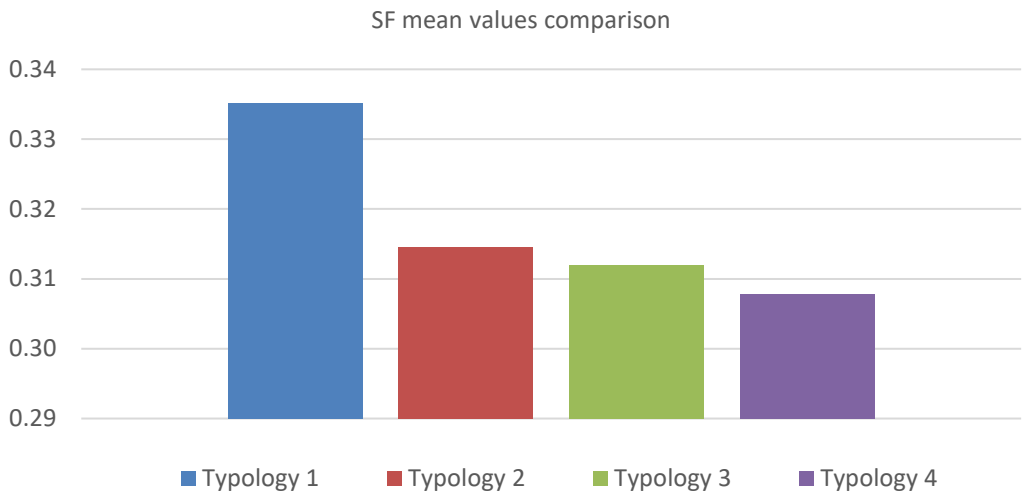

Figure 58. SF mean values comparison.

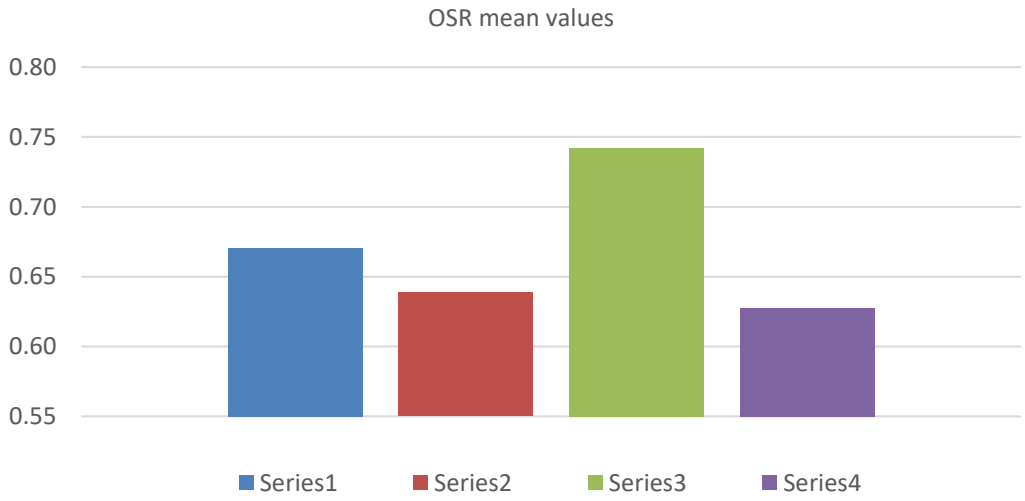

Figure 59. OSR mean values comparison.

3.4 Climate Description

Tirana has a humid subtropical climate according to Köppen climate classification as Cfa, lying in the boundaries of Mediterranean climate because of its insignificant inequality in the amount of rainfall during the summer. It is characterized by hot, dry summers and cool and wet winters. Its geographical location is 41.33°

north, 19.82° east, standing at 110 m above sea level. These data are calculated using the Meteonorm 7.3 software. The annual average temperature is 16.2 °C. They alter during the year from 6.3 °C in January to 23.8 °C in July. The coldest month is January with an average high-temperature of 29.2 °C and an aveage low-temperature of 2.9 °C. The warmest month is August with an average high temperature of f 29.2 ° C and an average low-temperature of 18.4 ° C, as shown in ***Figure 60***. The average solar radiation Tirana receives is 611 KWh/m2 yearly. The maximum global radiation value is marked in July reaching about 234 KWh/m². Tirana is one of the sunniest cities on the European Continent receiving 2500 hours of sun. The winter months receive the majority of the precipitation amounts. Both rain and snow occur with a peak in January (140 millimeters), November (170 millimeters), and December (150 millimeters). The average wind speed is 1.8 m. s-1; during winter, 2.6 m. s-1 in February; during spring and summer, 1.3 m. s-1 in May-August period.

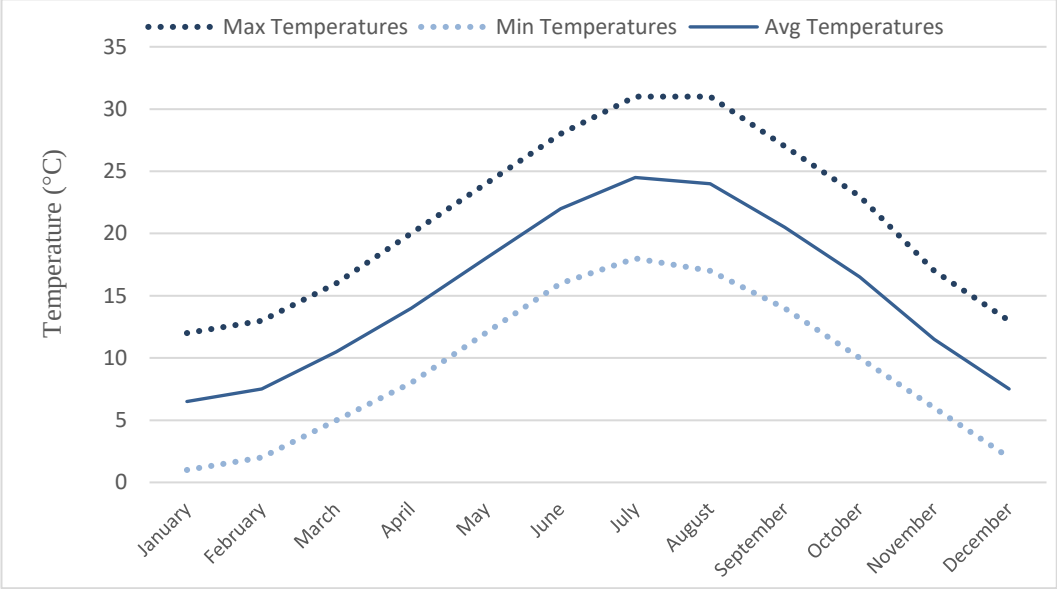

Figure 60. Annual temperatures for the city of Tirana.

3.5 Computational Simulation

3.5.1 Software Description

The softwares used for this study are a combination of 3D modelling softwares, that include AutoCAD 3D for building the overall site and each urban morphology chosen and Revit Architecture mass modelling option to build the model and run a detailed solar analysis with Insight Plugin for Revit, and energy simulation softwares such as CitySimPro, the main energy simulation software used for this research, which uses the files prepared from AutoCAD and examines several parameters, as shown in ***Figure 61***.

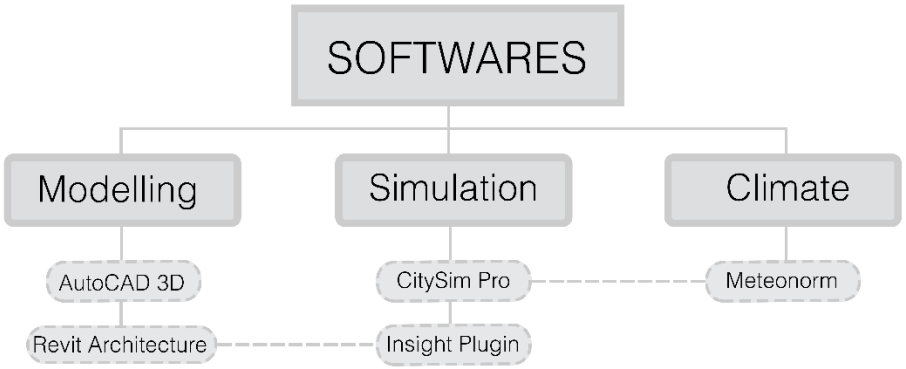

Figure 61. Softwares used for this study.

AutoCAD 3D is used here to extrude the building blocks from the site plans and other information provided for this project. The file is saved as an AutoCAD dxf 2000 with 3dface or polyline, in order to be imported later to CitySimPro software.

Revit Architecture covers the daylight analysis. Firstly, the site needs to be modeled with the Model in Place command and then proceed with Mass family. This is a necessary requirement as Insight Plugin for Revit can only execute solar analysis

on mass models surfaces. This proves to be a very useful tool as the final outputs are analyzed in a detailed manner for each surface of the envelope.

CitySimPro is the main software used for the purpose of urban energy simulations. It is a very reliable tool that requires the insertion of minimal input and produces detailed results for each building. The reason behind the selection of this software was that it provides detailed data about the physical model upon its import within the software. Such data include areas of: floors, roofs, walls etc. Moreover, this simulation instrument allows the user to change its defaults components to user-defined ones that are customizable through a database provided in advance. The results are shown hourly, daily, monthly and yearly about each of these outputs: short-wave irradiation, long-wave net irradiation, surface temperature, photovoltaic production, solar thermal production, heating demand, cooling demand, indoor temperature. The only result that remains unchanged throughout the whole year is sky view factor, because it relies on physical factors.

3.5.2 Simulation Input

CitySim Pro requires certain inputs, explained in detail in ***Table 3,*** to be included for the simulation in order for the results to be genuine. More specifically they are classified under the below mentioned categories:

The first one is *District Properties* which includes climate files (.cli) and horizon files (.hor). They both are generated from Meteonorm software and imported into CitySim. Second is *Building*, which consists of infiltration, T_{min}, T_{max}, shading device and cut-off irradiance. Minimum temperature is set to 20°C and maximum temperature to 25°C. Shading device and Cut-off irradiance are respectively 0.2 and 100.

Third is *Composites and Insulation* which has 4 main elements: walls (type and insulation thickness), roof (type and insulation thickness), floor (type and insulation

thickness), ground (type). The software has default composites of walls, roofs, floors and ground, but for this study are used typical ones for Tirana, as shown in ***Table 4***.

They are: *External walls* (plaster rendering, sand / extruded polystyrene / European standard clay brick / plaster rendering, sand), as shown in ***Figure 62***. *Insulated roof* (gravel / waterproof barrier / glass wool-fiber insulation / screed / concrete reinforced 2% steel / plaster rendering, sand), as shown in ***Figure 63 .*** *Internal floor* (ceramic tiles / screed / concrete reinforced 2% steel / plaster rendering, sand), as shown in ***Figure 64***.

Opening Properties is the fourth category that includes the glazing ratios of each orientation (north, south, east, west), U-value, g-value and openable fraction. The Glazing Ratio of each side is set to 40% (0.4), U-value of walls 0.435, glazing 1.761, roof 0.513, g-value set to 0.7 and openable fraction to 0.5, shown in ***Table 3***.

Fifth is *Visible Surface* that includes reflectance, solar panels (PV ratio and its type and thermal ratio and its type), as shown in ***Figure 65***.

Next one is *Grounds* that includes only the reflectance of the material used for the ground surface. The material used will be asphalt with a reflectance value of 0.2.

Final section is *Occupants* that has the subcategories of: number of people, density, sensible heat, radiant part, latent heat and occupancy profile. By setting the density to 25m^2/p the numer of people is automatically generated for each building. Sensible heat is 90 and the occupancy profile is set to ‘’year profile house’’.

Table 3. Input parameters energy simulation.

Family	Input parameters	Value
District properties	Climate	
	Horizon	
Building	Infiltration	0.10
	T_{min}	20
	T_{max}	25
	Shading device: λ	0.20
	Cut-off irradiance	100
Composites and insulation	Wall insulation	5
	Roof insulation	5
Opening properties	Glazing ratio	0.40 (N,S,E,W)
	U-value	1.761
	g-value	0.70
	Openable fraction	0.50
Visible surfaces	Reflectance	0.20
Ground	Reflectance	0.05
Occupants	Number	
	Density	$25m^2/p$
	Sensible heat	90
	Radiant part	0.60
	Occupancy profile	Year profile house

Table 4. Construction Properties.

		Density [kg/m³]	Conductivity [W/m °C]	Specific heat [J/kg °C]	Thickness [m]
External wall	Plaster rendering, sand	1600	0.8	1000	0.02
U-value=0.435 [W/m^2.K]	Extruded polystyrene	25	0.036	1400	0.05
	European standard clay brick	1100	0.44	900	0.20
	Plaster rendering, sand	1600	0.8	1000	0.02
Insulated roof					
U-value=0.513 [W/m^2.K]	Gravel	1900	0.7	800	0.05
	Waterproof barrier	1200	0.2	1600	0.001
	Glass wool-fiber insulation	22	0.031	1029	0.05
	Screed	1000	0.3	1000	0.05
	Concrete, reinforced (2% steel)	2400	2.5	1000	0.20
	Plaster rendering, sand	1600	0.8	1000	0.02
Internal floor					
U-value=1.942 [W/m^2.K]	Ceramic tiles	1900	1	1000	0.01
	Screed	1000	0.3	1000	0.05
	Concrete, reinforced (2% steel)	2400	2.5	1000	0.20
	Plaster rendering, sand	1600	0.8	1000	0.02

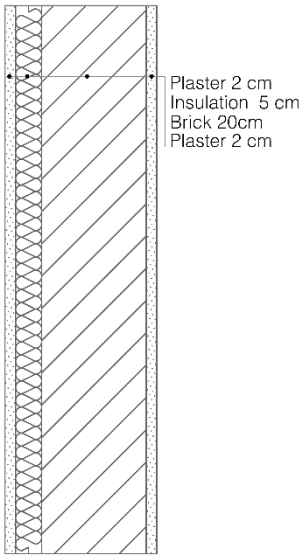

Figure 62. Section detail of external wall of the simulated model.

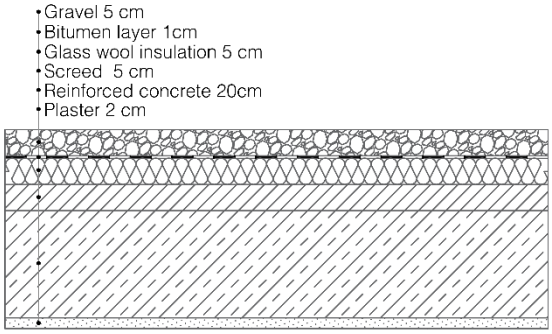

Figure 63. Section detail of terrace of the simulated model.

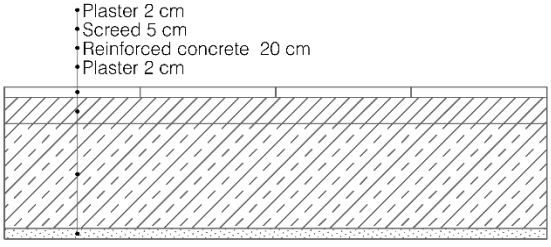

Figure 64. Section detail of internal floor of the simulated model.

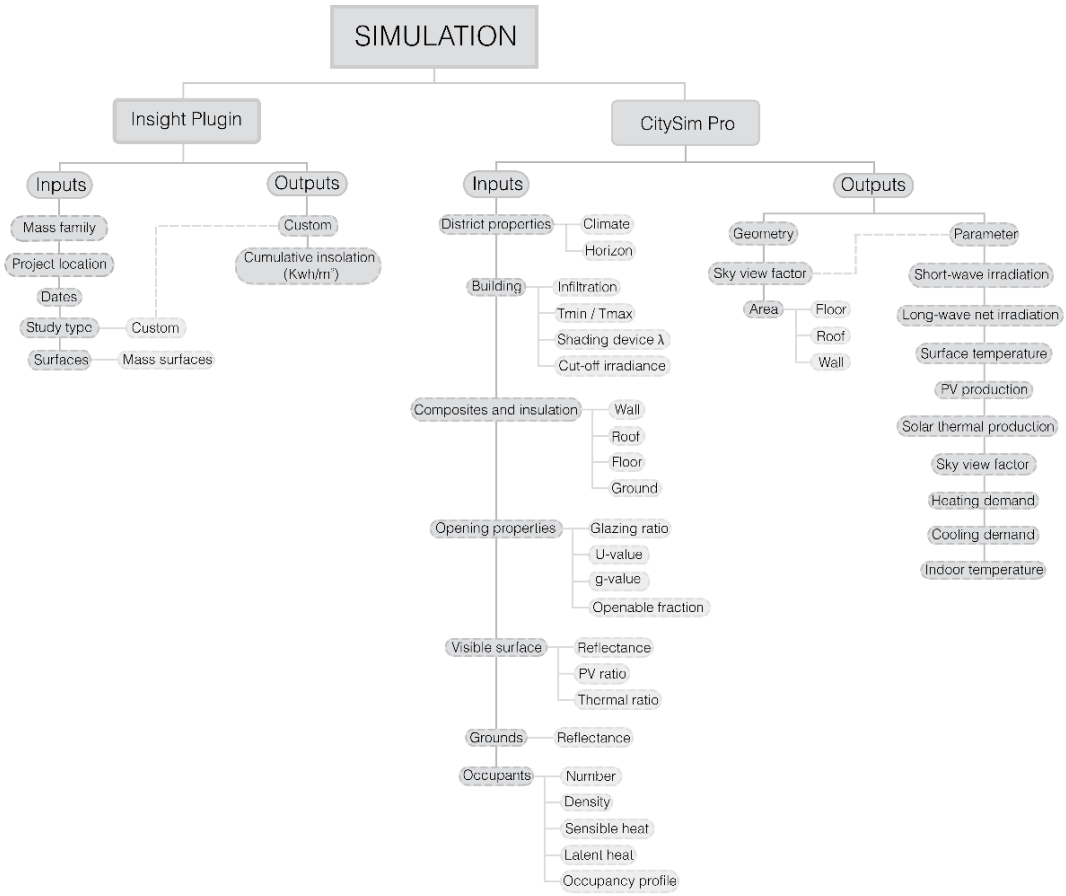

Figure 65. Simulation inputs scheme.

CHAPTER 4

RESULTS AND DISCUSSION

4.1 Typology 1

4.1.1 Overview

For *Typology 1*, the energy simulations are conducted with CitySim Pro. All the data is interpreted and categorized into monthly heating and cooling loads, in kwh/m^3. Also, the surface temperatures are generated and grouped for two days of the year: Summer Solstice and Winter Solstice. The results are sorted for a full day on both of them.

A single building block, *A10*, is chosen to analyze the surface temperatures results. All 8 facades are taken into account, and are assembled into two categories: inner facades, the ones facing the courtyard, shown in ***Figure 66***, and outer facades, the ones on the outer envelope of the building, shown in ***Figure 67***.

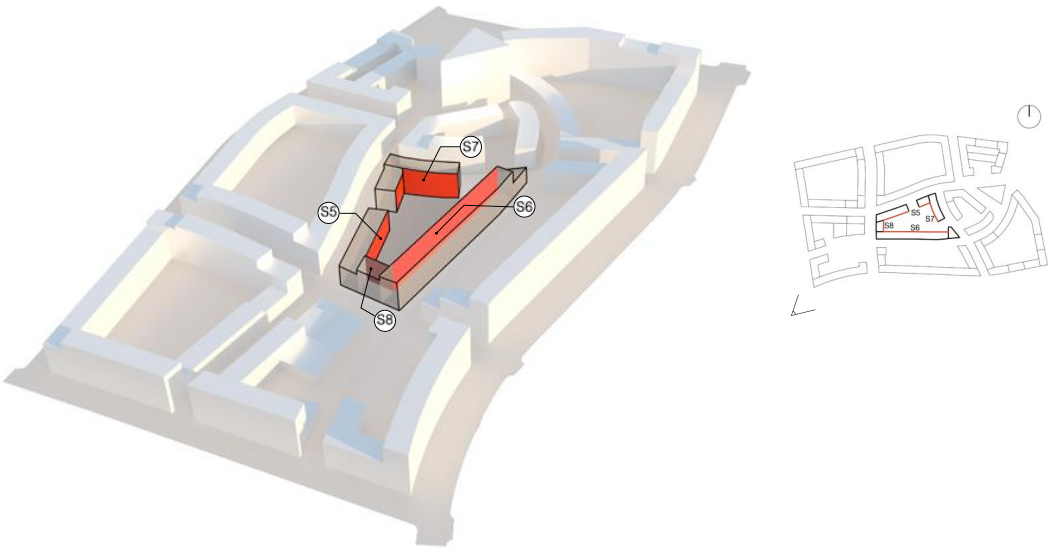

Figure 66. Inner facades of building A10, Typology 1.

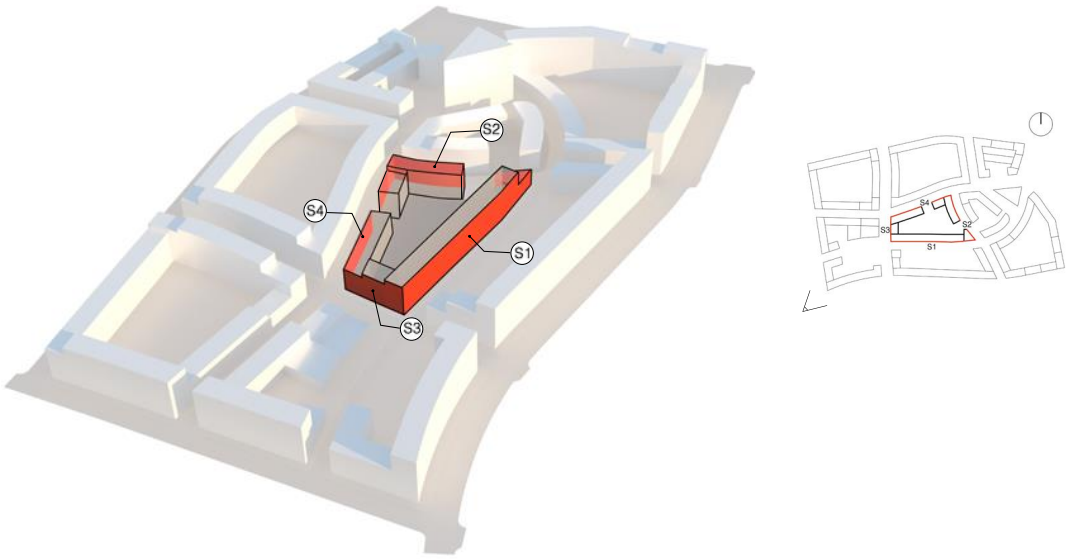

Figure 67. Outer facades of building A10, Typology 1.

4.1.2 Energy Consumption

4.1.2.1 Monthly Energy Consumption

Figure 68 to ***Figure 77*** illustrates the monthly heating and cooling energy consumption for each builing of the *Typology 1*. Concerning the heating demand, January is the month with the highest demand of energy in every building, with block *A2* having the highest loss of energy dedicated to heating, as shown in ***Figure 69***. On the other hand, the cooling demand is highest during the month of July, period when block *A2* has again the highest energy loss dedicated to cooling, shown in ***Figure 69***.

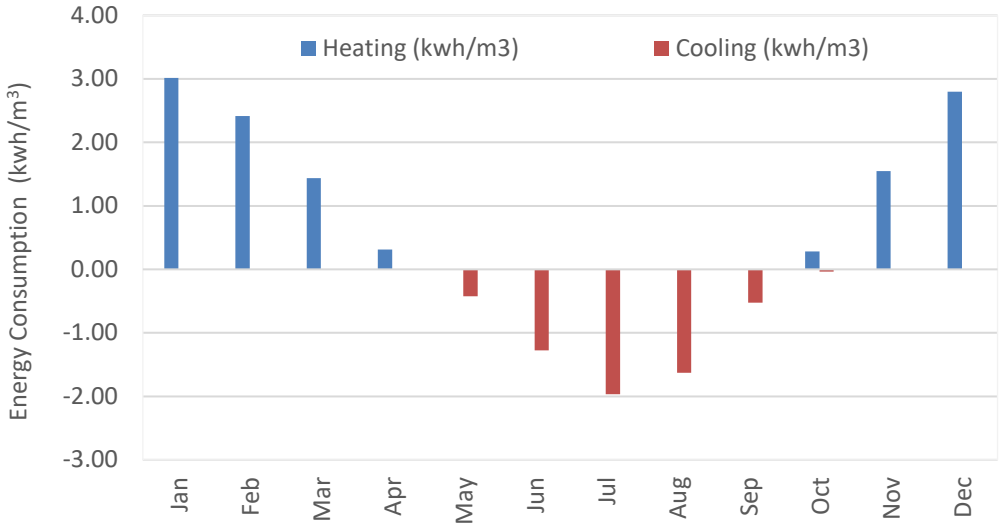

Figure 68. Monthly Heating and Cooling Energy Consumption (kWh/m3) of Building A1 of Typology 01.

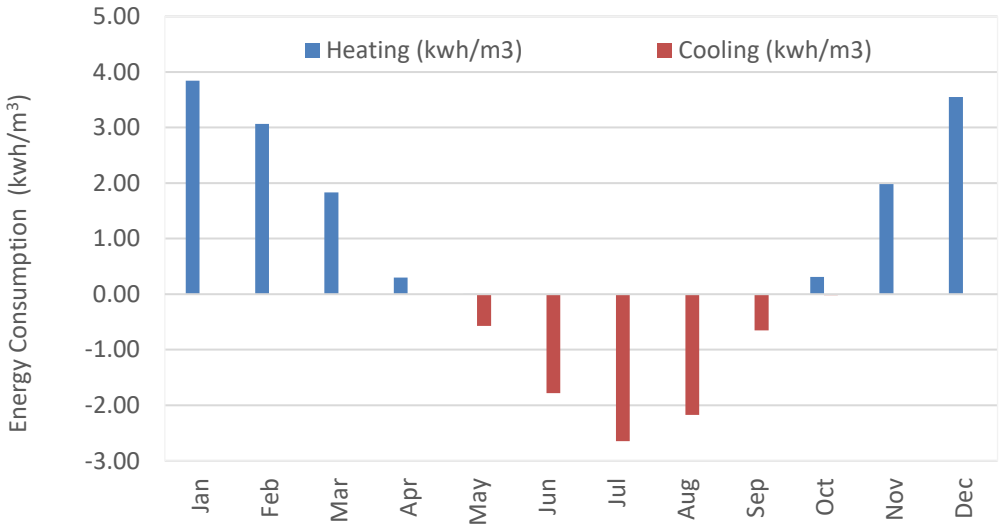

Figure 69. Monthly Heating and Cooling Energy Consumption (kWh/m3) of Building A2 of Typology 01.

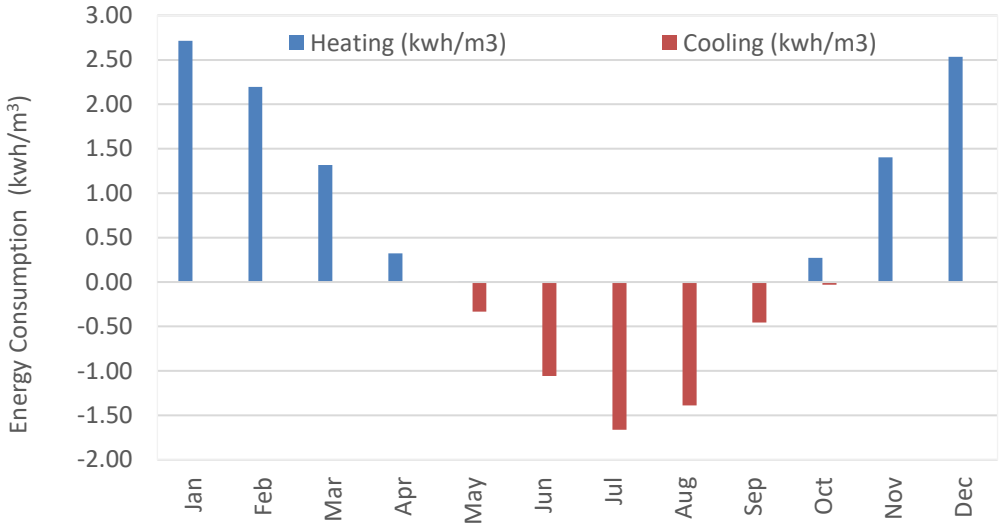

Figure 70. Monthly Heating and Cooling Energy Consumption (kWh/m3) of Building A3 of Typology 01.

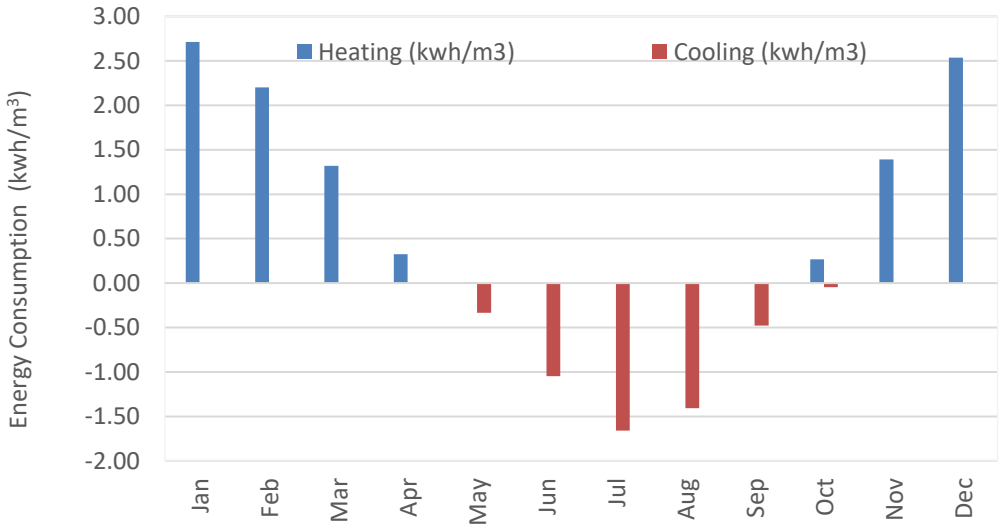

Figure 71. Monthly Heating and Cooling Energy Consumption (kWh/m3) of Building A4 of Typology 01.

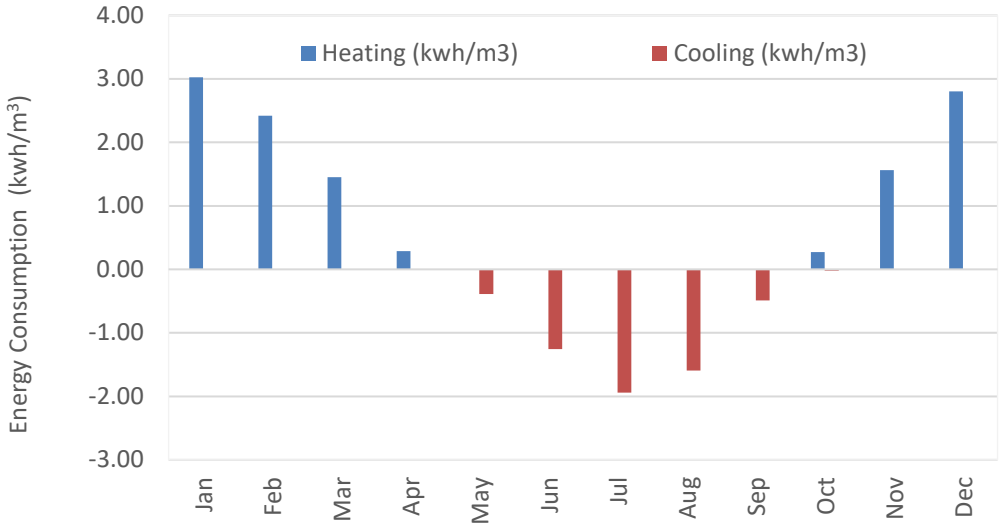

Figure 72. Monthly Heating and Cooling Energy Consumption (kWh/m3) of Building A5 of Typology 01.

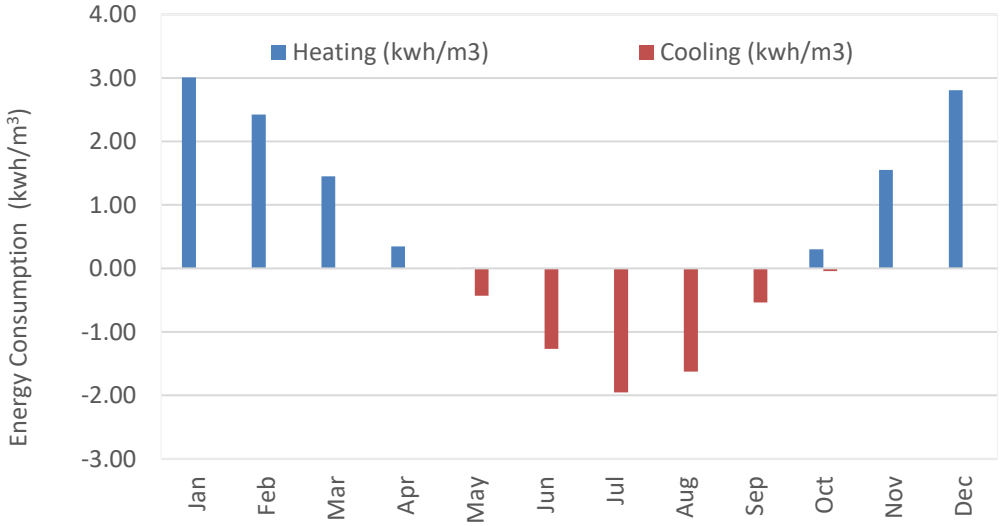

Figure 73. Monthly Heating and Cooling Energy Consumption (kWh/m3) of Building A6 of Typology 01.

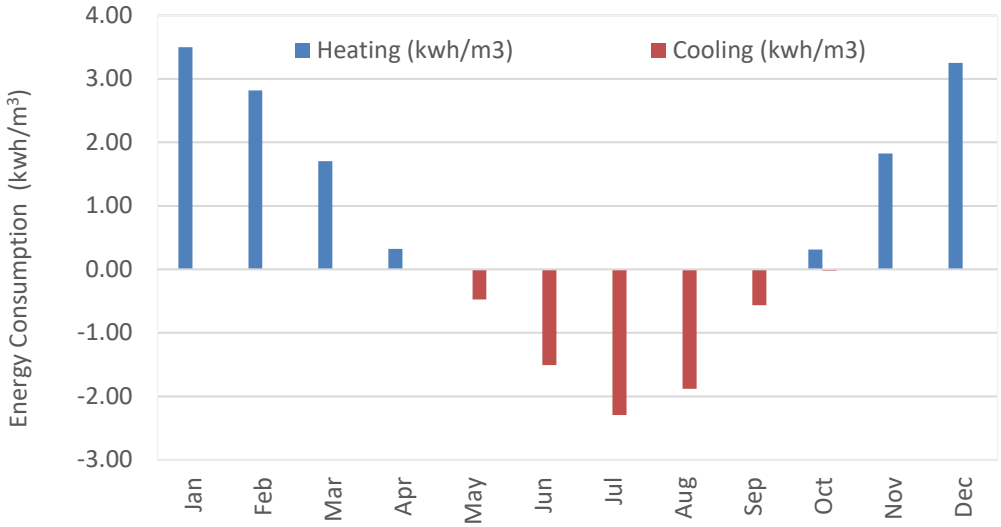

Figure 74. Monthly Heating and Cooling Energy Consumption (kWh/m3) of Building A7 of Typology 01.

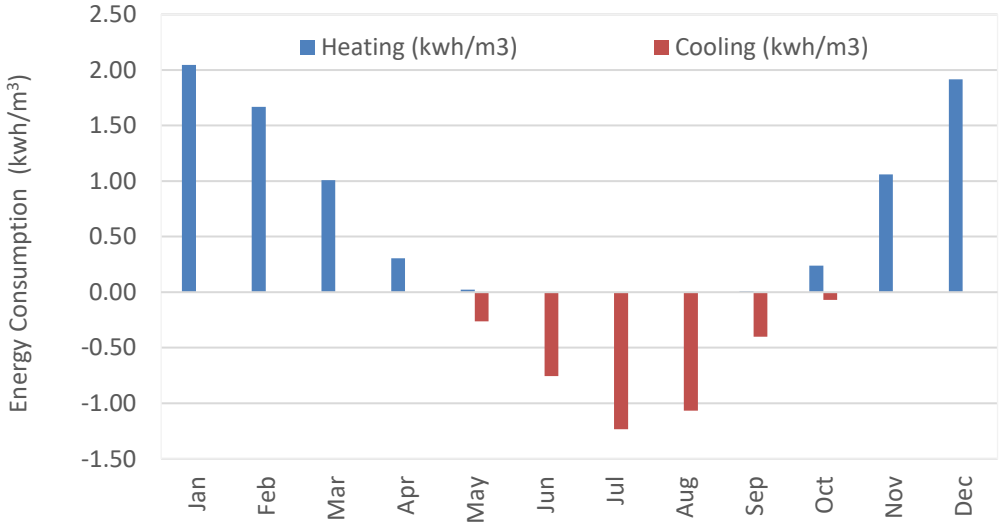

Figure 75. Monthly Heating and Cooling Energy Consumption (kWh/m3) of Building A8 of Typology 01.

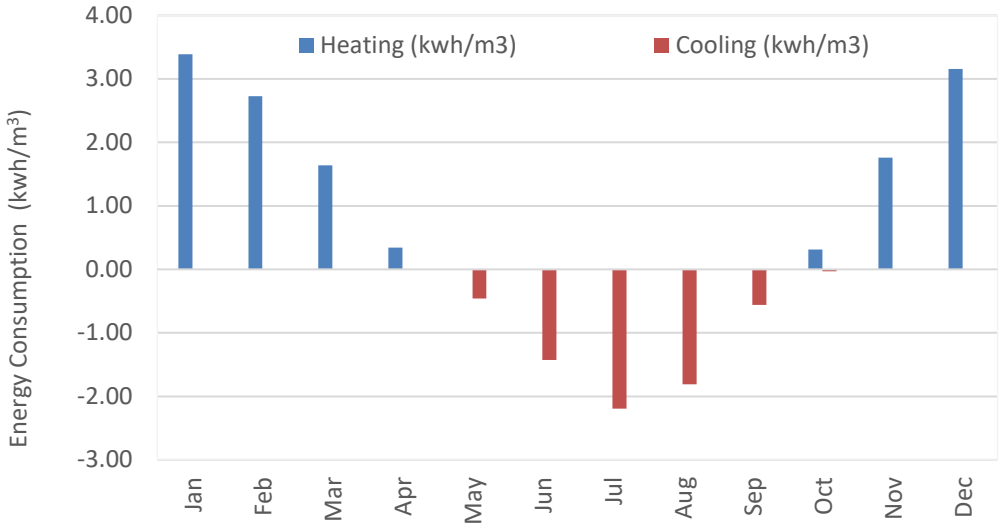

Figure 76. Monthly Heating and Cooling Energy Consumption (kWh/m3) of Building A9 of Typology 01.

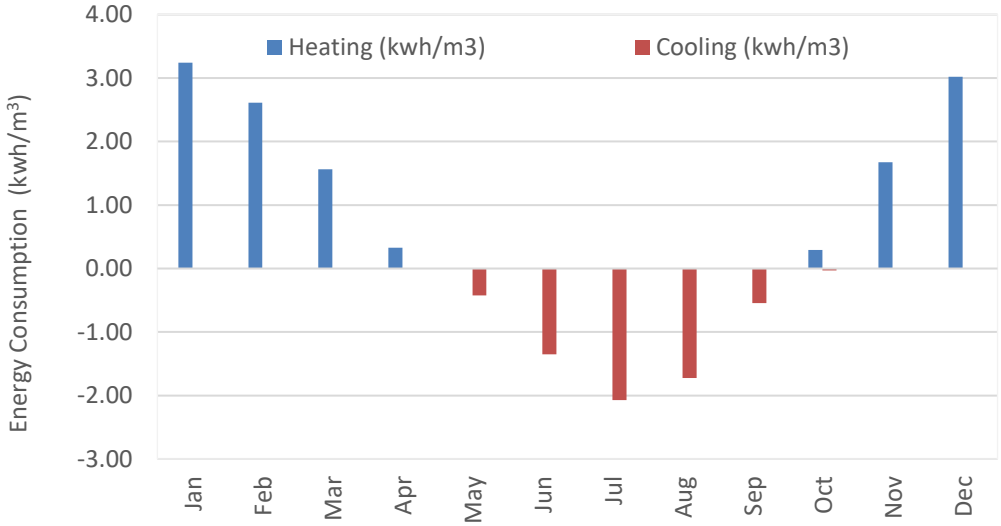

Figure 77. Monthly Heating and Cooling Energy Consumption (kWh/m3) of Building A10 of Typology 01.

4.1.2.2 Annual Energy Consumption

The annual energy consumption results show that throughout a full year, block *A2***,** located in the western part of *Typology 1*, consumes the most energy dedicated to heating (14.89 kWh/m^3), as shown in ***Figure 78*** and cooling (7.52 kWh/m^3), as shown in ***Figure 79***, while block *A8* spends the least energy for heating and cooling purposes, (8.27 kWh/m^3) and (3.50 kWh/m^3) respectively. The overall energy consumption for both heating and cooling, has the highest value (22.41 kWh/m^3) in block *A2* and the lowest value (11.77 kWh/m^3) in block *A8,* as shown in ***Figure 80.***

Block *A2* is situated on the western side of the site and has the highest *GSI* value (0.42), as shown in ***Figure 20 Chapter 3***, lowest *FSI* (1.90), as shown in ***Figure 21 Chapter 3,*** lowest *Hbld* (15.77), as shown in ***Figure 23 Chapter 3,*** lowest *V/A* ratio with a value of (6.65), as shown in ***Figure 24 Chapter 3,*** highest *Building Aspect ratio* with a value of (0.24), as shown in ***Figure 25 Chapter 3***, lowest *OSR*, with a value of 0.58, as shown in ***Figure 27 Chapter 3***.

Block *A8* is located on the eastern part of *Typology 1* and has the highest value for *FSI* (5.55), as shown in ***Figure 21 Chapter 3***, the highest value for VH_{urb} (2.89), as shown in ***Figure 22 Chapter 3***, highest value for H_{bld} (51.01), as shown in ***Figure 23 Chapter 3***, highest value for *V/A ratio* (16.66), as shown in ***Figure 24 Chapter 3***, lowest value for *Building Aspect Ratio* (0.17), as shown in ***Figure 25 Chapter 3*** and highest value for *SF* (0.42), as shown in ***Figure 26 Chapter 3***.

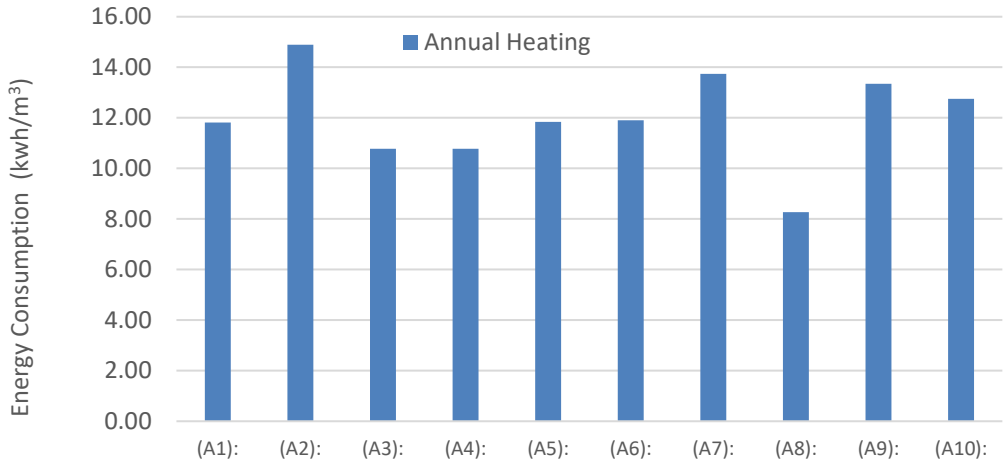

Figure 78. Annual Heating Energy Consumption (kWh/m^3) of Typology 1.

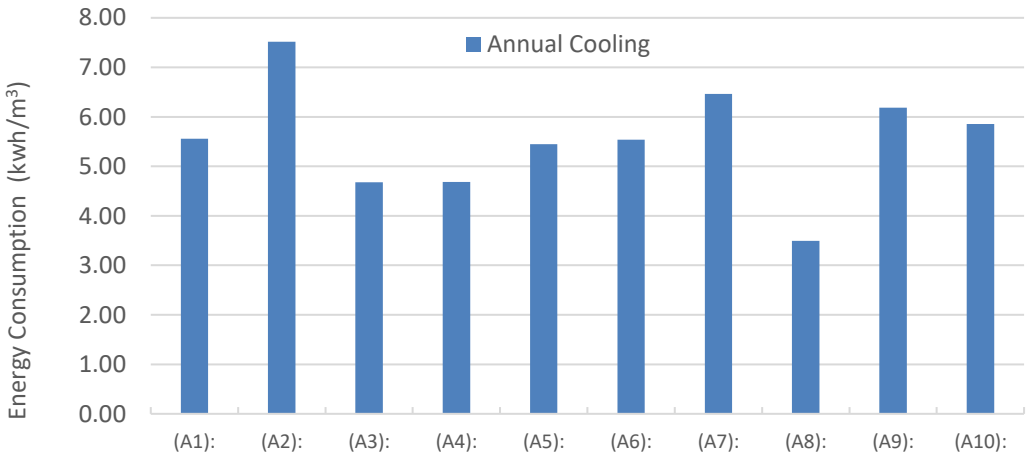

Figure 79. Annual Cooling Energy Consumption (kWh/m^3) of Typology 1.

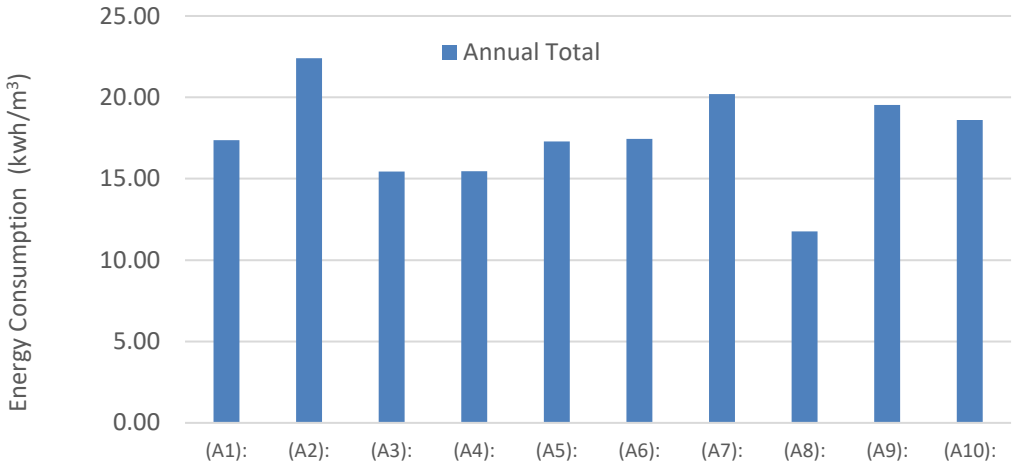

Figure 80. Annual Total Energy Consumption (kWh/m^3) of Typology 1.

4.1.2.3 Surface Temperature

Figure 81 shows the surface temperature variations, for block *A10* of *Typology 1*, outer and courtyard facades, during a full day on Summer Solstice, while ***Figure 82,*** shows the surface temperature variations for the same block and same facades during a full day on Winter Solstice.

On Summer Solstice, the highest temperatures are reached by façade *S3*, which is an outer façade, oriented towards west and has the highest temperature value reaching up to 92 °C, at 16:00, closely followed by *S7* with 88 °C, a western façade located in the inner courtyard of the building. On the other hand, both outer and inner facades reach the lowest temperatures at 4:00-5:00 AM, with S2 facing east and S4 facing North, both reaching a temperature of 17 °C during Summer Solstice, as shown in ***Figure 81***.

During Winter Solstice, the highest temperatures are reached between 12:00 PM and 15:00 PM, with outer façade *S1*, facing south, reaching a temperature of 63 °C, closely followed by the inner façade *S7*, facing west, reaching a temperature of 60 °C. The lowest temperature values are reached between 7:00 AM-8:00 Am, with all of them going as low as -1 °C, as shown in ***Figure 82***.

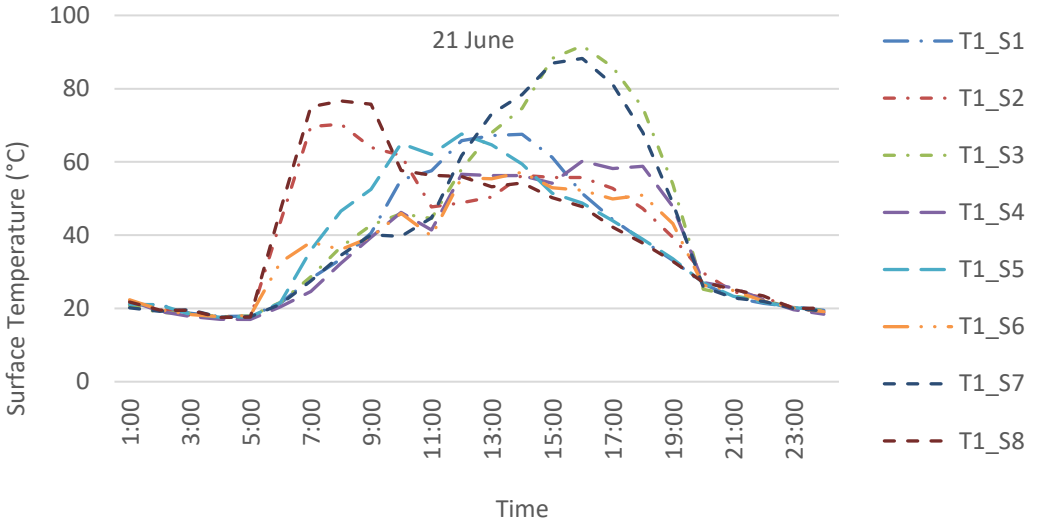

Figure 81. Surface temperatures for building A10 of Typology 1, on Summer Solstice.

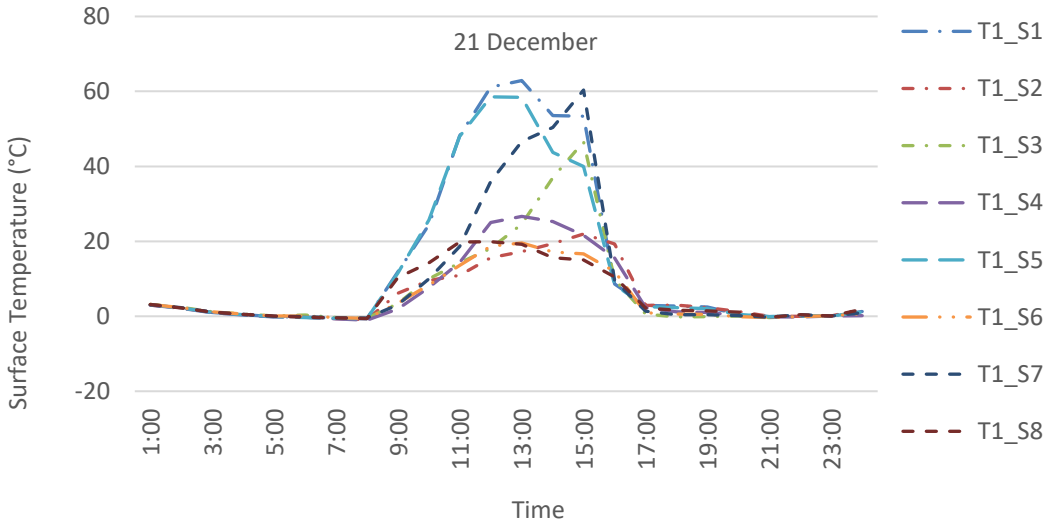

Figure 82. Surface temperatures for building A10 of Typology 1, on Winter Solstice.

4.2 Typology 2

4.2.1 Overview

For Typology 2, the energy simulations are conducted with CitySim Pro. All the data is interpreted and categorized into monthly heating and cooling loads, in kwh/m^3. Also, the surface temperatures are generated and grouped for two days of the year: Summer Solstice and Winter Solstice. The results are sorted for a full day on both of them.

A single building block, *A101*, is chosen to analyze the surface temperatures results. All 8 facades are taken into account, and are assembled into two categories: Inner facades, the ones facing the courtyard, shown in ***Figure 83*** and outer facades, the ones on the outer envelope of the building, shown in ***Figure 84***.

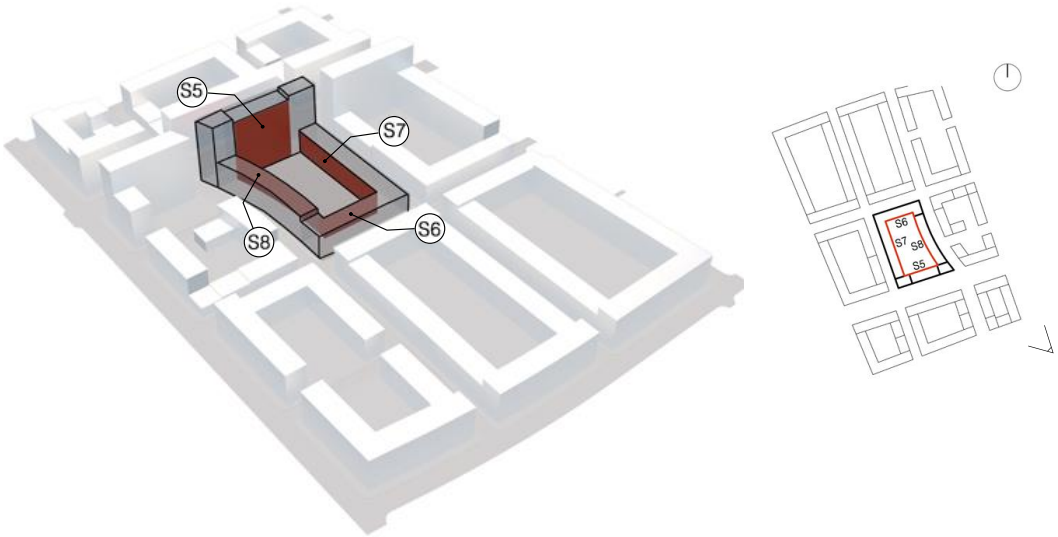

Figure 83. Inner facades of building A101, Typology 2.

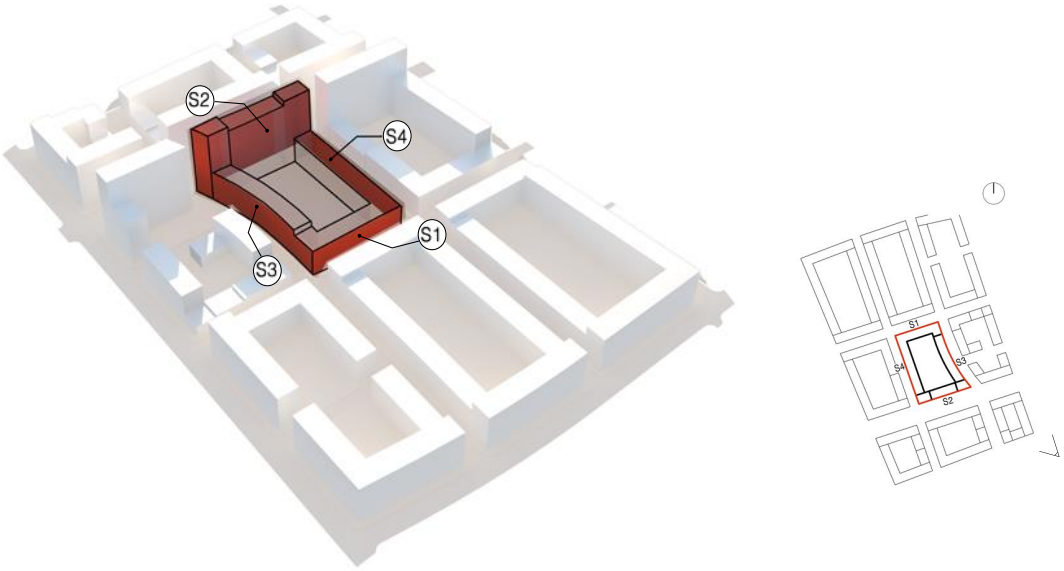

Figure 84. Outer facades of building A101, Typology 2.

4.2.2 Energy Consumption

4.2.2.1 Monthy Energy Consumption

Figure 85 to ***Figure 95*** illustrates the monthly heating and cooling energy consumption for each builing of the *Typology 2*. The month of January has the highest heating demand throughout all the buildings, with block *A100* spending the most during this period of time (4.36 kwh/m^3), as shown in ***Figure 90***. For the cooling demand, during the month of July, every building in this typology has the highest energy consumption. Again, the same block, *A100*, consumes the most energy for cooling purposes during this interval, shown in ***Figure 90***.

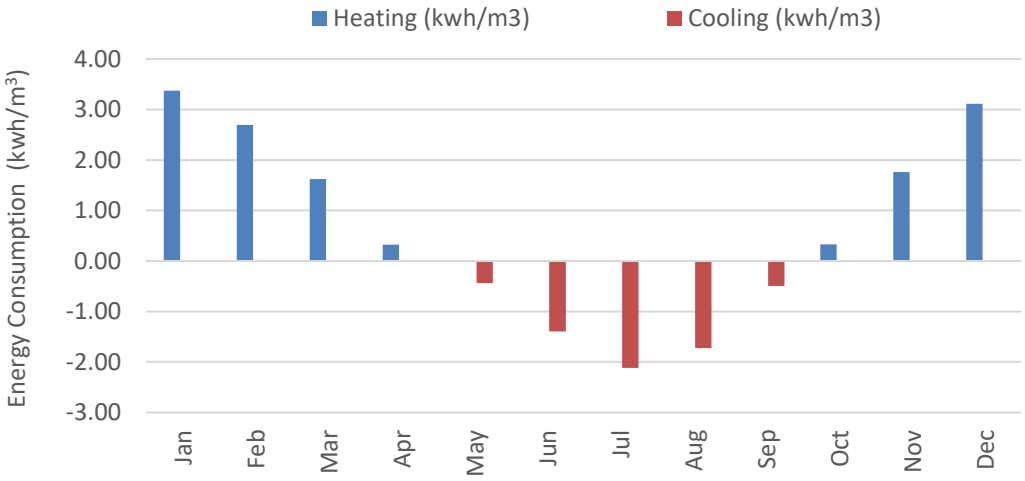

Figure 85. Monthly Heating and Cooling Energy Consumption (kWh/m3) of Building A86 of Typology 2.

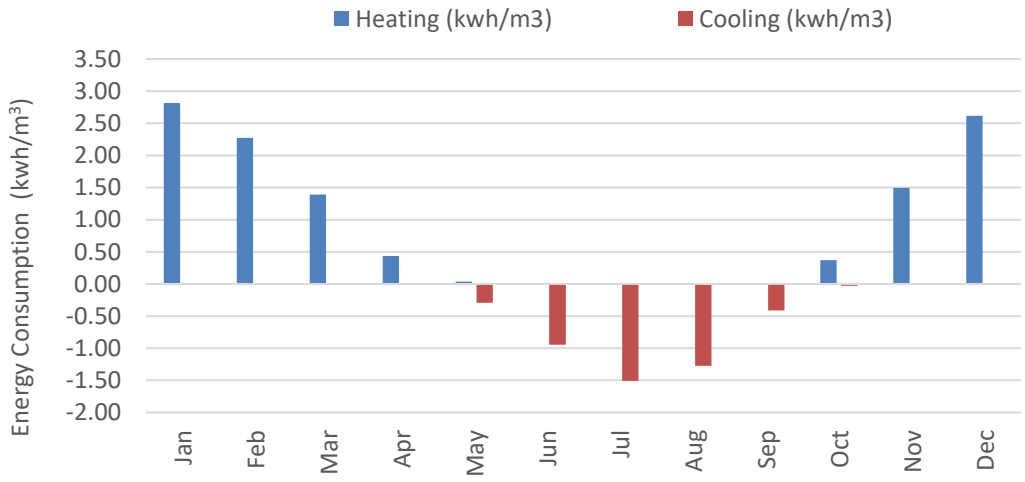

Figure 86. Monthly Heating and Cooling Energy Consumption (kWh/m3) of Building A87 of Typology 2.

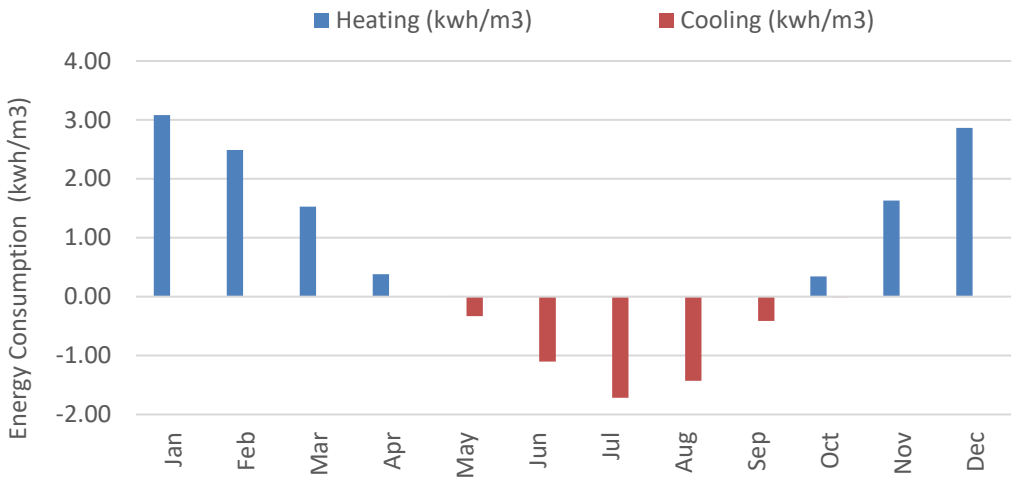

Figure 87. Monthly Heating and Cooling Energy Consumption (kWh/m3) of Building A97 of Typology 2.

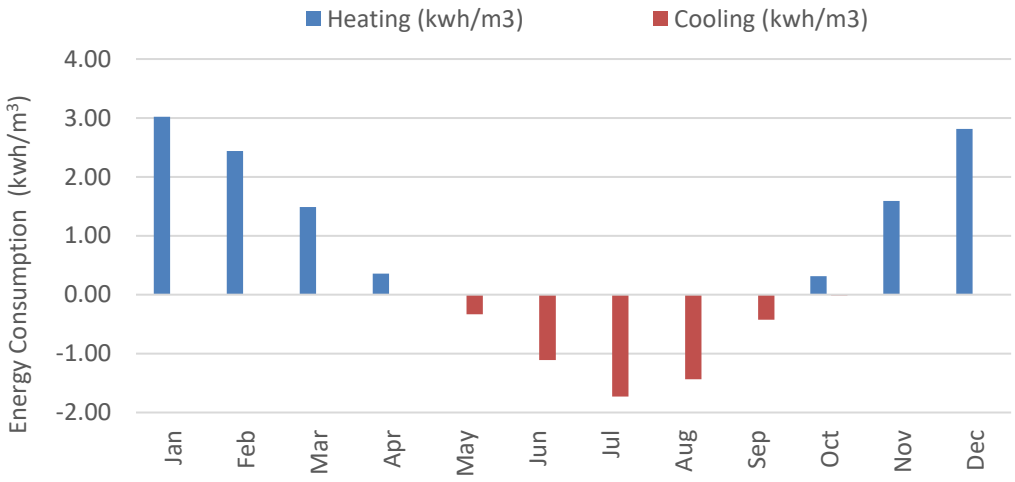

Figure 88. Monthly Heating and Cooling Energy Consumption (kWh/m3) of Building A98 of Typology 2.

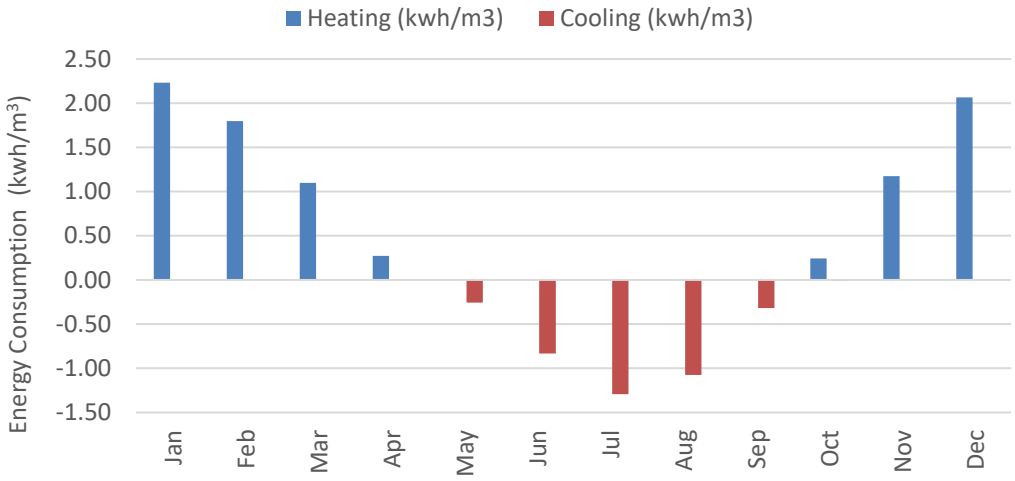

Figure 89. Monthly Heating and Cooling Energy Consumption (kWh/m3) of Building A99 of Typology 2.

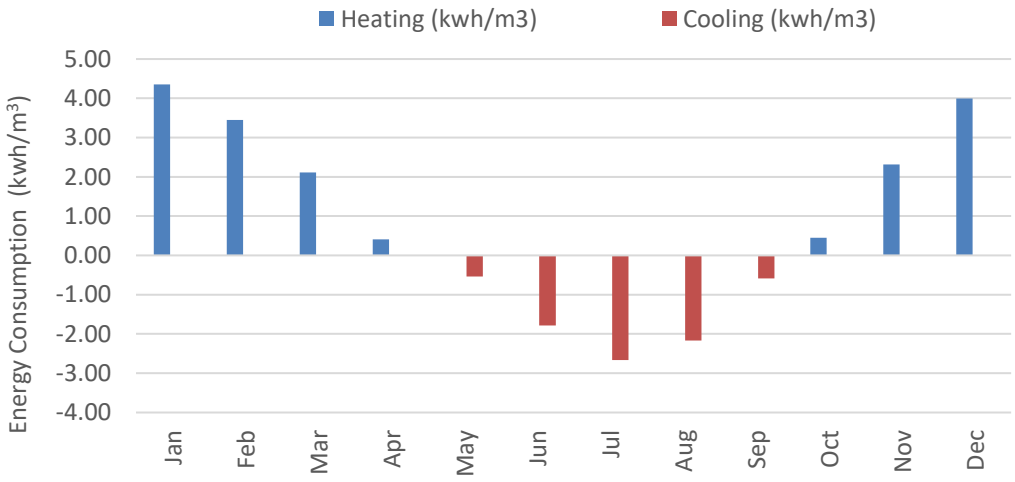

Figure 90. Monthly Heating and Cooling Energy Consumption (kWh/m3) of Building A100 of Typology 2.

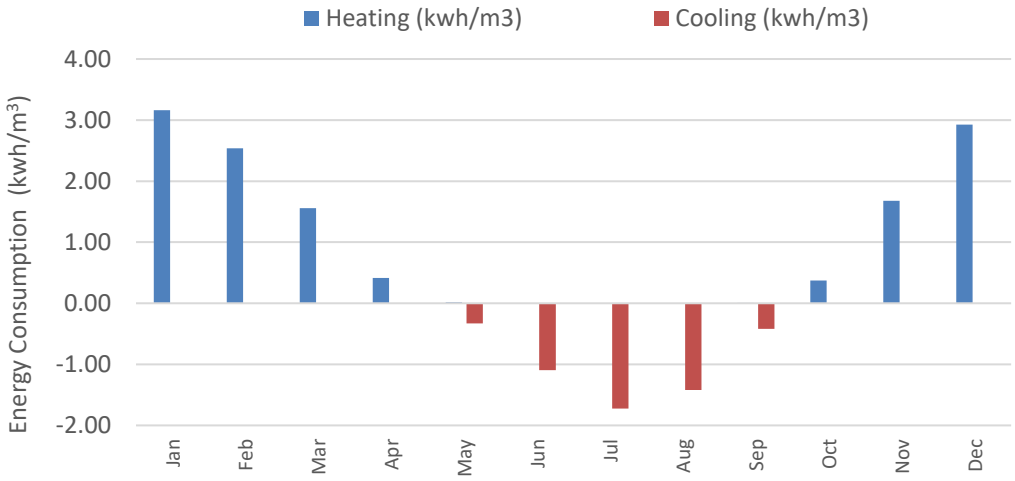

Figure 91. Monthly Heating and Cooling Energy Consumption (kWh/m3) of Building A101 of Typology 2.

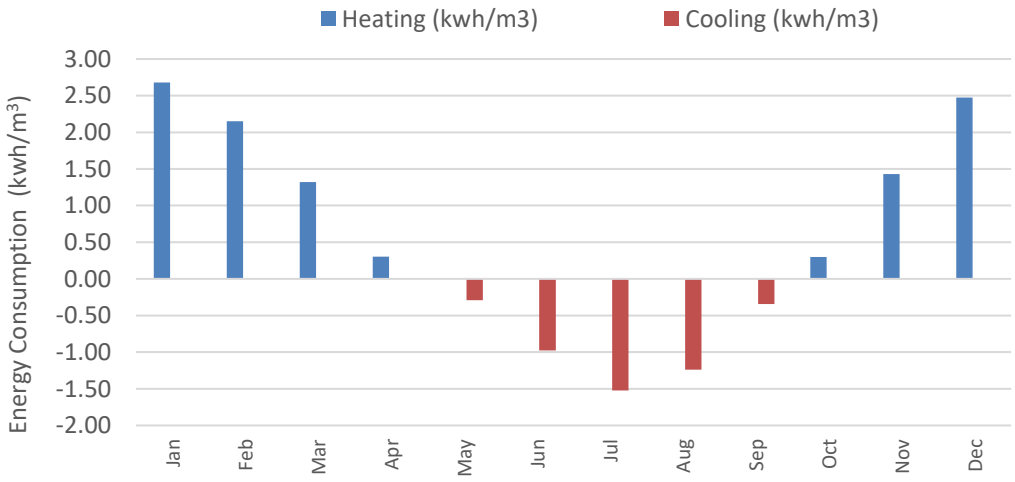

Figure 92. Monthly Heating and Cooling Energy Consumption (kWh/m3) of Building A102 of Typology 2.

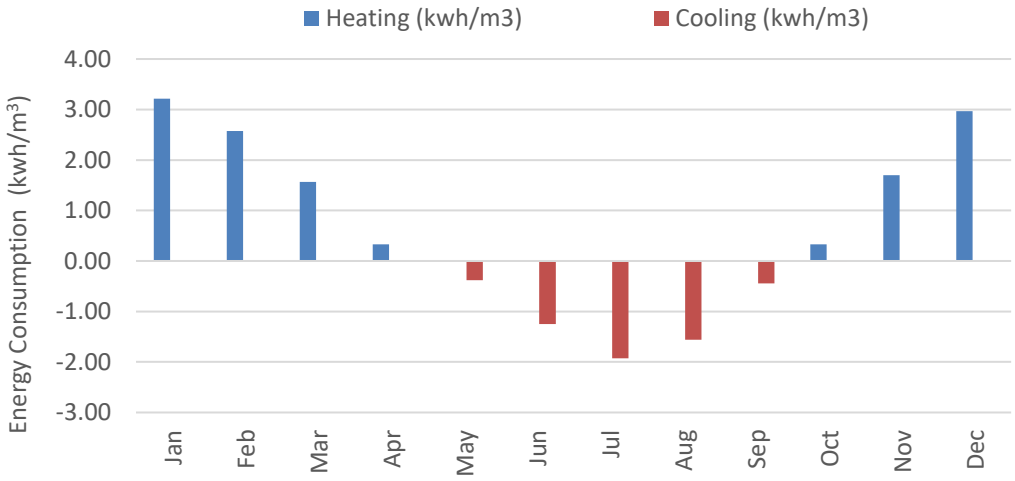

Figure 93. Monthly Heating and Cooling Energy Consumption (kWh/m3) of Building A103 of Typology 2.

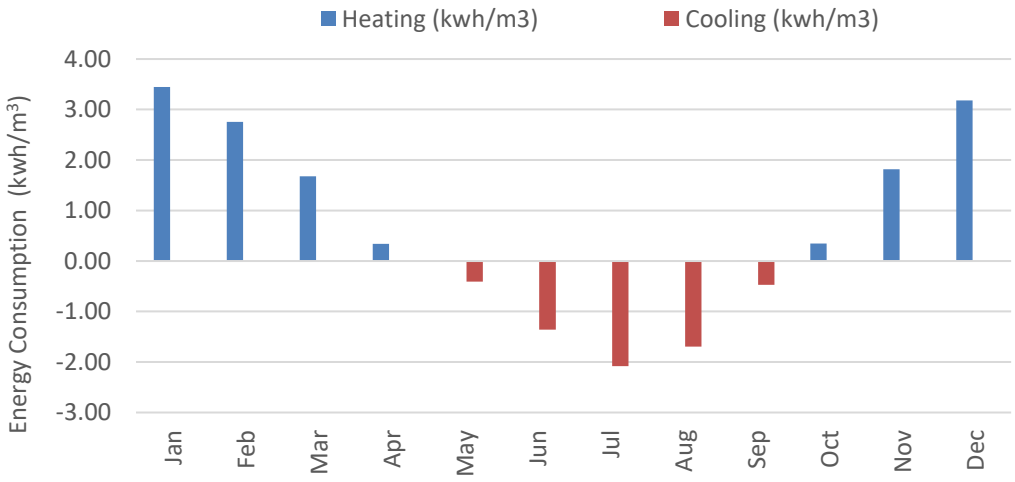

Figure 94. Monthly Heating and Cooling Energy Consumption (kWh/m3) of Building A104 of Typology 2.

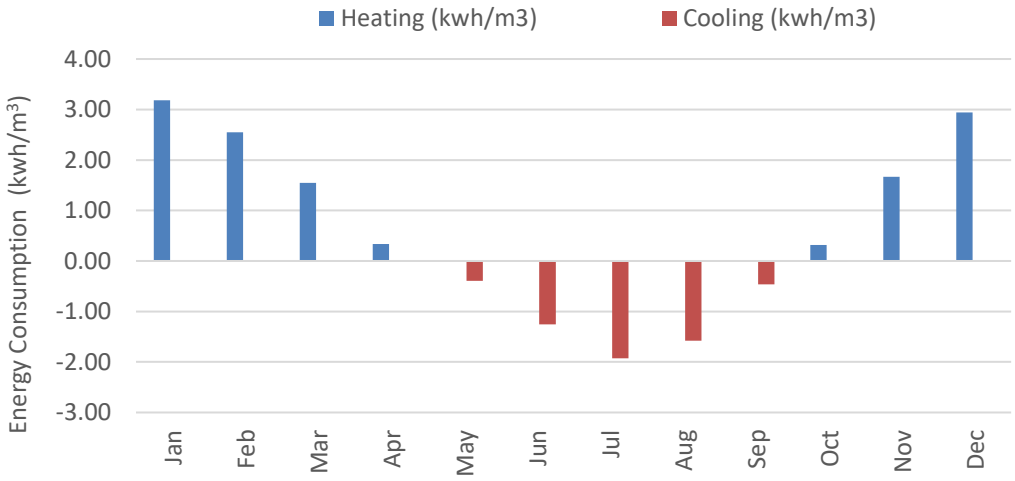

Figure 95. Monthly Heating and Cooling Energy Consumption (kWh/m3) of Building A105 of Typology 2.

4.2.2.2 Annual Energy Consumption

The annual energy consumption results show that throughout a full year, block *A100**,*** located in the eastern part of *Typology 2*, consumes the most energy dedicated to heating (17.09 kWh/m^3), as shown in ***Figure 96*** and cooling (7.51 kWh/m^3), as shown in ***Figure 97***, while block *A99* spends the least energy for heating and cooling purposes, (8.90 kWh/m^3) and (3.63 kWh/m^3) respectively. The overall energy consumption for both heating and cooling, has the highest value (24.60 kWh/m^3) in block *A100* and the lowest value (12.53 kWh/m^3) in block *A99*, as shown in ***Figure 98.***

A100 is located on the eastern side of the site and has the lowest *FSI* value (1.89) as shown in ***Figure 29 Chapter 3***, lowest H_{bld} value (14.82), as shown in ***Figure 31 Chapter 3***, lowest *V/A* ratio value (5.68), as shown in ***Figure 32 Chapter 3***,and lowest *SF* value (0.28), as shown in ***Figure 34 Chapter 3***.

Block *A99* is located on the south-eastern part of *Typology 2* and has the highest value for *GSI* (0.40), as shown in ***Figure 28 Chapter 3***, the highest value for *FSI* (4.78), as shown in ***Figure 29 Chapter 3***, the highest value for VH_{urb} (3.32), as shown in

Figure 30 Chapter 3, highest value together with building *A87* which is slightly higher, for H_{bld} (35.47), as shown in ***Figure 31 Chapter 3***, highest value for *V/A ratio* (14.34), as shown in ***Figure 32 Chapter 3***, lowest value for *OSR* (0.60), as shown in ***Figure 35 Chapter 3***.

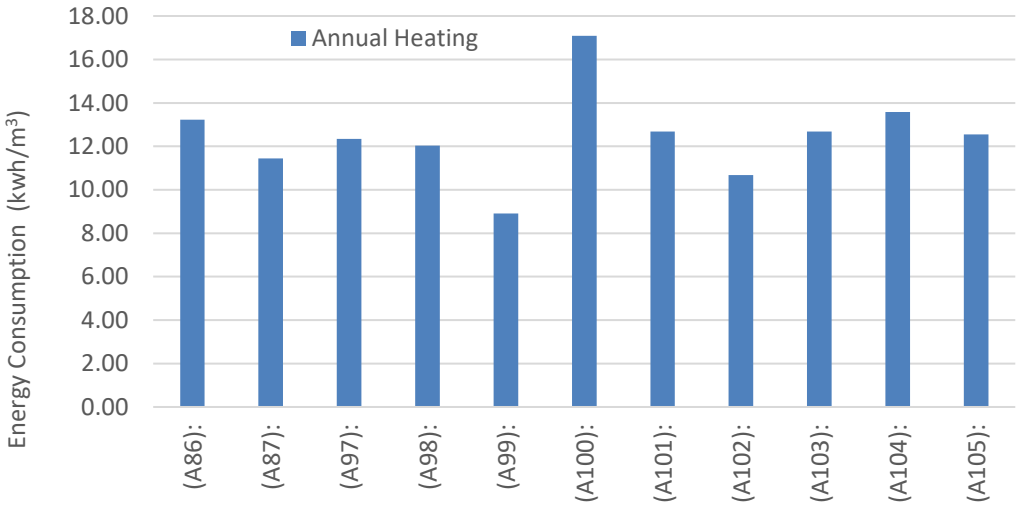

Figure 96. Annual Heating Energy Consumption (kWh/m^3) of Typology 2.

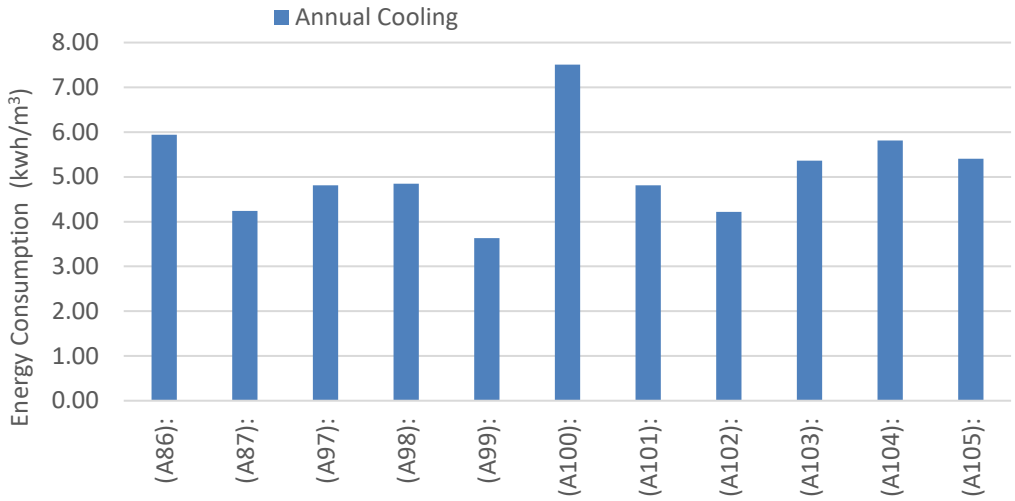

Figure 97. Annual Cooling Energy Consumption (kWh/m^3) of Typology 2.

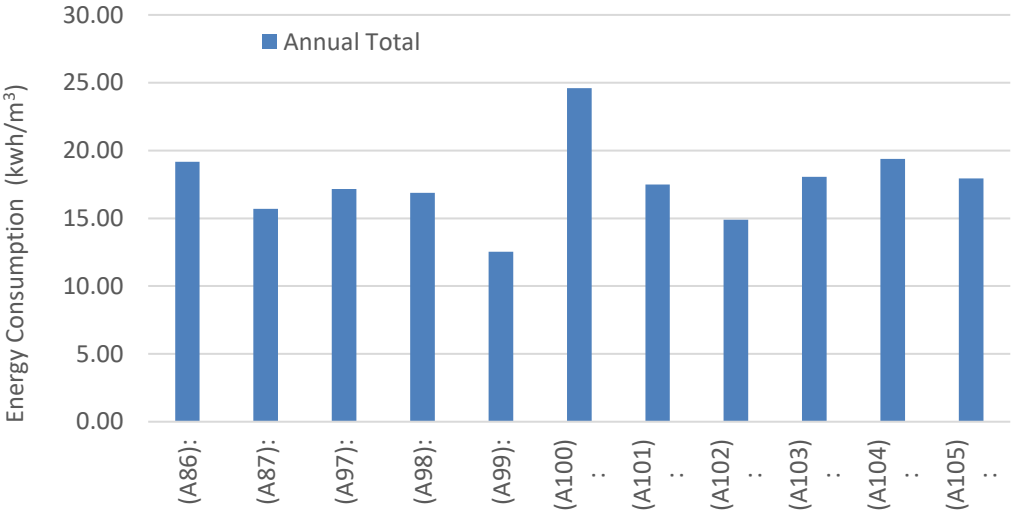

Figure 98. Annual Total Energy Consumption (kWh/m^3) of Typology 2.

4.2.2.3 Surface Temperature

Figure 99 shows the surface temperature variations, for block *A101* of *Typology 2*, outer and courtyard facades, during a full day on Summer Solstice, while ***Figure 100,*** shows the surface temperature variations for the same block and same facades during a full day on Winter Solstice.

On Summer Solstice, the highest temperatures are reached by façade *S8*, which is an inner façade, oriented towards west and has the highest temperature value reaching up to 88 °C, at 15:00, followed by *S4* with 81 °C, a western façade located on the outer part of the building. On the other hand, both outer and inner facades reach the lowest temperatures at 4:00-5:00 AM, with all of them having temperatures of 17 °C-18 °C during Summer Solstice, as shown in ***Figure 99***.

During Winter Solstice, the highest temperatures are reached between 12:00 PM and 15:00 PM, with inner façade *S6*, facing south, reaching a temperature of 51 °C, followed by the outer façade *S2*, facing south, reaching a temperature of 41 °C. The lowest temperature values are obtained between 7:00 AM-8:00 Am, with all of them going as low as -1 °C, as shown in ***Figure 100***.

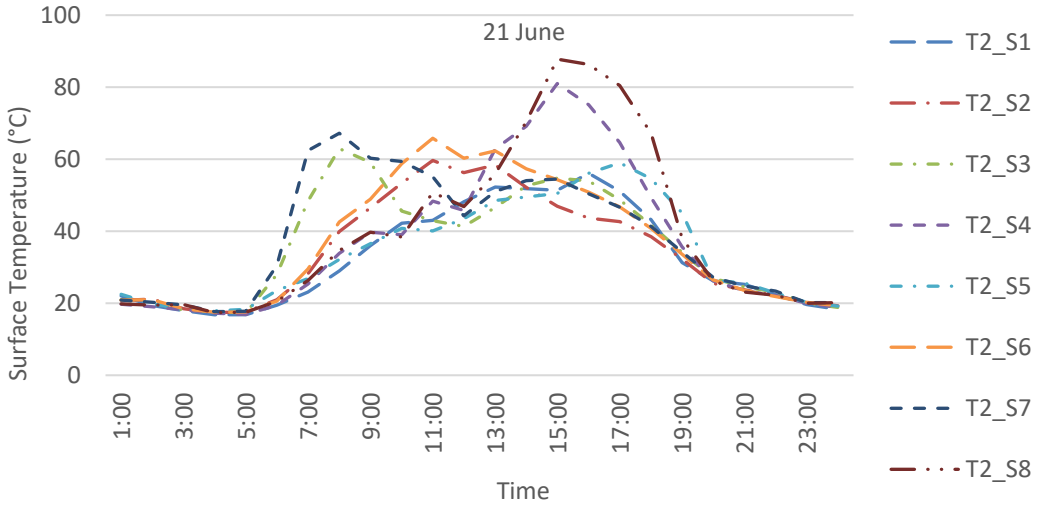

Figure 99. Surface temperatures for building A101 of Typology 2, on Summer Solstice.

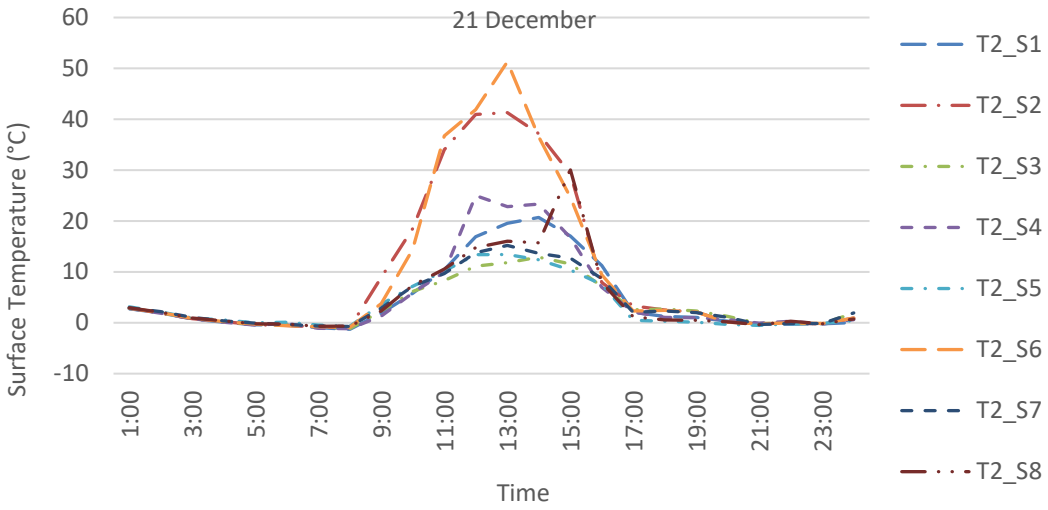

Figure 100. Surface temperatures for building A101 of Typology 2, on Winter Solstice.

4.3 Typology 3

4.3.1 Overview

For *Typology 3*, the energy simulations are conducted with CitySim Pro. All the data is interpreted and categorized into monthly heating and cooling loads, in kwh/m^3. Also, the surface temperatures are generated and grouped for two days of the year: Summer Solstice and Winter Solstice. The results are sorted for a full day on both of them.

A portion of building block *A28*, is chosen to analyze the surface temperatures results. Five facades are considered for this geometry, as the original block has a distinct shape differing from the rest of the typologies, and are assembled into two categories: inner facades, the ones facing the courtyard, shown in ***Figure 101*** and outer facades, the ones on the outer envelope of the building, shown in ***Figure 102***. The first has 4 chosen facades facing the courtyard while the latter has only one facing the main axis of the site.

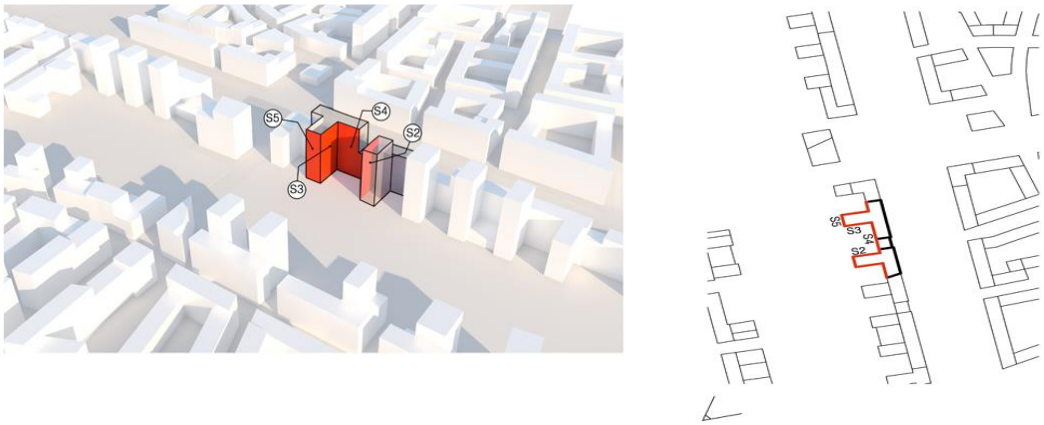

Figure 101. Inner facades of building A28, Typology 3.

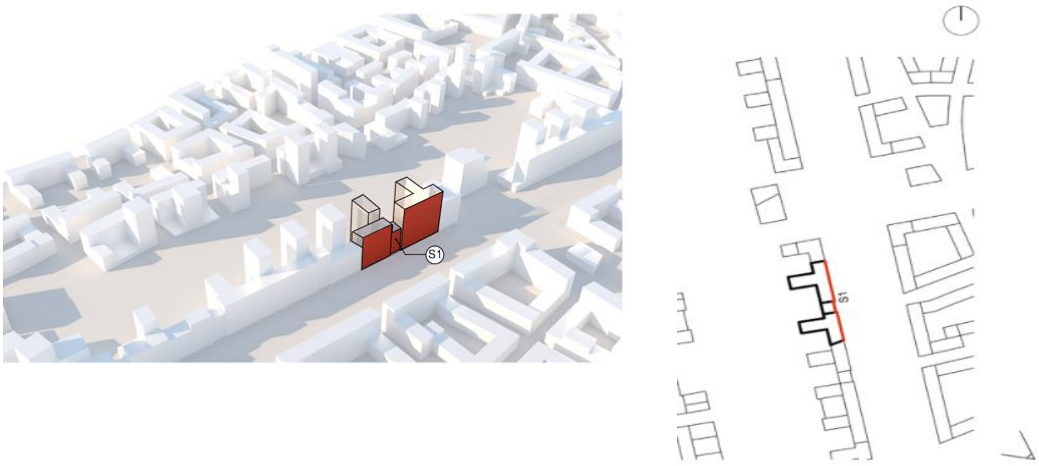

Figure 102. Outer facades of building A28, Typology 3.

4.3.2 Energy Consumption

4.3.2.1 Monthly Energy Consumption

Figure 103 and ***Figure 104*** show the monthly heating and cooling energy consumption of both building blocks of Typology 3. January is the month with the highest heating energy consumption, while July is the month with the highest cooling energy consumption. Specifically block *A28* has the highest demand for both of them

with (3.10 kwh/m^3) for heating and (1.53 kwh/m^3) for cooling, as shown in ***Figure 104.***

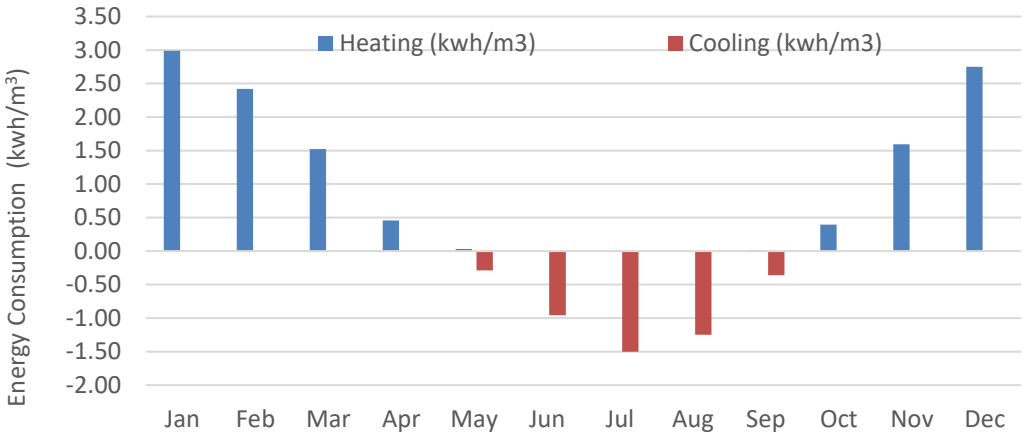

Figure 103. Monthly Heating and Cooling Energy Consumption (kWh/m3) of Building A27 of Typology 3.

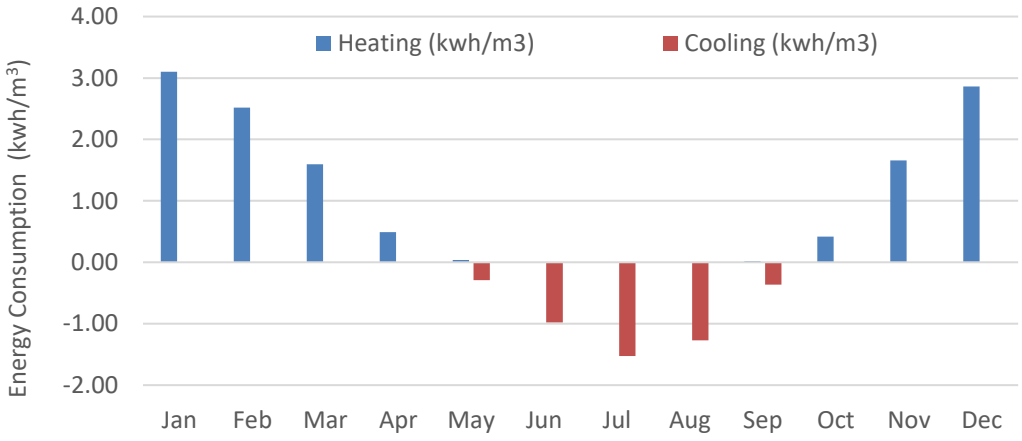

Figure 104. Monthly Heating and Cooling Energy Consumption (kWh/m3) of Building A28 of Typology 3.

4.3.2.2 Annual Energy Consumption

The annual energy consumption results show that throughout a full year, block ***A28,*** located in the southern part of *Typology 3*, consumes the most energy dedicated to heating (12.71 kWh/m^3), as shown in ***Figure 105*** and cooling (4.28 kWh/m^3), as shown in ***Figure 106***, while block *A27* spends the least energy for heating and cooling purposes, (12.19 kWh/m^3) and (4.20 kWh/m^3) respectively. The overall energy consumption for both heating and cooling, has the highest value (16.98 kWh/m^3) in block *A28* and the lowest value (16.38 kWh/m^3) in block *A27*, as shown in ***Figure 107.***

Both *A27* and *A28* blocks are similar in morphological terms with the only distinction that block *A28* is located more southwards and has a larger volume, which makes for larger building walls area and thus to a larger value of VH_{urb} (1.87), as shown in ***Figure 38 Chapter 3***.

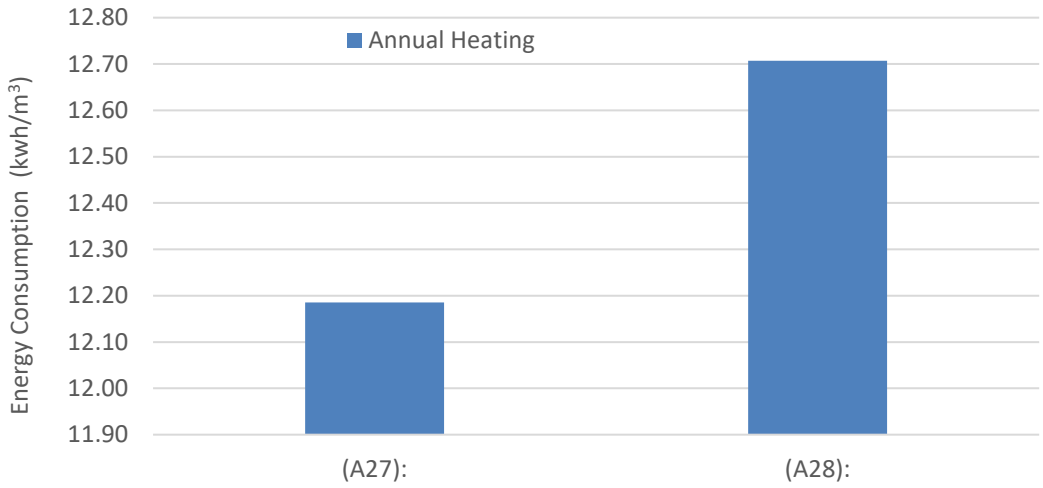

Figure 105. Annual Heating Energy Consumption (kWh/m^3) of Typology 3.

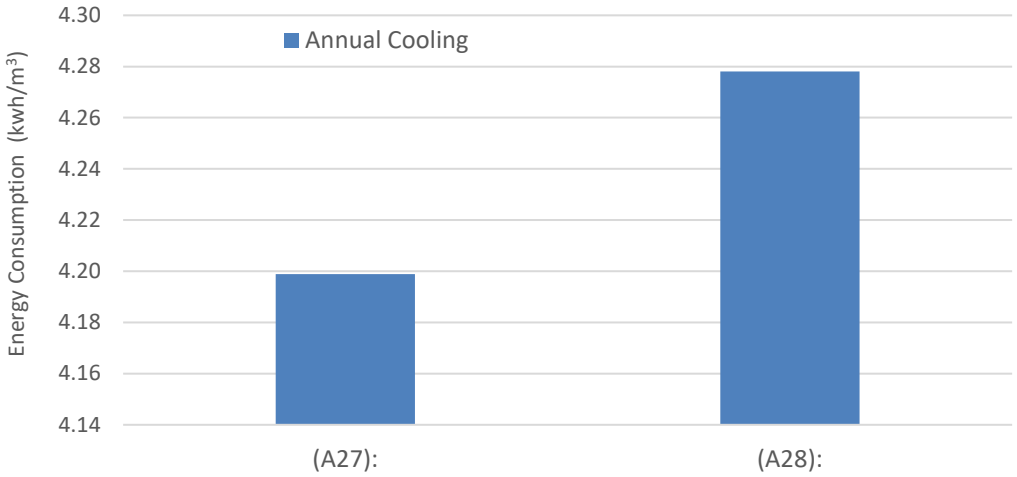

Figure 106. Annual Cooling Energy Consumption (kWh/m^3) of Typology 3.

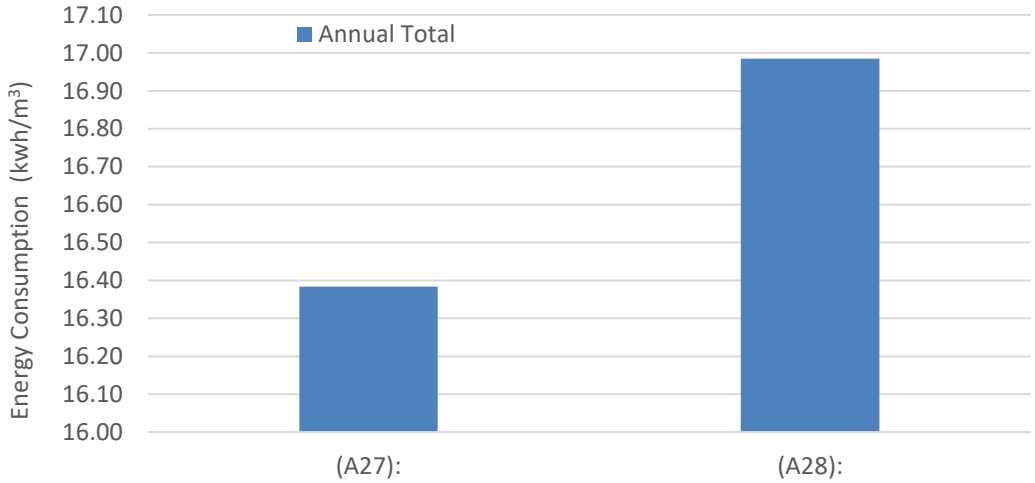

Figure 107. Annual Total Energy Consumption (kWh/m^3) of Typology 3.

4.3.2.3 Surface Temperature

Figure 108 shows the surface temperature variations, for block *A28* of *Typology 3*, outer and courtyard facades, during a full day on Summer Solstice, while ***Figure 109,*** shows the surface temperature variations for the same block and same facades during a full day on Winter Solstice.

On Summer Solstice, the highest temperatures are reached by façade *S5*, which is an inner façade, oriented towards west and has the highest temperature value reaching up to 88 °C, at 16:00, followed by *S4* with 80 °C, also an adjacent western façade located on the inner part of the building. On the other hand, both outer and inner facades reach the lowest temperatures at 4:00-5:00 AM, with all of them having temperatures of 17 °C-18 °C during Summer Solstice, as shown in ***Figure 108***.

During Winter Solstice, the highest temperatures are reached between 12:00 PM and 14:00 PM, with inner façade *S3*, facing south, reaching a temperature of 48 °C, followed by the other inner façade *S5*, facing west, reaching a temperature of 39 °C. The lowest temperature values are obtained between 7:00 AM-8:00 Am, with all of them going as low as -1 °C, as shown in ***Figure 109***.

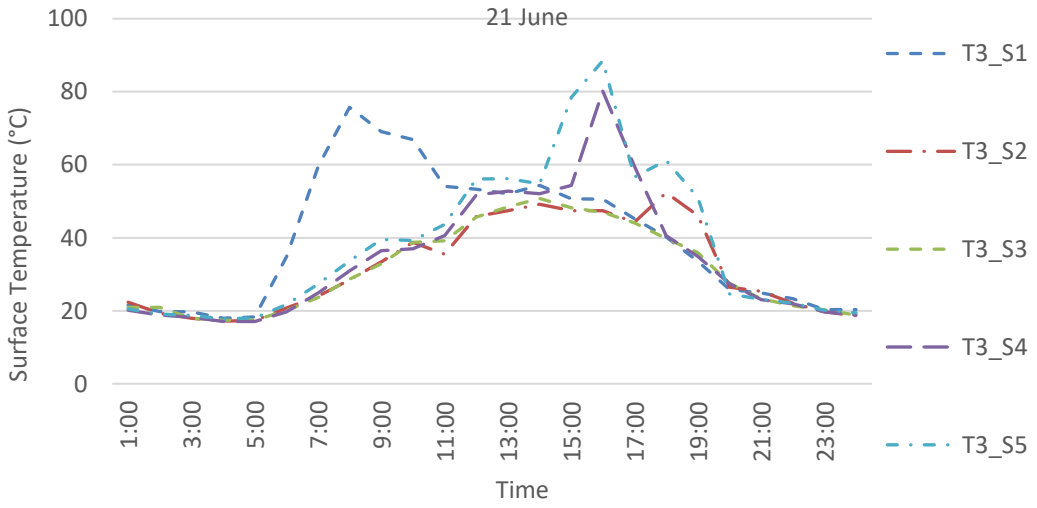

Figure 108. Surface temperatures for building A28 of Typology 3, on Summer Solstice.

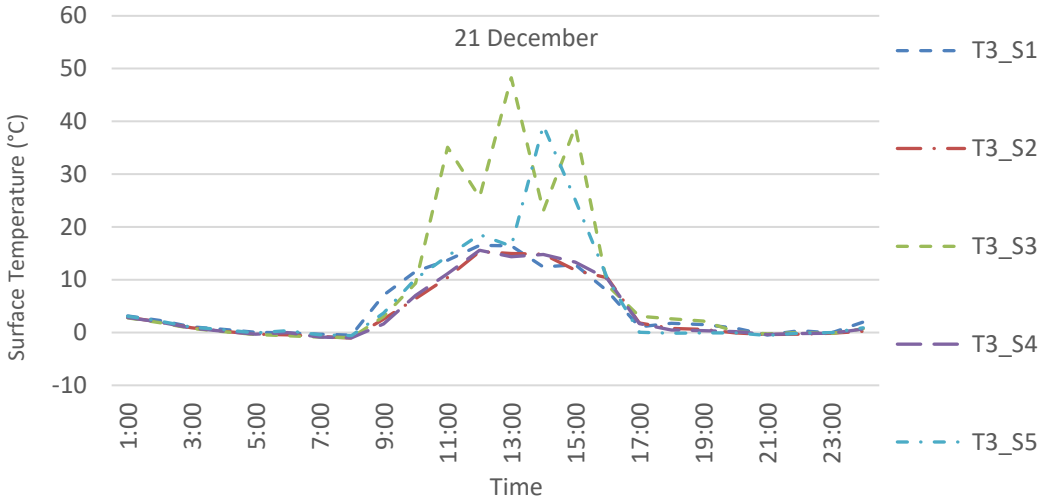

Figure 109. Surface temperatures for building A28 of Typology 3, on Winter Solstice.

4.4 Typology 4

4.4.1 Overview

For *Typology 4*, the energy simulations are conducted with *CitySim Pro*. All the data is interpreted and categorized into monthly heating and cooling loads, in kwh/m^3. Also, the surface temperatures are generated and grouped for two days of the year: Summer Solstice and Winter Solstice. The results are sorted for a full day on both of them.

A single building block, *A42*, is chosen to analyze the surface temperatures results. All 8 facades are taken into account, and are assembled into two categories: inner facades, the ones facing the courtyard, shown in ***Figure 110*** and outer facades, the ones on the outer envelope of the building, shown in ***Figure 111***.

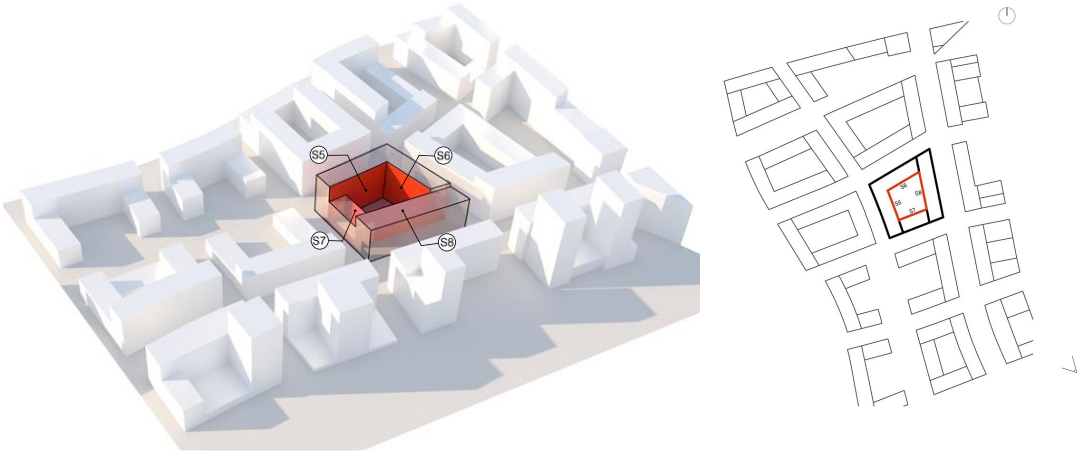

Figure 110. Inner facades of building A42, Typology 4.

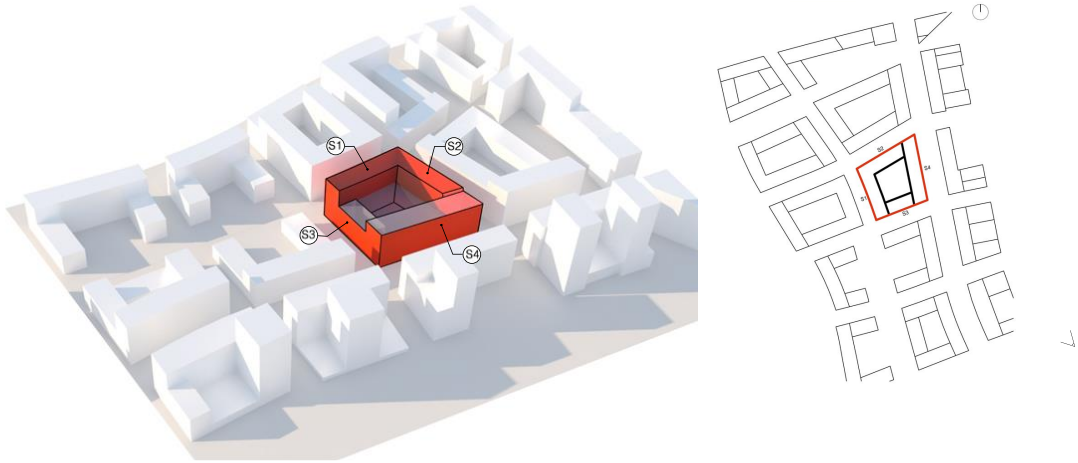

Figure 111. Outer facades of building A42, Typology 4.

4.4.2 Energy Consumption

4.4.2.1 Monthly Energy Consumption

Figure 112 to ***Figure 119*** illustrates the monthly heating and cooling energy consumption of each building of *Typology 4*. The month with the highest heat energy demand is January with block *A44* consuming (4.24 kwh/m^3), as shown in ***Figure 116***,

while July is the month with the highest demand for cooling energy, with the same block, *A44*, consuming (2.63 kwh/m^3), as shown in ***Figure 116***.

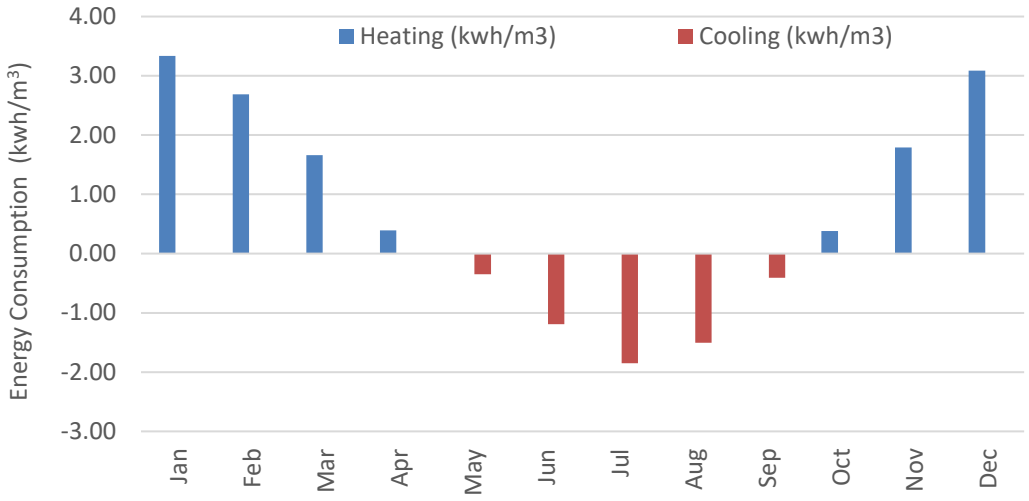

Figure 112. Monthly Heating and Cooling Energy Consumption (kWh/m3) of Building A40 of Typology 4.

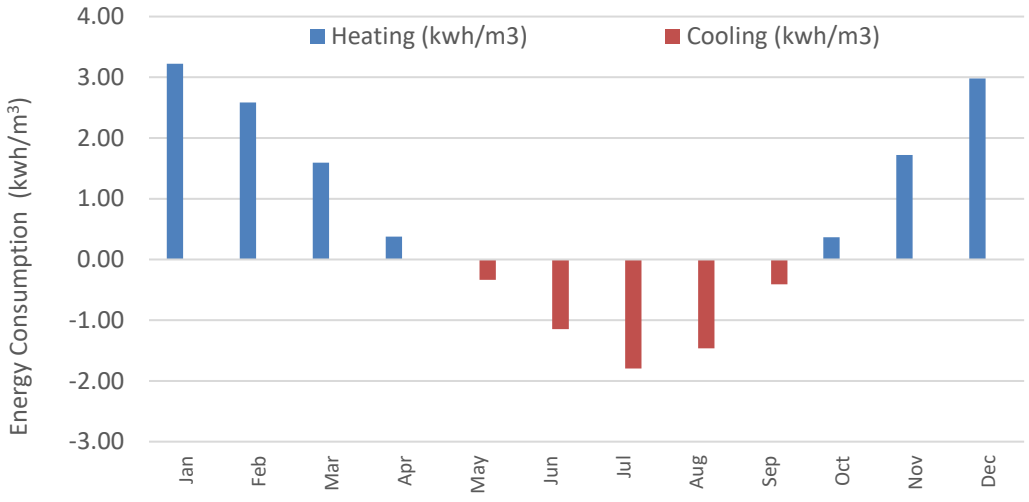

Figure 113. Monthly Heating and Cooling Energy Consumption (kWh/m3) of Building A41 of Typology 4.

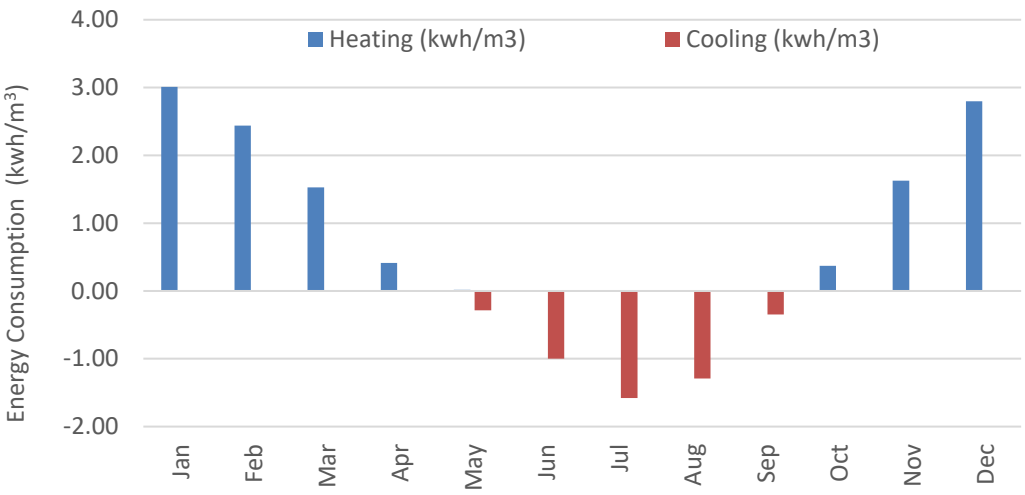

Figure 114. Monthly Heating and Cooling Energy Consumption (kWh/m3) of Building A42 of Typology 4.

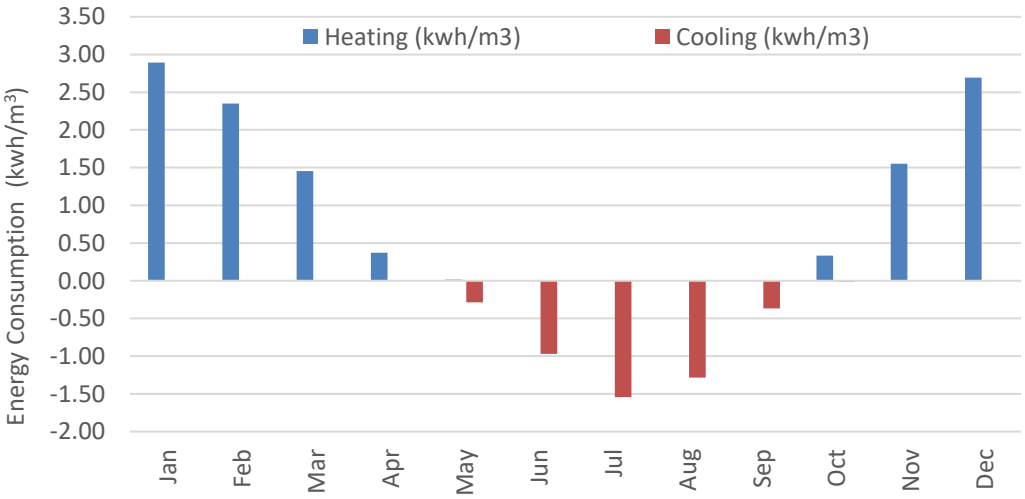

Figure 115. Monthly Heating and Cooling Energy Consumption (kWh/m3) of Building A43 of Typology 4.

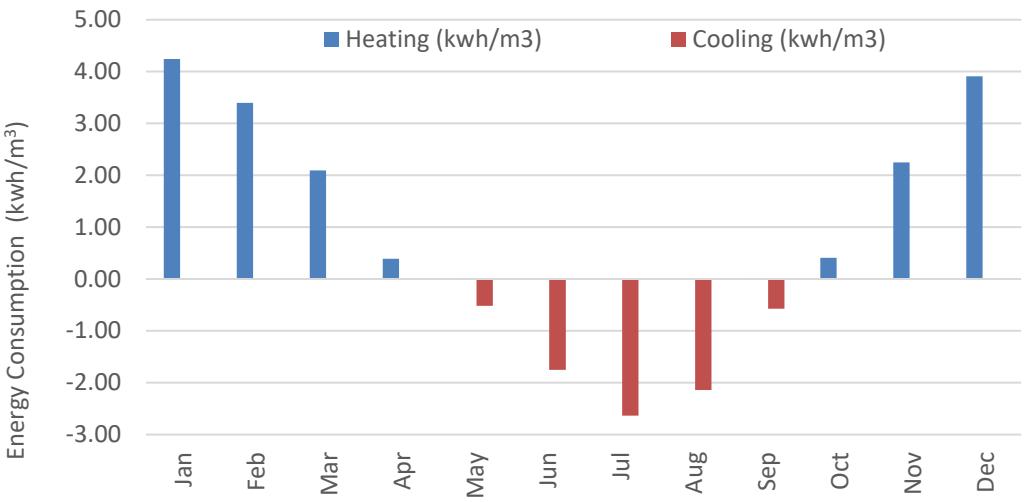

Figure 116. Monthly Heating and Cooling Energy Consumption (kWh/m3) of Building A44 of Typology 4.

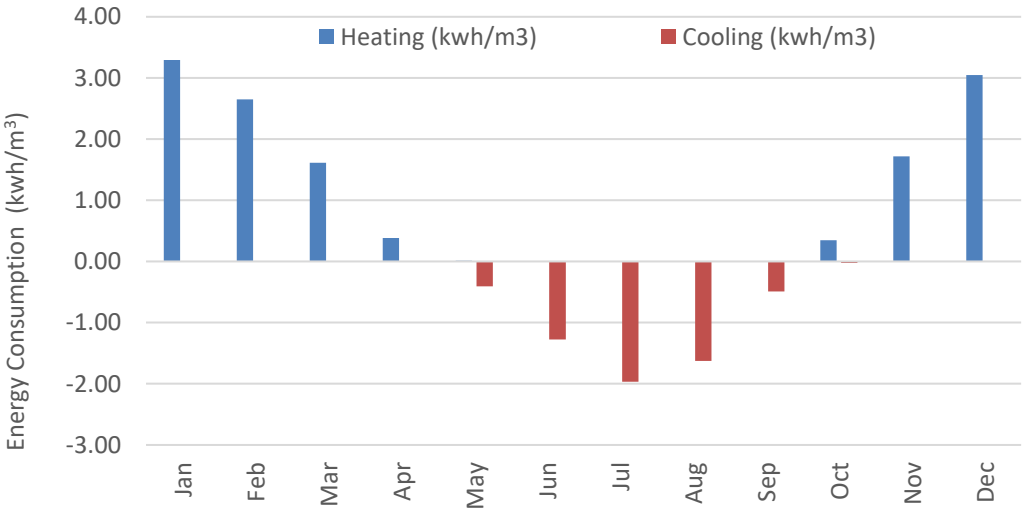

Figure 117. Monthly Heating and Cooling Energy Consumption (kWh/m3) of Building A45 of Typology 4.

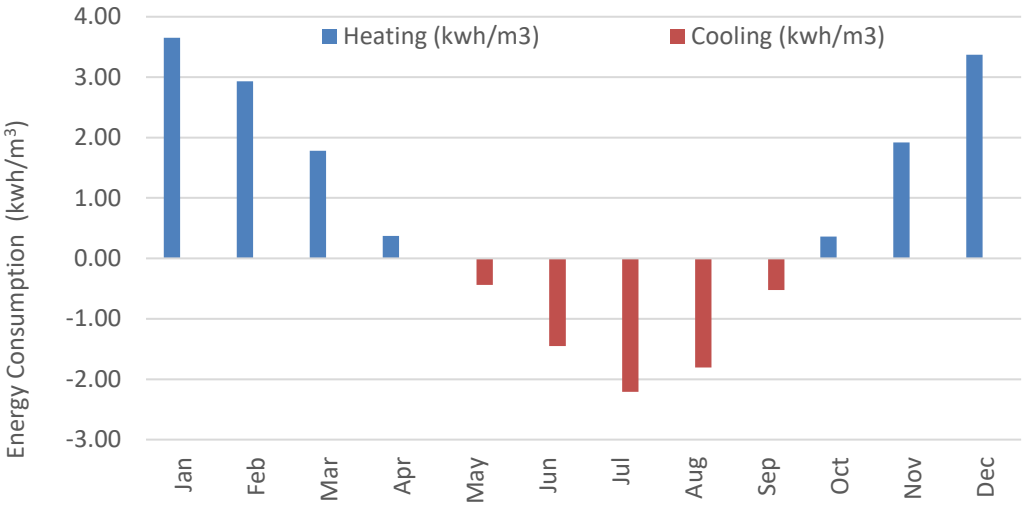

Figure 118. Monthly Heating and Cooling Energy Consumption (kWh/m3) of Building A46 of Typology 4.

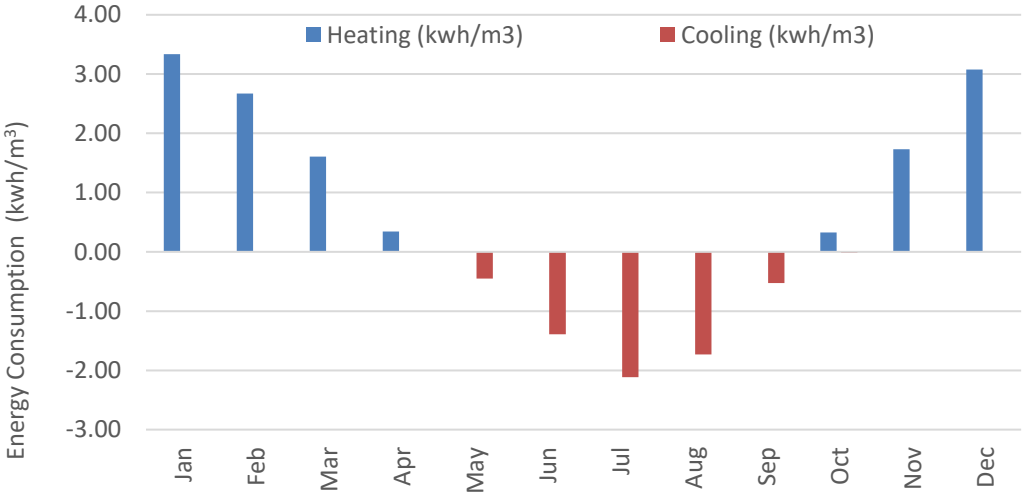

Figure 119. Monthly Heating and Cooling Energy Consumption (kWh/m3) of Building A47 of Typology 4.

4.4.2.2 Annual Energy Consumption

The annual energy consumption results show that throughout a full year, block *A44***,** located in the eastern part of *Typology 4*, consumes the most energy dedicated to

heating (16.72 kWh/m^3), as shown in ***Figure 120*** and cooling (7.39 kWh/m^3), as shown in ***Figure 121***, while block *A43* spends the least energy for heating and cooling purposes, (11.68 kWh/m^3) and (4.30 kWh/m^3) respectively. The overall energy consumption for both heating and cooling, has the highest value (24.11 kWh/m^3) in block *A44* and the lowest value (15.97 kWh/m^3) in block *A43*, as shown in ***Figure 122.***.

Block *A44* is located on the eastern part of *Typology 4* and has the lowest values for *FSI* (1.73), shown in ***Figure 45 Chapter 3***, VH_{urb} (1.31) shown in ***Figure 46 Chapter 3***, *Hbld* (14.56) shown in ***Figure 47 Chapter 3***, *V/A* ratio (5.19) shown in ***Figure 48 Chapter 3***, *SF* (0.24) shown in Figure 45 Chapter 3. On the other hand, it has the highest value for *Building aspect ratio* (0.25) shown in ***Figure 49 Chapter 3***.

Block *A43* is located on the western part of *Typology 4* and has the highest value for *FSI* (3.94), as shown in ***Figure 45 Chapter 3***, highest value for H_{bld} (27.43), as shown in ***Figure 47 Chapter 3***, highest value for *V/A ratio* (11.83), as shown in ***Figure 48 Chapter 3***, lowest value for *Building Aspect Ratio* (0.20), as shown in ***Figure 49 Chapter 3***.

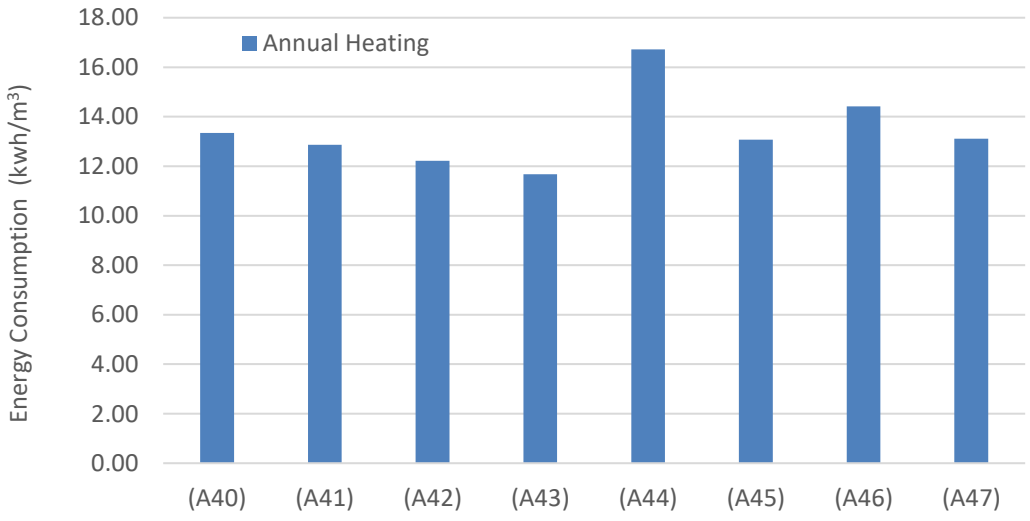

Figure 120. Annual Heating Energy Consumption (kWh/m^3) of Typology 4.

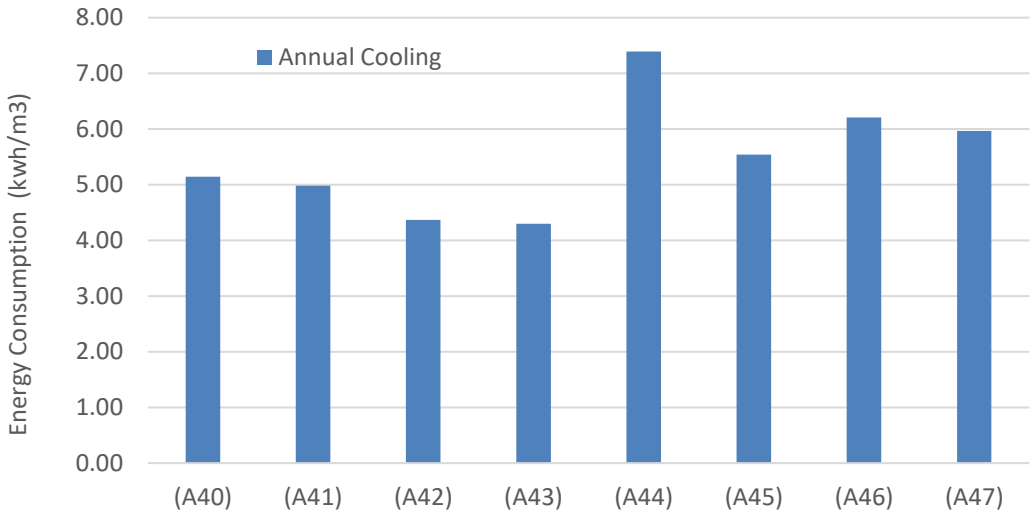

Figure 121. Annual Cooling Energy Consumption (kWh/m^3) of Typology 4.

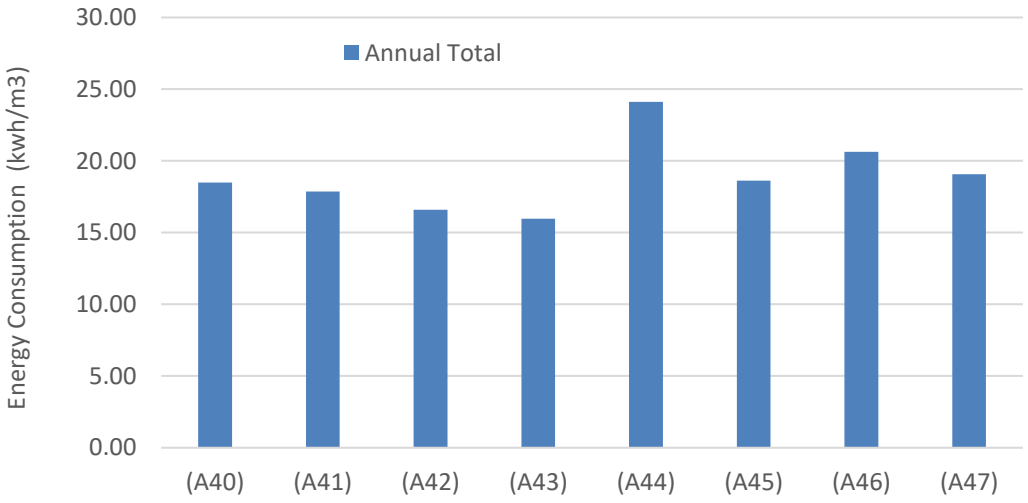

Figure 122. Annual Total Energy Consumption (kWh/m^3) of Typology 4.

4.4.2.3 Surface Temperature

Figure 123 shows the surface temperature variations, for block *A42* of *Typology 4*, outer and courtyard facades, during a full day on Summer Solstice, while

Figure 124, shows the surface temperature variations for the same block and same facades during a full day on Winter Solstice.

On Summer Solstice, the highest temperatures are reached by façade *S8*, which is an inner façade, oriented towards west and has the highest temperature value reaching up to 67 °C, at 15:00, followed by *S1* with 65 °C, a western façade located on the outer part of the building. On the other hand, both outer and inner facades reach the lowest temperatures at 4:00-5:00 AM, with all of them having temperatures of 16 °C-17 °C during Summer Solstice, as shown in ***Figure 123***.

During Winter Solstice, the highest temperatures are reached between 12:00 PM and 15:00 PM, with outer façade *S3*, facing south, reaching a temperature of 58 °C, followed by the other inner façade *S6*, facing south, reaching a temperature of 44 °C. The lowest temperature values are obtained between 7:00 AM-8:00 Am, with all of them going as low as -1 °C, as shown in ***Figure 124***.

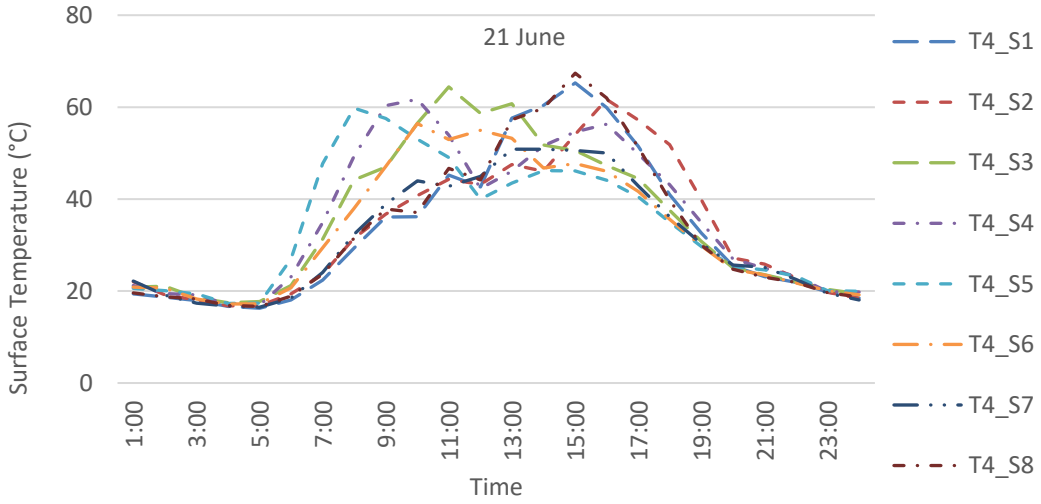

Figure 123. Surface temperatures for building A42 of Typology 4, on Summer Solstice.

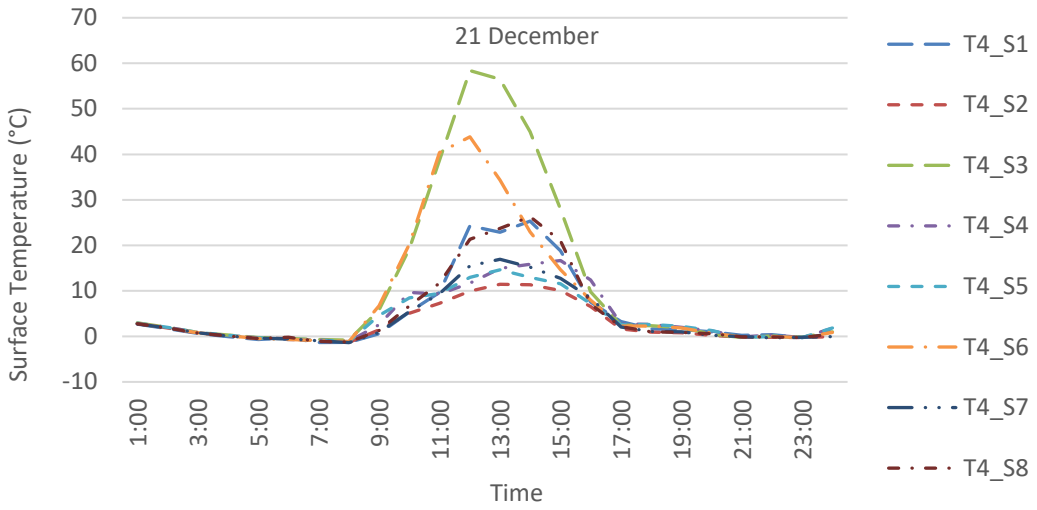

Figure 124. Surface temperatures for building A42 of Typology 4, on Winter Solstice.

4.5 Comparison

4.5.1 Energy Consumption

As reflected from the annual energy consumption results, the building blocks with the most energy usage are: *A2* in *Typology 1*, *A100* in *Typology 2*, *A28* in *Typology 3* and *A44* in *Typology 4*, while the blocks with the least energy spendings are *A8* in *Typology 1*, *A99* in *Typology 2*, *A27* in *Typology 3* and *A43* in *Typology 4*, as shown in ***Table 5***. Total annual energy values vary from 24.60 kWh/m^3 being the highest, in building *A100* of *Typology 2*, to 11.77 kWh/m^3 being the lowest, in building *A8* of *Typology 1*.

- After having made the UMIs distinctions for each typology, on the blocks that spend the highest and the lowest, one indicator that is related to all 8 buildings is H_{bld}. For all the buildings that spend the most energy, H_{bld} is the lowest throughout the typology, while for all the buildings that spend the least energy, H_{bld} is the highest throughout the typology. The lowest value of this parameter (14.56) is reached in block *A44* of *Typology 4*, while the highest value (51.01) is reached in block *A8* of *Typology 1*.

- Another indicator that is related to all 8 blocks is *FSI*. For all the buildings that spend the most energy *FSI* is lowest throughout the typology, while for all the buildings that spend the least energy *FSI* is highest. The lowest value for this parameter (1.73) is reached in block A44 of Typology 4, while the highest value (5.55) is reached in block *A8* of *Typology 1*.
- *V/A ratio* also has an impact on all 8 blocks. For all the buildings that have the highest energy demand, *V/A ratio* is the lowest, while for the ones that have the lowest energy demand, *V/A ratio* is the highest. This indicator has the lowest value (5.19) in block *A44* of *Typology 4* and the highest value (16.66) in block *A8* of *Typology 1*.
- The building that has the highest energy consumption (24.60 kWh/m^3) is block *A100* of *Typology 2*, while block *A8* of *Typology* 1 has the lowest energy consumption (11.77 kWh/m^3).

Despite all the abovementioned indicators having a relation with the buildings that spend the most and the ones that spend the fewest energy annually, only H_{bld} has the highest correlation in accordance with the total energy consumption of all building blocks throughout the site, as shown in ***Figure 125***.

Table 5. Heating and Cooling simulation results obtained for all buildings.

		Annual heating demand	Annual cooling demand	Annual energy demand
Typologies	Buildings	Total heating [kWh]	Total cooling [kWh]	Total energy demand [kWh]
T1	A1	11.82	-5.56	17.38
	A2	14.89	-7.52	22.41
	A3	10.77	-4.68	15.45
	A4	10.77	-4.69	15.46
	A5	11.84	-5.45	17.28
	A6	11.91	-5.54	17.45
	A7	13.74	-6.46	20.21
	A8	8.27	-3.50	11.77
	A9	13.34	-6.19	19.53
	A10	12.75	-5.86	18.61

	A86	13.22	-5.94	19.16
	A87	11.45	-4.24	15.69
	A97	12.34	-4.81	17.15
	A98	12.03	-4.85	16.88
	A99	8.90	-3.63	12.53
T2	A100	17.09	-7.51	24.60
	A101	12.68	-4.81	17.49
	A102	10.68	-4.22	14.90
	A103	12.69	-5.37	18.05
	A104	13.57	-5.81	19.39
	A105	12.55	-5.40	17.95
T3	A27	12.19	-4.20	16.38
	A28	12.71	-4.28	16.98
	A40	13.35	-5.14	18.49
	A41	12.87	-4.98	17.86
	A42	12.22	-4.37	16.58
	A43	11.68	-4.30	15.97
T4	A44	16.72	-7.39	24.11
	A45	13.08	-5.54	18.62
	A46	14.42	-6.21	20.62
	A47	13.11	-5.97	19.07

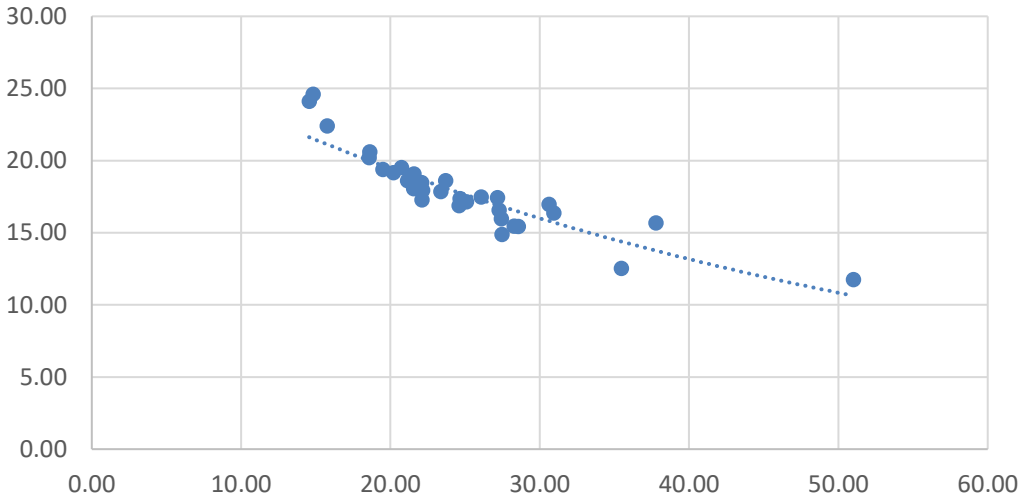

Figure 125. H_{bld} correlation with total energy consumption of all buildings in all 4 typologies.

4.5.2 Surface Temperatures

The building blocks chosen from each typology are compared to one another and the results, shown in ***Table 6***, indicate the following:

- The maximum surface temperature for block *A10* of *Typology 1*, is reached in Summer Solstice, on façade *S3* with a value of 92 °C, while the minimum surface temperature is reached in Winter Solstice, on all facades *S1-S8* with a value of -1 °C.
- The maximum surface temperature for block *A101* of *Typology 2*, is reached in Summer Solstice, on façade *S8* with a value of 88 °C, while the minimum surface temperature is reached in Winter Solstice, on all facades *S1-S8* with a value of -1 °C.
- The maximum surface temperature for block *A28* of *Typology 3*, is reached in Summer Solstice, on façade *S5* with a value of 88 °C, while the minimum surface temperature is reached in Winter Solstice, on all facades *S1-S5* with a value of -1 °C.
- The maximum surface temperature for block *A42* of *Typology 4*, is reached in Summer Solstice, on façade *S8* with a value of 67 °C, while the minimum surface temperature is reached in Winter Solstice, on all facades *S1-S8* with a value of -1 °C.

Table 6. Summary of the simulation results for the exterior surface temperatures of the facades for the chosen building blocks calculated for a full day on Summer Solstice and Winter Solstice.

		Summer Solstice			Winter Solstice		
Building	Facade	Max	Min	Avg	Max	Min	Avg
T1_A10	S1	68	18	36	63	-1	14
	S2	70	17	41	22	-1	6
	S3	92	18	43	47	-1	7
	S4	60	17	36	27	-1	6
	S5	68	18	37	59	-1	13
	S6	57	18	36	20	-1	5
	S7	88	18	42	60	-1	10
	S8	77	18	41	20	-1	6
T2_A101	S1	56	17	33	21	-1	5
	S2	60	17	34	41	-1	10
	S3	63	17	36	13	-1	4
	S4	81	17	37	25	-1	5
	S5	59	18	34	13	-1	3
	S6	66	18	37	51	-1	10
	S7	67	18	38	15	-1	4
	S8	88	17	40	30	-1	5
T3_A28	S1	76	18	40	17	0	5
	S2	52	17	32	15	-1	4
	S3	51	17	31	48	-1	8
	S4	80	17	34	16	-1	4
	S5	88	18	38	39	-1	6
T4_A42	S1	65	16	33	25	-1	5
	S2	62	17	34	11	-1	3
	S3	64	17	36	58	-1	11
	S4	62	17	36	17	-1	4
	S5	60	17	34	15	-1	4
	S6	56	17	33	44	-1	8
	S7	51	16	32	17	-1	4
	S8	67	17	34	26	-1	5

CHAPTER 5

CONCLUSIONS

Despite the fact that UMI studies have been previously conducted for the Mediterranean region, the outcomes still remain on a more theoretical than practical level. This research displays an attempt to better understand what is the impact of a buildings form in its energy efficiency. Thus, the final results reveal the accuracy of the preliminary design phase and a way to check the architects design decisions, if they are informed or not.

This study reveals the following findings:

- H_{bld} is the main urban morphology indicator that has the most impact on the total energy consumption on a building block in the Mediterranean context. The higher the building the less energy it spends, while the lower the building the most energy it spends for heating and cooling purposes. The correlation of this indicator and the buildings in this site is up to a factor of 0.9.
- The surrounding buildingst have a huge impact to adjacent ones as they indirectly shape the energy loads of one another.
- The shape of the courtyard plays an important role in the total energy consumption of a building. Despite the fact that block *A44* of *Typology 4*, had the lowest H_{bld}, *FSI* and *V/A* (the common contrasting urban morphology indicators across all buildings) values throughout the site, the building with the most energy consumption is block *A100* of *Typology 2*. Both have the same UMIs values. The main physical differentiation between them is on their courtyard form, A100 contains a courtyard that is not fully closed while block *A44* is fully open from one side, as shown in ***Figure 126***.

The use of very detailed inputs in the software has further helped the precision of the final data, the literature review chapter describes previous studies that have taken few inputs into consideration. To further develop this research area more

observations need to be made on several building geometries in this climate and other sub-climate regions of it.

Overall, the final results of this study reveal insightful data for the given site in Tirana. It represents a well documented initiative towards new observations for this field in the future.

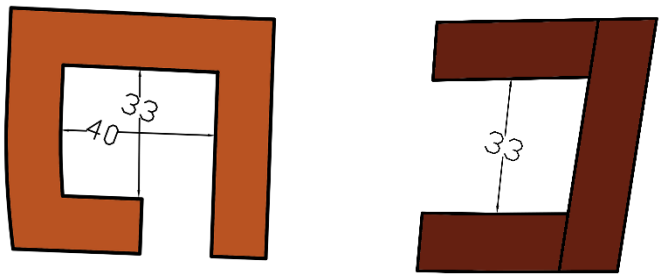

Figure 126. Block A100 on the left and Block A44 on the right.

REFERENCES

[1] "Wang, L., Yuan, G., Long, R., & Chen, H. (2017). An urban energy performance evaluation system and its computer implementation. Journal of Environmental Management, 204, 684–694. https://doi.org/10.1016/j.jenvman.2017.09.041"

[2] "Rode, P., Keim, C., Robazza, G., Viejo, P., & Schofield, J. (2014). Cities and energy: Urban morphology and residential heat-energy demand. Environment and Planning B: Planning and Design, 41(1), 138–162. https://doi.org/10.1068/b39065"

[3] "Allen, A., Henze, G., Baker, K., & Pavlak, G. (2020). Evaluation of low-exergy heating and cooling systems and topology optimization for deep energy savings at the urban district level. Energy Conversion and Management, 222. https://doi.org/10.1016/j.enconman.2020.113106"

[4] "Wong, N. H., Jusuf, S. K., Syafii, N. I., Chen, Y., Hajadi, N., Sathyanarayanan, H., & Manickavasagam, Y. V. (2011). Evaluation of the impact of the surrounding urban morphology on building energy consumption. Solar Energy, 85(1), 57–71. https://doi.org/10.1016/j.solener.2010.11.002"

[5] "Urquizo, J., Calderón, C., & James, P. (2017). Metrics of urban morphology and their impact on energy consumption: A case study in the United Kingdom. Energy Research and Social Science, 32, 193–206. https://doi.org/10.1016/j.erss.2017.03.011"

[6] "Salvati, A., Palme, M., Chiesa, G., & Kolokotroni, M. (2020). Built form, urban climate and building energy modelling: case-studies in Rome and Antofagasta. Journal of Building Performance Simulation, 13(2), 209–225. https://doi.org/10.1080/19401493.2019.1707876"

[7] "Pérez-Lombard, L., Ortiz, J., & Pout, C. (2008). A review on buildings energy consumption information. Energy and Buildings, 40(3), 394–398. https://doi.org/10.1016/j.enbuild.2007.03.007"

[8] "Kämpf, J. H., Montavon, M., Bunyesc, J., Bolliger, R., & Robinson, D. (2010). Optimisation of buildings' solar irradiation availability. Solar Energy, 84(4), 596–603. https://doi.org/10.1016/j.solener.2009.07.013"

[9] "Holden, E. (2004). Ecological footprints and sustainable urban form. Journal of Housing and the Built Environment, 19(1), 91–109. https://doi.org/10.1023/B:JOHO.0000017708.98013.cb"

[10] "Allegrini, J., Dorer, V., & Carmeliet, J. (2012). Influence of the urban microclimate in street canyons on the energy demand for space cooling and heating of buildings. Energy and Buildings, 55, 823–832. https://doi.org/10.1016/j.enbuild.2012.10.013

[11] "Allegrini, J., Orehounig, K., Mavromatidis, G., Ruesch, F., Dorer, V., & Evins, R. (2015, December 29). A review of modelling approaches and tools for the simulation of district-scale energy systems. Renewable and Sustainable Energy Reviews. Elsevier Ltd. https://doi.org/10.1016/j.rser.2015.07.123"

[12] "Allegrini, J., Dorer, V., & Carmeliet, J. (2016). Impact of radiation exchange between buildings in urban street canyons on space cooling demands of buildings. Energy and Buildings, 127, 1074–1084. https://doi.org/10.1016/j.enbuild.2016.06.073"

[13] "Orehounig, K., Mavromatidis, G., Evins, R., Dorer, V., & Carmeliet, J. (2014). Towards an energy sustainable community: An energy system analysis for a village in Switzerland. Energy and Buildings, 84, 277–286. https://doi.org/10.1016/j.enbuild.2014.08.012

[14] "Calvillo, C. F., Sánchez-Miralles, A., & Villar, J. (2016, March 1). Energy management and planning in smart cities. Renewable and Sustainable Energy Reviews. Elsevier Ltd. https://doi.org/10.1016/j.rser.2015.10.133"

[15] "Chatzipoulka, C., Compagnon, R., & Nikolopoulou, M. (2016). Urban geometry and solar availability on façades and ground of real urban forms: using London as a case study. Solar Energy, 138, 53–66. https://doi.org/10.1016/j.solener.2016.09.005"

[16] "Chatzipoulka, C., & Nikolopoulou, M. (2018). Urban geometry, SVF and insolation of open spaces: London and Paris. Building Research and Information, 46(8), 881–898. https://doi.org/10.1080/09613218.2018.1463015"

[17] Tardioli, G., Narayan, A., Kerrigan, R., Oates, M., O'Donnell, J., & Finn, D. P. (2020). A methodology for calibration of building energy models at district scale using clustering and surrogate techniques. Energy and Buildings, 110309. doi: 10.1016/j.enbuild.2020.110309"

[18] Keirstead, J., Jennings, M., & Sivakumar, A. (2012, August). A review of urban energy system models: Approaches, challenges and opportunities. Renewable and Sustainable Energy Reviews. https://doi.org/10.1016/j.rser.2012.02.047"

[19] "Javanroodi, K., Mahdavinejad, M., & Nik, V. M. (2018). Impacts of urban morphology on reducing cooling load and increasing ventilation potential in hot-arid climate. Applied Energy, 231, 714–746. https://doi.org/10.1016/j.apenergy.2018.09.116"

[20] "Chen, H. C., Han, Q., & de Vries, B. (2020). Urban morphology indicator analyzes for urban energy modeling. Sustainable Cities and Society, 52. https://doi.org/10.1016/j.scs.2019.101863"

[21] "Cheng, V., Steemers, K., Montavon, M., & Compagnon, R. (2006). Urban form, density and solar potential. In PLEA 2006 - 23rd International Conference on Passive and Low Energy Architecture, Conference Proceedings."

[22] "Evins, R., Orehounig, K., & Dorer, V. (2016). Variability between domestic buildings: the impact on energy use. Journal of Building Performance Simulation, 9(2), 162–175. https://doi.org/10.1080/19401493.2015.1006526"

[23] "Fichera, A., Frasca, M., Palermo, V., & Volpe, R. (2018). An optimization tool for the assessment of urban energy scenarios. Energy, 156, 418–429. https://doi.org/10.1016/j.energy.2018.05.114"

[24] "Frayssinet, L., Merlier, L., Kuznik, F., Hubert, J. L., Milliez, M., & Roux, J. J. (2018, January 1). Modeling the heating and cooling energy demand of urban buildings at city scale. Renewable and Sustainable Energy Reviews. Elsevier Ltd. https://doi.org/10.1016/j.rser.2017.06.040"

[25] "Futcher, J. A., Kershaw, T., & Mills, G. (2013). Urban form and function as building performance parameters. Building and Environment, 62, 112–123. https://doi.org/10.1016/j.buildenv.2013.01.021"

[26] "Futcher, J., Mills, G., & Emmanuel, R. (2018). Interdependent energy relationships between buildings at the street scale. Building Research and Information, 46(8), 829–844. https://doi.org/10.1080/09613218.2018.1499995"

[27] "Hui, S. C. M. (2001). Low energy building design in high density urban cities. Renewable Energy, 24(3–4), 627–640. https://doi.org/10.1016/S0960-1481(01)00049-0"

[28] "Jamei, E., Rajagopalan, P., Seyedmahmoudian, M., & Jamei, Y. (2016, February 1). Review on the impact of urban geometry and pedestrian level greening on outdoor thermal comfort. Renewable and Sustainable Energy Reviews. Elsevier Ltd. https://doi.org/10.1016/j.rser.2015.10.104

[29] "Lauzet, N., Rodler, A., Musy, M., Azam, M. H., Guernouti, S., Mauree, D., & Colinart, T. (2019, December 1). How building energy models take the local climate into account in an urban context – A review. Renewable and Sustainable Energy Reviews. Elsevier Ltd. https://doi.org/10.1016/j.rser.2019.109390"

[30] "Mauree, D., Naboni, E., Coccolo, S., Perera, A. T. D., Nik, V. M., & Scartezzini, J. L. (2019). A review of assessment methods for the urban environment and its energy sustainability to guarantee climate adaptation of future cities. Renewable and Sustainable Energy Reviews, 112, 733–746. https://doi.org/10.1016/j.rser.2019.06.005"

[31] "Morganti, M., Salvati, A., Coch, H., & Cecere, C. (2017). Urban morphology indicators for solar energy analysis. In Energy Procedia (Vol. 134, pp. 807–814). Elsevier Ltd. https://doi.org/10.1016/j.egypro.2017.09.533"

[32] "Naboni, E., Coccolo, S., Meloni, M., & Scartezzini, J.-L. (2018). Outdoor Comfort Simulation of Complex Architectural Designs a Review of Simulation Tools from the Designer Perspective. 2018 Building Performance Analysis Conference and SimBuild, (Anon 2017), 659–666."

[33] "Okeil, A. (2010). A holistic approach to energy efficient building forms. Energy and Buildings, 42(9), 1437–1444. https://doi.org/10.1016/j.enbuild.2010.03.013"

[34] "Perera, A. T. D., Javanroodi, K., & Nik, V. M. (2021). Climate resilient interconnected infrastructure: Co-optimization of energy systems and urban morphology. Applied Energy, 285. https://doi.org/10.1016/j.apenergy.2020.116430

[35] "Salvati, A., Coch, H., & Morganti, M. (2017). Effects of urban compactness on the building energy performance in Mediterranean climate. In Energy Procedia (Vol. 122, pp. 499–504). Elsevier Ltd. https://doi.org/10.1016/j.egypro.2017.07.303"

[36] "Salvati, A., Monti, P., Coch Roura, H., & Cecere, C. (2019). Climatic performance of urban textures: Analysis tools for a Mediterranean urban context. Energy and Buildings, 185, 162–179. https://doi.org/10.1016/j.enbuild.2018.12.024"

[37] "Sola, A., Corchero, C., Salom, J., & Sanmarti, M. (2018, December 1). Simulation tools to build urban-scale energy models: A review. Energies. MDPI AG. https://doi.org/10.3390/en11123269"

[38] "Steadman, P., Hamilton, I., & Evans, S. (2014). Energy and urban built form: An empirical and statistical approach. Building Research and Information, 42(1), 17–31. https://doi.org/10.1080/09613218.2013.808140"

[39] "Tardioli, G., Narayan, A., Kerrigan, R., Oates, M., O'Donnell, J., & Finn, D. P. (2020). A methodology for calibration of building energy models at district scale using

clustering and surrogate techniques. Energy and Buildings, 226. https://doi.org/10.1016/j.enbuild.2020.110309"

[40] "Salvati, A., Coch Roura, H., & Cecere, C. (2015). Urban morphology and energy performance: the direct and indirect contribution in mediterranean climate. PLEA 2015 Architecture in (R)Evolution – 31st International PLEA Conference – Bologna 9-11 September, 1–8."

[41] "Wu, R., Mavromatidis, G., Orehounig, K., & Carmeliet, J. (2017). Multiobjective optimisation of energy systems and building envelope retrofit in a residential community. Applied Energy, 190, 634–649. https://doi.org/10.1016/j.apenergy.2016.12.161"

[42] "Sharifi, A., & Yamagata, Y. (2016, July 1). Principles and criteria for assessing urban energy resilience: A literature review. Renewable and Sustainable Energy Reviews. Elsevier Ltd. https://doi.org/10.1016/j.rser.2016.03.028"

[43] Tardioli, G., Narayan, A., Kerrigan, R., Oates, M., O'Donnell, J., & Finn, D. P. (2020). A methodology for calibration of building energy models at district scale using clustering and surrogate techniques. Energy and Buildings, 110309. doi: 10.1016/j.enbuild.2020.110309